12-17-2009

Design and Synthesis of Boronic Acid-Modified Nucleotides for Fluorescent Sensing and Cell Imaging

Xiaochuan Yang
Georgia State University

DESIGN AND SYNTHESIS OF BORONIC ACID-MODIFIED NUCLEOTIDES FOR FLUORESCENT SENSING AND CELL IMAGING

by

XIAOCHUAN YANG

Under the Direction of Professor Binghe Wang

ABSTRACT

With the rapidly increasing interest in the field of glycomics, which is the comprehensive study of the roles carbohydrates play in a living system, urgent need for developing quick and highly selective carbohydrate sensors is growing. The boronic acid group, with its electron-deficient structure (6 valence electrons with an open shell), acts as a Lewis acid with high intrinsic affinity towards Lewis bases such as fluoride, cyanide and hydroxyl groups. Specifically, formation of a 5- or 6- membered ring between the boronic acid moiety and a1,2- or 1,3-diol in aqueous solution has been fully explored as a strategy of carbohydrate sensor design. Along this line, those binders were termed as “boronolectins” because of their similar functions as lectins.

One challenge in developing boronic acid-based carbohydrate sensors is to enhance the discriminating ability among various carbohydrate analytes with diverse building blocks and complex linkage patterns. One approach is using polypeptide or

oligonucleotide as a backbone or scaffold with functionalized boronic acid moiety to create a molecular library, and then selecting binders with favorable properties.

The work presented here includes three general research parts: synthesis of a naphthalimide-based boronic acid-conjugated thymidine triphosphate (NB-TTP), fluorescence property studies of NB-TTP incorporated DNA (NB-DNA), and cellular imaging studies using NB-TTP:

1) 4-Amino-1,4-naphthalimide (Nap) was chosen as the fluorophore because of its relatively long excitation and emission wavelengths, and stability. The synthesis of naphthalimide-based boronic acid (NB) followed similar route as previously published work. Tethering of boronic acid moiety and TTP was accomplished through Cu(I)-catalyzed azide-alkyne cyclization (CuAAC), known as click chemistry. The synthesized NB-TTP showed fluorescence enhancements at long wavelength (λ_{em}: 540 nm) upon sugar addition.

2) NB-TTP was incorporated into DNA through Klenow fragment-catalyzed primer extension reactions. Different DNA sequences were designed with varying number and spacing for NB-TTP incorporation. The preliminary study provided certain insight into several factors that affect the fluorescent properties of different NB -DNA.

3) NB-TTP was added into Hela cell culture medium to study its cell imaging properties. With the observation under fluorescent microscope, it was demonstrated that NB-TTP showed good cell membrane permeability and significant accumulation in cell nucleus.

INDEX WORDS: Boronic acid, Fluorescence, DNA, Carbohydrate sensor, Cell imaging

DESIGN AND SYNTHESIS OF BORONIC ACID-MODIFIED NUCLEOTIDES FOR FLUORESCENT SENSING AND CELL IMAGING

by

XIAOCHUAN YANG

A Dissertation Submitted in Partial Fulfillment of the Requirements for the Degree of

Doctor of Philosophy

in the College of Arts and Sciences

Georgia State University

2010

DESIGN AND SYNTHESIS OF BORONIC ACID-MODIFIED NUCLEOTIDES FOR FLUORESCENT SENSING AND CELL IMAGING

by

XIAOCHUAN YANG

Committee Chair: Dr. Binghe Wang

Committee: Dr. Al Baumstark
Dr. Jenny Yang

Electronic Version Approved:

Office of Graduate Studies
College of Arts and Sciences
Georgia State University
May 2010

ACKNOWLEDGEMENTS

Here I would like to express my deep gratitude towards my advisor Prof. Wang, for the whole work was carried out under his direction and guidance. During the entire process, Prof. Wang consistantly worked with me closely, not only providing advice on solving acadmic research problems, but also helping keep me in good shape of personality development. I benefit a lot through learning from him and thus get a high-level starting point in my career. Besides, I would also like to sincerely thank Prof. Baumstark and Prof. Yang for their time and patience in helping me through out my PhD program. In addition to the professional knowledge I gained from their courses, their enthusiasm and passion in scientific research and teaching has also affected me in so many positive ways. This dissertation would not have been possible without their guidance. Many other people of Department of Chemistry have also offered their support and help during my 5 years of study, making this time a precious piece of memory in my life. Among them, I would especially thank Dr. Shilong Zheng and Dr. Guojing Sun for their intimate hands-on teaching and training of my lab skills, without whom I would struggle much more with entangling trouble shootings. Also, I am obliged to Dr. Na Lin and Dr. Minyong Li for their initiation of the project and helping me as a good starter on track. Technical support from Dr. Siming Wang and Dr. Sekar Chandrasekaran in Mass Spectrum and NMR data collection should also be acknowledged. In addition, I would like to address my appreciation to my other coworkers in the lab, Nanting Ni, Junfeng Wang, Gurpreet Kaur, Shan Jin, Jun Yan, Chaofeng Dai and Weixuan Chen for their daily discussions and help in research, which is quite an enjoyable personal experience for me. This work is supported by grants from the NIH (CA123329, CA113917, and

GM084933). Finally, my very special thanks go out to my parents Zhenhua Yang and Huizhen Cao, who I want to dedicate this dissertation to for their love and care that nothing can compare to in the whole world.

TABLE OF CONTENTS

LIST OF TABLES

LIST OF FIGURES

LIST OF SCHEMES

LIST OF ABBREVIATIONS

DNA	Deoxyribonucleic acid
TTP	Thymidine triphosphate
CuAAC	Cu(I)-catalyzed azide-alkyne cyclization
PTM	Post-translational modification
GlcNAc	*N*-Acetylglucosamine
PAMP	Pathogen associated molecular patterns
HBP	Hepatic binding proteins
vWF	von Willebrand factor
CDG	Congenital disorder of glycosylation
PSA	Prostate cancer antigen
hCG	Human chorionic gonadotropin
GBP	Glycan binding protein
CRD	Carbohydrate recognition domain
MBP	Mannose Binding Proteins
NMR	Nuclear magnetic resonance
ESI	Electrospray ionization
MALDI	Matrix-Assisted Laser Desorption/ionization
WGA	Wheat germ agglutinin
PBA	Phenylboronic acid
ARS	Alizarin Red S.
PET	Photoninduced electron transfer
HPTS	8-Hydroxypyrene-1,3,6-trisulfonic acid trisodium salt
BBV	Bis(benzyl-2-boronic acid)-viologen
sLe^x	sialic Lewis acid X
SAM	Self-assembled monolayer
QCM	Quartz crystal microbalance
SPR	Surface plasma resonance
HRP	Horseradish peroxidase
EDTA	Ethylenediaminetetraacetic acid
HbA1c	Glycated hemoglobin
HbA0	Non-glycated hemoglobin
DTBA	Dithiobis(4-butylamino)
VPB	(4-Vinylphenyl)boronic acid
EGDMA	Ethylene glycol dimethacrylate
UV	Ultraviolet
ISFET	Ion-sensitive field effect transistor
IF	Imprinting factor
PBL	Peptide-based boronolectin
NBL	Nucleic acid-based boronolectin
RBR	resin-bound receptor
LDA	Linear Discriminant Analysis
SELEX	Systematic evolution of ligands with exponential enrichment
Nap	4-amino-1,8-naphthalimide
aNap	Alkylated 4-amino-1,8-naphthalimide

NB	Naphthalimide-based boronic acid
B-TTP	Boronic acid-modified TTP analogue
NB-TTP	Naphthalimide-based boronic acid modified TTP
NB-DNA	Naphthalimide based boronic acid conjugated DNA
dsDNA	Double stranded DNA
ssDNA	Single stranded DNA
RNA	Ribonucleic acid
PCR	Polymerase chain reaction
PAGE	Polyacrylamide gel electrophoresis
ICT	Internal charge transfer
DFT	Density function theory
PCM	Polarizable continuum model
TEA	Triethyl amine
TFA	Trifluoroacetic acid
THF	Tetrahedrofuran
TLC	Thin layer chromatography
DMF	Dimethylformamide
TBTA	*tris*-(benzyltriazolylmethyl)amine

1. INTRODUCTION

1.1. Glycomics study and natural carbohydrate sensors

With the completion of the Human Genome Project and the mapping of approximately 20,000-25,000 genes in the human genome,[1-3] the world is entering into a post-genomics era of investigating how genes function in a coordinated fashion *in vivo* and in response to outside environment. It is well known that after transcription and translation from the genomic DNA sequences, the expressed proteins or peptide sequences sometimes undergo further modifications (post-translational modification, PTM) in order to gain full function properly.[4-7] Glycosylation, the attachment of oligosaccharide moieties to the protein, is perhaps the most complicated form of PTM.[8-10] In fact, the differences contributed by the various glycoforms are so significant that the microdiversity of proteins created by glycosylation can determine their functions and properties.[11-15] Collectively, the vast diversity of glycans arises from its non-template driven biosynthetic routes, a lack of proof-reading machinery, and a large number of tissue-specific isoforms of glycosyltransferase and glycosidase.[16-17] Differences in sequence, composition and branching patterns also provide the chemical basis for the structural complexity of glycans. Such complexity rivals or exceeds that of proteins and nucleic acids. On one hand, the inherent chemical heterogeneity and structural diversity makes it convenient for cells to coordinate together and be individual and specific in the whole body context. On the other hand, it also creates a great challenging scenario in the research field of glycosylation. Thus, there is an urgent need for developing tools to

detect and differentiate so many different forms of glycans. Currently, the word “glycan” refers to a general term including oligosaccharides, polysaccharides and carbohydrates.[17] The term of “glycomics” also emerged correspondingly, which is defined as the comprehensive study of the biological roles glycans play in living organisms, as in parallel with terms like genomics, proteomics and lipidomics.

1.1.1 Brief introduction of glycan structures

Briefly, there are nine monosaccharides used by mammals in enzymatic glycosylation processes. These are galactose, glucose, glucuronic acid, fucose, mannose, *N*-acetylgalactosamine, *N*-acetylglucosamine, sialic acid and xylose (Figure 1.1).[17] For glycans on cell membranes or extracellular compartment in the forms of glycoproteins and glycolipids, their assembling is through the Golgi apparatus where the glycan oligomers elongate and branch.[12,18] There are three major glycosylation patterns of protein: *O*-glycan, *N*-glycan and glycosaminoglycan. Specifically, *N*-glycans are attached to the asparagine residues in the Asn-X-Ser/Thr motif of proteins.[19-21] *O*-Glycans are linked to either Ser or Thr residues.[19,22] Glycosaminoglycans are also Ser or Thr anchored but in linear instead of branched, and often highly sulfated oligo-forms.[23-25] Glycosylation on lipids is in the form of sialic acid-bearing gangliosides.[26-27] Besides those glycosylations that happen through the Golgi apparatus secretory pathways, many cytoplasmic and nuclear proteins are glycosylated by *N*-acetylglucosaminidase in cytoplasm. *N*-Acetylglucosamines attached to Ser or Thr residues (*O*-GlcNAc) of those proteins are found to be a very important PTM regulated for many mammalian cell types’

viability, probably as nutrient sensors or protein turnover regulation factors.[28-31] Again, all the glycosylation patterns with α or β anomers linking through 1,2 (donor) → 2,3,4,6 (acceptor) glycosidic bonds contribute to a repertoire of tremendous number of glycan structures.[17]

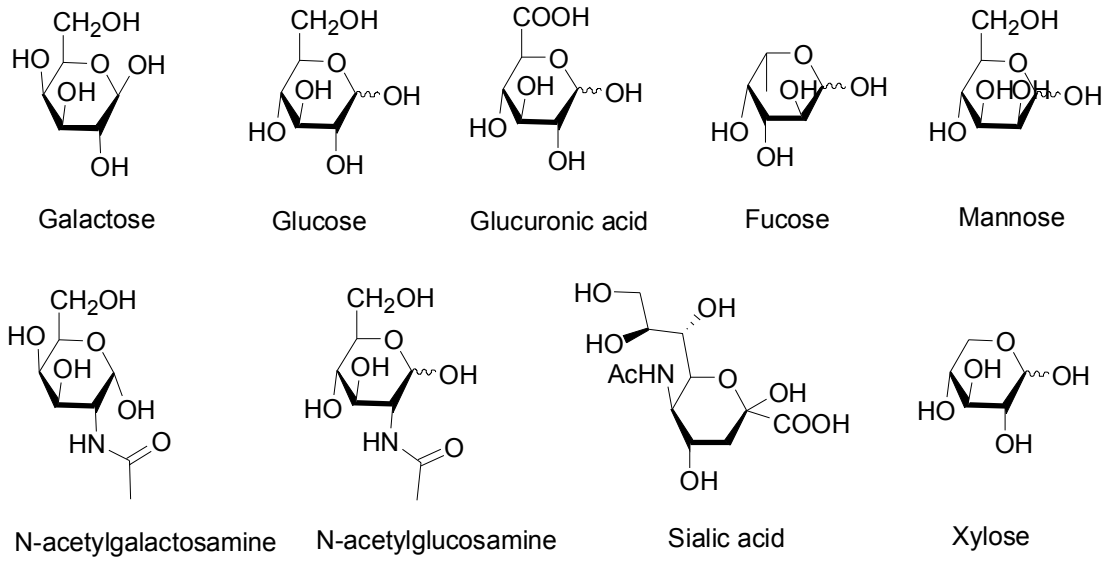

Figure 1.1. Monosaccharides used in mammalian enzymatic glycosylations

1.1.2 Brief introduction of glycosylation functions

Glycosylation in animal body functions is important. For example, in transgenic mice with GlcNAcT-1 glycosyltransferase deficiency, the embryos showed severe defects in the cardiovascular system and other morphogenic abnormalities.[32-33] In general, there are several biological processes that involve glycosylation. For example, cell-cell adhesion mediated by glycan-protein interactions is critical for trafficking lymphocytes, neutrophils, CD4+ T cells, natural killer cells and other immuno-responsive cells to the

site of inflammation;[34-37] the mammalian immunoreaction is directed by molecular recognition mechanisms including a key fucose linkage on sialyl-Lewis X oligosaccharide;[38] self/non-self recognition through discrimination of pathogen glycans by mammalian cells is responsible for the initiation of some immunoreactions;[39-40] pathogen-associated molecular patterns (PAMP), once recognized and bound, can initiate phagocytosis by macrophages to clear up the invading organisms.[41-45] Glycan recognition is also responsible for the body's metabolism regulation, such as turnover of endogenous glycoproteins. One case in point is the hepatic asialoglycoprotein receptors (or hepatic binding proteins, HBP), which can bind to and internalize the glycoproteins with fewer or without any sialic acid linkages.[46] In mice with decreasing thrombosis resulting from defective sialytransferase expression, both platelets and the von Willebrand factor (vWF) glycoproteins are targets for asialoglycoprotein receptors.[47] Moreover, some glycosylation recognitions are involved in cellular receptor activation and signal transduction processes. For example, specific heparan sulfate, as one kind of glycosylaminoglycans, can bind to fibroblast growth-factor receptors and induce receptor dimerization and activation.[48] It is also found that some morphogenesis and organogenesis in early embryo stages can be regulated through glycosylaminoglycan-receptor binding.[49] Of course, listing all the examples of glycosylation importance will be laborious work and not practical. Illustrating a few examples above helps to highlight the meaning and need for developing tools for glycan sensing and study.

Given the importance of glycosylation in normal mammalian body functions, it is conceivable that abnormality of certain glycosylation patterns could result in dysfunction or even disease of human body. For example, the lack of dolicol-oligosaccharide precursor resulting in a decrease in *N*-glycosylation frequency is found to be responsible for congenital disorders of glycosylation (CDG) syndromes of children, many of which are discovered especially in their early life years.[50-52] I-cell disease, resulting from the failure of mannose-6-phosphate modification of *N*-glycan in the Golgi body, causes a protein storage disorder, due to the lack of trafficking signal of hydrolase into lysosome.[53-54] Furthermore, unusual glycosylation patterns serve as good indicators for specific diseases such as cancer and serve as biomarkers in clinical diagnosis.[55-60] In one case, elevated T-antigen levels (truncated O-glycan) were correlated with the prognosis of low survival rate of certain cancer patients.[14,61] Another example is the prostate cancer antigen (PSA) from tumor cells, which contains a higher level of fucose and absence of sialic acid compared with PSA from normal cells.[62-65] Also, different glycosylated forms of hCG can be diagnostic biomarkers for cancer, Down syndrome, or pregnancy failure.[66-67] Specifically, hyperglycosylated hCGs (hCG-H, also known as invasive trophoblast antigen-ITA), are very different from normal hCG (human chorionic gonadotropin) in terms of both functions, origins, and glycosylation paterns. While hCG-H is essential for successful human implantation, it is also an invasive promoter in choriocarcinoma.[68] One last but not least example is human RNase 1, which has completely different glycosylation patterns when secreted by pancreatic tumor cells

compared with those by normal cells.[58,69-70] For a more comprehensive compiling of glycan-based biomarkers, some excellent reviews are recommended.[71-73] However, even with those well-documented glycosylation related diseases, the discovery process is more serendipitous than well-planned.[17] Commonly used protein separation methods through isoelectric focusing and electrophoresis are not able to catch most glycosylation defects. Thus, developing tools that can primarily focus on the glycosylation microdomain (sweet spots) should have great meaning and implication in clinical practice.

1.1.3 Conventional tools and methods for glycosylation studies

Conventional chemistry analytical approaches, such as mass spectrometry,[74-79] HPLC[80-81] and NMR,[82-84] have been used together with computational informatics as an integral method for glycan primary structure characterization.[16,85-86] As powerful as those essential tools are, they suffer from the shortcomings of time consuming, and the need for advanced expertise and large sample amounts (for NMR). Besides, analysis of the glycan moieties using those methods requires removal of the saccharides from proteins and seperate characterizations. Due to the inherent heterogeneity nature of glycans, systematic analysis of a large number of glycans demands a more efficient approach.

The above-mentioned proteins that bind to *N*- or *O*-glycans and mediate various biological processes are generally termed glycan-binding proteins (GBP). So far, three major classes of natural GBPs have been identified in mammalian system: C-type lectins, siglecs and galactins.[9-10,16] The C-type lectins are so named because of their

requirement of Ca^{2+} for proper functions.[87-88] C-type lectins are further divided into three sub-classes: endocytic lectins, collectins and selectins. Previously discussed hepatic binding proteins (HBP) are the prototype of endocytic lectins, specific for galactose/N-acetylgalactosamine moiety.[46,89-90] Endocytic lectins are all transmembrane proteins with extracellular carbohydrate recognition domain (CRD).[88] In contrast, collectins are soluble proteins with a cysteine-rich amino terminal and a CRD carboxyl terminal.[91-92] Mannose-binding proteins (MBP A and MBP C) are typical examples of collectins.[93-96] The third subclass, selectins are so named because of their mediation in selective contact between cells. Three members of selectins, E-selectin, P-selectin and L-selectins, are all membrane bound proteins with CRD located at amino terminal part.[97-101] In total, there are hundreds of lectins identified and characterized, among which about 60 of them are commercially available from companies like Sigma-Aldrich and Fisher Scientific.[71] Due to the flexibility around glycosidic linkage, oligosaccharides exist with highly dynamic conformations. The lectin-glycan binding affinity is quite structure-dependent so that saccharides with different chemical compositions but similar topographic properties can bind to the same lectin.[88] In contrast, different lectins for the same saccharide could focus on separate regions of the saccharide structure. However, once bound by lectins, specific conformation of the glycan is locked and fixed and the rotational freedom around glycosidic linkage is reduced. Thus, lectins bind saccharides in a reversible and specific way, but they all have cross-reactivity issues.[71,88] Different from C-type lectins, siglecs are a subgroup of immunoglobulin superfamily, termed I-type

lectins.[102-103] The *N*-terminal of siglecs specifically recognizes sialic acid-containing ligands. The third type of GBPs, galectins are so named because their selective affinity towards galactose-containing ligands on cell-surface.[104-106]

All three types of GBPs are involved in previously discussed cell-cell adhesion, cell trafficking and signal transduction processes through target glycan bindings. Among them, lectins are the most widely used tools in glycan research.[34,37,44,60,88,91-92,99,102-103,105-110] Binding between lectin and carbohydrate happens on the shallow cavity of lectin surface and primarily relys on hydrogen bond formations and hydrophobic interactions.[71,88] Thus, single lectin-glycan interaction is very week with K_d at the mM level. Tight binding is achieved through cooperative multivalent interactions of lectin towards oligosaccharides (K_d to μM range),[111-112] while lectin-monosaccharide interaction remains at the same level. Application of lectins in glycosylation research has been achieved in recent years through a lectin-microarray method.[108-110,113] Basically, different types of selected lectins are immobilized on the array surfaces and analytes with fluorescence labeling are applied on the microarray. Through analyzing the binding profiles generated on the arrays, each glycosylation pattern has one corresponding fingerprint profile. Through such method, general glycan information such as *N*- or *O*-glycosylated form, mannose and fucose content and sialylated level could be acquired. Furthermore, even real-time monitoring of glycosylation pattern changes was achieved using this approach.[109]

Given the efficiency of lectin microarray in glycan detection, the technique is still

limited by the availability of lectins. First of all, only about 40 commercially available lectins can be obtained conveniently, compared to hundreds and thousands of glycan targets are on the list of being analyzed. Second, the cost is still much higher using biological generated lectins than using usual chemically synthesized sensors.

1.1.4 Conclusion

In general, carbohydrates are very important in glycosylation modification of proteins. Acurate detection and characterization of those glycans have great implication in terms of both fundamental biological research and clinical diagnostic applications. However, the complexity and numerous varieties of the carbohydrate analytes constitute an inviting challenge for people to develop rapid and efficient research tools in area of carbohydrate recognition. Lectins as natural carbohydrate binders showed great promise in their high affinity and somehow selectivity towards oligosaccharides sensing. However, in order to address the issues of their high cost, limited availability and certain degree of cross reactivity, there is an urgent demand for developing artificial lectin-mimetics that are low in cost, easy to make and highly selective. For such purpose, great amount of efforts have been carried out in developing synthetic lectin-mimetics using chemical approaches, among which one specific class is the boronic acid-based carbohydrate sensor utilizing the intrinsic affinity of boronic acid towards carbohydrate diols.

1.2 Boronic acid: a powerful tool to detect carbohydrates

1.2.1 Brief introduction of boronic acid chemistry

As introduced in the previous chapter, the importance of glycomics studies requires the development of novel powerful tools to assist and complement currently using biological approaches. Under the “biology-driven chemistry” impetus, great effort has been undertaken to develop artificial sensors for carbohydrate. Besides the need in glycosylation research, those sensors may even be further applied for clinical diagnostic and therapeutic purposes. In terms of their functions, those sensors act as lectin mimics. In general, there are two chemical design strategies: boronic acid-based and non-boronic acid-based sensors. The boronic acid-based lectin mimics using the strong and reversible interactions between boronic acids and hydroxyl groups as recognition moieties are termed “boronolectins”.[114] In contrast, most of the non-boronic acid-based lectin mimics rely on hydrogen bond, hydrophobic and ionic interactions in building up the intrinsic affinity.[71,115-116] It should be noticed that in an ideal application situation, the carbohydrate sensing should be best performed in an aqueous environment. Most of the non-boronic acid lectin mimics designed so far only function under aprotic solvent system.[116-118]

Since for chemosensing purpose the solvent system is not a major issue, it is understandable since those interaction studies could provide insightful information about non-covalent interactions between carbohydrates and sensors, which is the strategy that nature adapts in lectin-glycan binding processes. One noticeable exception of them is

the elegant work by the Davis group. In this case, a binding cavity was created to accommodate sugar moiety with parallel aryl rings as the roof and floor for hydrophobic interactions, and with four amide linkers as pillars for hydrogen bond interactions (Figure 1.2).[116,119] Thus, the sensor designed spatially complement saccharides possessing axial CH groups (CH-π interaction) and equatorial hydroxyl groups (hydrogen bond interaction) (Scheme 1.1). Then dodecacarboxylate side chains were linked to sensor to provide it with good solubility for entering into the aqueous phase.[120] The sensor and β-*N*-acetyl-D-glucosaminyl (β-GlcNAc) have a association constant of 630 M^{-1},[121] which was strong enough to rival natural β-GlcNAc lection, wheat germ agglutinin (WGA).

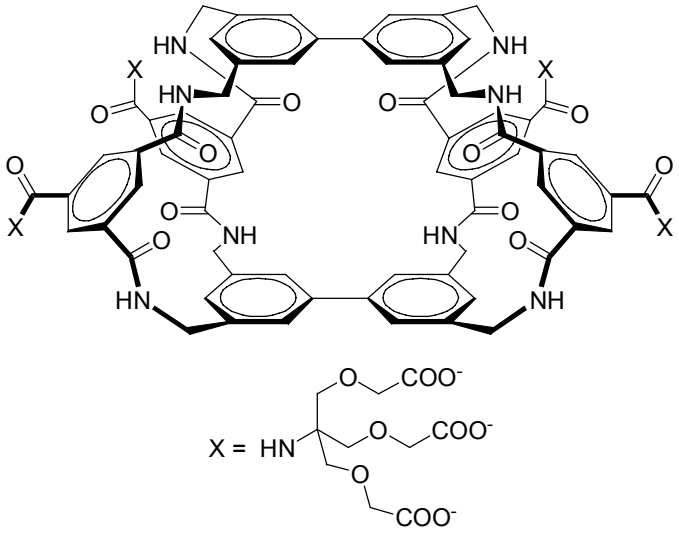

Figure 1.2 Non-boronic acid water-soluble lectin mimics by the Davis Group[120]

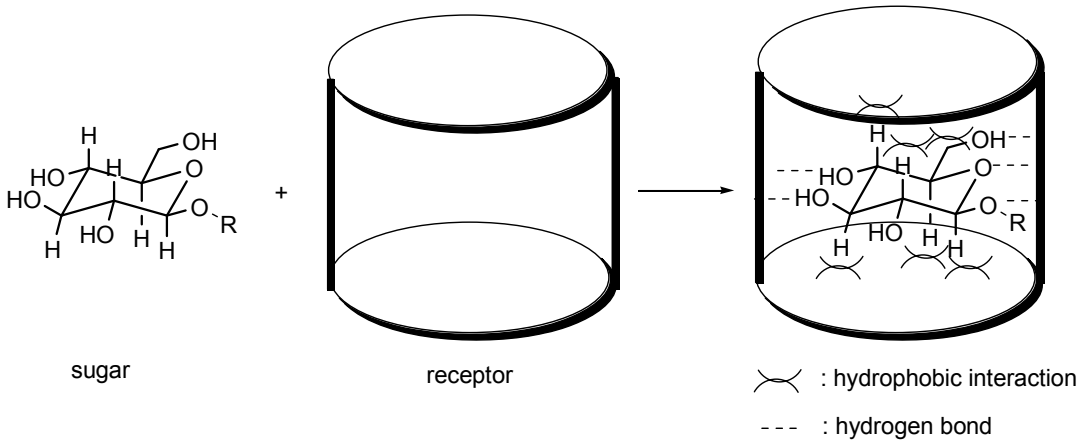

Scheme 1.1 Proposed interaction model between sugar and non-covalent receptors by the Davis group[116]

Meanwhile, there are many water soluble boronlectins designed, which have promise for potential biological applications in the future. The nature of biological studies and clinical diagnostics makes water solubility a primary requisite of sensing tools. Due to the widely spread effort in using boronic acid as a carbohydrate recognition motif from a great many active labs including that of Strongin, Shinkai, Czarnik, Anslyn, Lavigne, Heagy, Duggan, Hall, Asher, James, Wang, Lakowicz, Geddes, Norrild, Hindsgaul, Singaram, Tao, Lowe, Eggert, Smith, Okano, Taylor, Takeuchi, Ishihara, Katterle, Sporzynski, Freund, Mattiasson, Yoon, Scheller, Tuncel, Anzai, Houston etc,[122-123] it would be necessary to get a comprehensive understanding of the chemistry nature of boronic acid first.

The boron atom of boronic acid in its neutral form is in sp^2 hybridization status with 6 valence electrons forming 3 pairs in a trigonal plane and a vacant *p* orbital perpendicular

to it. Thus, the electron deficiency nature of boronic acid makes it a ready lone pair electrons acceptor to fill its open shell and achieve a stable octet state. Because of such unique electronic structural property of the boron atom, boronic acid has a high tendency to react with a Lewis base such as hydroxyl, amino, and carboxylate groups.[124-131] Boronic acids are also known to bind with simple Lewis bases such as fluoride[132-135] and cyanide.[136-137] All these features have stimulated great interest in utilizing boronic acid as a key functional group for designing receptors and sensors for carbohydrates,[138-143] hydroxyacids,[144-147] amino alcohols,[127,148-149] cyanide,[136-137] and fluoride.[132-135,150]

Among all the boronic acid sensor applications, we are particularly interested in the carbohydrate sensing area. In fact, boronic acid's specialty in the carbohydrate recognition field is widely acknowledged by chemists, especially due to its unique high affinity towards 1,2- or 1,3- carbohydrate diols. For a detailed discussion of boronic acid-carbohydrate complex formation, it will be helpful to begin with an illustration of several features of the boronic acid-diol interaction. Firstly, the acidity of a boronic acid arises differently from that of a conventional BrØnsted acid, which releases a proton. Taken phenylboronic acid (PBA, **1**, Scheme 1.2) as an example. In a protic solvent such as water or alcohol, solvent molecules will first react with boronic acid by donating lone pair electrons to occupy the boron *p* orbital, which converts the hybridization state of B from sp^2 to sp^3. The coordination complex will then release one proton to form an anionic tetrahedral phenylboronate (**2**, Scheme 1.2). Since the deprotonation of the boronic acid hydroxyl group is much harder (higher pK_a), the acidity of a boronic acid actually results

from its Lewis acidity *per se*. In an aprotic solvent, boronic acids act as a pure Lewis acid. For this reason, boronic acids are frequently used as Lewis acid catalysts and chelating agents for reaction controls in organic synthesis.[151] Secondly, the boronic acid is transformed to its corresponding boronic ester once it reacts with carbohydrate diol (**3**, Scheme 1.2). The driven force is partially due to the 5- or 6- membered ring formation, depending on whether it's 1,2- or 1,3- diols respectively. It should be noticed that the acidity of the boronic ester still remains due to the existence of the boron open shell. The boronic ester can react with a protic solvent molecule, release a proton, and generate the boronate ester anion (**4**, Scheme 1.2) much the same way as a boronic acid. Determined by the dihedral angles and ring strains of the formed complex, boronic ester acidity is also affected by the stabilizing energy of sp^3-boron accordingly. In most of the cases, boronic acids are more readily binding towards linear diols and diols on five-membered rings than diols on six-membered rings.[71] Exceptions do exist such as pinandiol,[152-154] which is a six-membered ring and binds boronic acid very tightly. The key is still the dihedral angle. Smaller O-C-C-O dihedral angles favor binding by driving the reaction equilibrium to forming more stable anionic boronate esters with tetrahedral geometry, making boronic esters usually more acidic than boronic acids. This also partially explains the reason for the high affinities that catechols display towards boronic acid. One useful method for determining boronic acid-diol binding constant using Alizarin red S (ARS) was developed by our group based on competitions,[155] which will be discussed later. Thirdly, because of the intrinsic Lewis acidity of both boronic acids and

boronic esters, it is conceivable that the boronic acid-carbohydrate binding affinity will be affected by boronic acid/diol pK_a values and solution pH. Most of the time, low boronic acid pK_a values and high pH conditions are commonly believed to favor binding.[126] However, this is not always the case. Optimal binding conditions involve the interplay of the pK_a values of the boronic acid and diol, solution pH, and the nature and concentration of the buffer solution.[114,126] It was found that the optimal binding pH is often between the pK_a values of the boronic acids and diols. For example, the optimal pH for the binding between ARS and a phenyl boronic acid is close to or below 7.4,[126,155] while in other cases of boronic acid-carbohydrate binding the preferred binding pH is within basic condition. Beside those, several other factors such as solvent system, buffer composition, temperature and steric hindrance can also affect intrinsic affinities of diols for a boronic acid. [114,125-126]

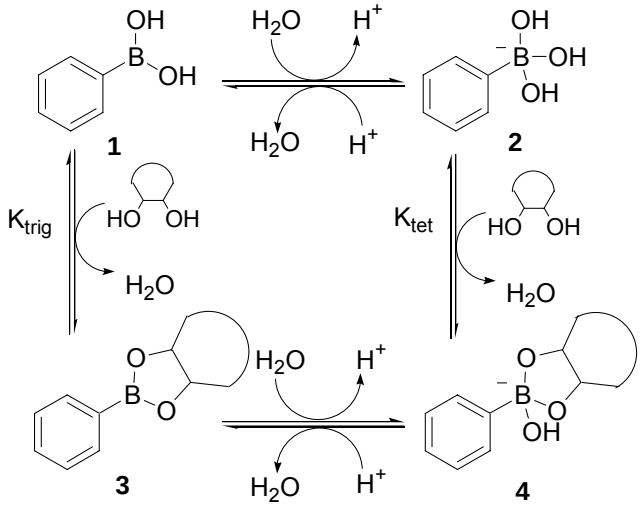

Scheme 1.2 Binding of phenylboronic acid with a diol

From the above discussions about boronic acid-diol binding, it is easy to see that with all the factors affecting the binding process, not all boronic acids have the same affinity toward a given diol and not all diols have the same affinity for a given boronic acid. Thus, for the design of boronic acid-based carbohydrate sensors, taking multiple factors as a whole picture into consideration with detailed analysis is required for building binders of high intrinsic affinity and selectivity with the best chance for success. For measuring and comparing the boronic acid-diol binding affinities, binding constant K_a or dissociation constant K_d is often used. However, in this case, binding constant K_a is really referred to as the apparent overall binding constant, K_{app}, which does not considerate the ionization states of boronic acids or boronic esters (Scheme 1.3).[125-126] From the overall binding equation, the real binding event happens among all four molecular forms as trigonal boronic acid **1**, tetrahedral boronate **2**, trigonal boronic ester **3** and tetrahedral boronate ester **4** (Scheme 1.3). Using either binding constant K_{trig} (equilibrium constant between the trigonal forms of boronic acid and boronic ester) or K_{tet} (equilibrium between the tetrahedral boronate form and boronate ester) will not be representative enough to describe the process in a general way.[114] To simplify the situation but not leaving out the essential information, an overall equilibrium to represent the binding between a phenylboronic acid and a diol is used without digging up the exact ionization status distribution of all forms. After all, K_{app} is directly related to the binding/dissociation equilibrium and informative enough for binding affinity evaluation.

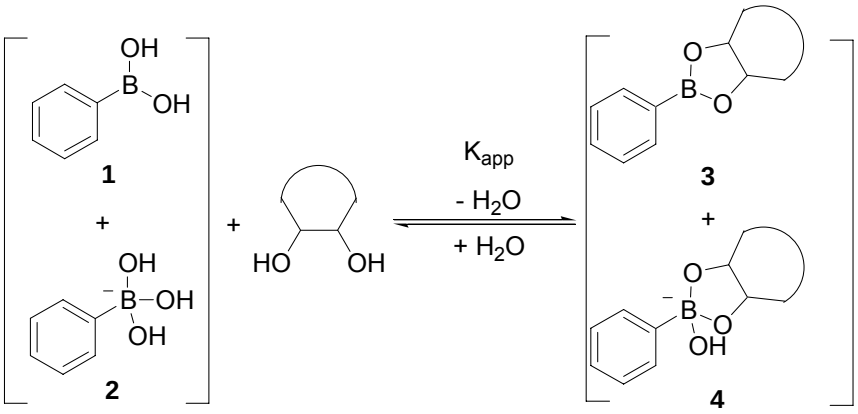

Scheme 1.3 Overall binding equilibrium of phenylboronic acid with a diol

In conclusion, this chapter has discussed about the basic chemistry of boronic acid and some fundamental features of boronic acid-diol binding process. Those background knowledge and information should have laid a good foundation of rational design and synthesis of boronic acid-based carbohydrate sensors.

1.2.2 Small molecular boronic acid sensors for carbohydrates

Due to the tremendous development in the glycobiology and glycomics areas, carbohydrate sensing represents an area of enormous biological importance, which requires a large number of tools that allow for high affinity and high specificity recognitions. Binders and sensors for such glycans are very useful as potential diagnostic tools and therapeutic agents. In the boronic acid-based carbohydrate sensing field, there have been hundreds of publications. Instead, the focus will be on key issues and approaches to consider in designing and selecting boronic acid sensors/binders for carbohydrates and catechols.

The ability for the boronic/boric acid group to bind “tightly” to carbohydrates was

recognized over a century ago. In the 1940's and 50's, there were a number of excellent papers examining such interactions in detail.[124,156-159] In the early 1990's Czarnik[138,160] and Shinkai[161] started the modern wave of interests and activities in using the boronic acid moiety for the design and synthesis of sensors/binders of carbohydrates. Now boronic acid-hydroxyl group interactions are probably the most widely used single pair functional group interactions in the design of sensors and "binders".[71,114,162]

In applying boronic acid-nucleophile interactions for the design of boronolectins, three factors need to be kept in mind: relatively low affinity, reversibility, and pH dependence. If these factors are not considered, one could be led to propose applications that have little theoretical chance of success. The pH dependence has been studied and reviewed extensively[71,114,126,163] and will not be discussed again. The reversibility in binding is ideal for sensor design where "regeneration" is necessary, but may not be desirable in other applications. As with any binding event, the "devil is in the detail," which is the binding constant. For example, the apparent binding constant between phenylboronic acid and glucose is only about 5 M^{-1} at near physiological pH.[163] For fructose, mannose, galactose, sialic acid, mannitol, and sorbitol, the apparent binding constants are 160, 13, 15, 21, 120, and 370 M^{-1} respectively. Such numbers are far greater than what can be achieved with single pair functional group interactions involving, e.g., hydrogen bond, ionic interactions, and ion-dipole interactions in an aqueous environment. However these numbers also mean that at below mM concentrations of these sugar, binding is minimal. Therefore, single boronic acid interactions are rarely useful as "sensors" except in rare cases[164] and with

boronic acids that have enhanced affinities.[165-166] On the other hand, the “bulk” properties of boronic acids can be used for crude separation purposes with one caveat that one has to keep in mind that the intrinsic affinity differences of a boronic acid for different carbohydrates may bias the results if one is not careful. When the boronic acid moiety is used in sensor/binder design for carbohydrates, inevitably additional interactions, either a second boronic acid or other groups, are needed for reinforcement of the interactions. Of course, the three-dimensional scaffold that holds the appropriate functional groups is also very important.

Another important issue in using boronic acid as the key recognition moiety for the design of lectin mimics (boronolectins) is the availability of boronic acids that change spectroscopic properties upon bindings. The incorporation of such spectroscopic reporter compounds allows for the generation of an intrinsic signal during binding and can greatly simplify detection. Along this line, many such reporter compounds have been reported.[161,167-178] Detailed discussions are not presented here. Readers are referred to several extensive reviews that have covered this topic very thoroughly.[71,114,179] In such an approach, also need to be considered are the wavelengths of the fluorophores, the requirement for large intensity changes for quantitation work, the requirement for the K_d to be comparable to the detection concentration, and covalent immobilization of the boronic acid in the solid-phase matrix. In this chapter, we would like to present a discussion of several small molecular boronic acid sensors for carbohydrate detection, most of which involved fluorescence change as reporting signal for binding evaluations.

Norrild reported a bisboronic acid-based sensor (**5**, Figure 1.3) capable of selectively binding glucose.[180] In this case, two pyridylboronic acids were functionalized at both sides of anthracene as the bisdentate recognition moieties. The positive pyridinium groups serve to increase both water solubility and binding affinity of the sensor at neutral pH. NMR studies showed that glucose was bound at the 1,2;3,5-OH positions in its α-D-furanose form by the sensor (Figure 1.3). The sensor showed about 1.9- and 1.8-fold fluorescence intensity increases upon glucose and galactose addition (10^{-5}~10^{-1} M, pH 7.4, λ_{ex}: 377 nm, λ_{em}: 427 nm), respectively, while fructose addition resulted in no more than 10% fluorescence intensity changes under similar condition. The glucose-sensor binding constant (K_a) was calculated to be 2.5×10^3 M^{-1} using this method.

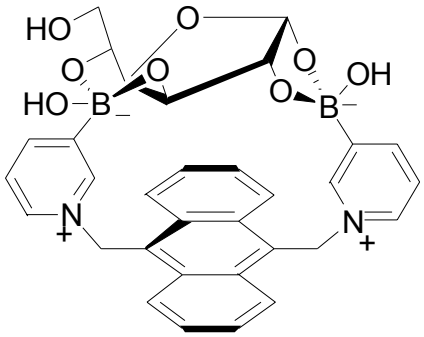

Glucose-**5** complex

Figure 1.3 Complex of bisdentate boronic acid **5** with α–D-furanose glucose 1,2;3,5-OH groups by Norrild

The Shinkai lab has successfully synthesized another boronic acid-based bisdentate glucose sensor (**6R** or **6S**, Figure 1.4), with chiral discrimination ability.[181] With a 1,1'-binaphthyl moiety as the chiral and fluophore building block, saccharide-boronic acid

binding could affect the fluorescence intensity through photoinduced electron transfer (PET) involving intramolecular boron-amine interactions. The mechanism of such interactions has recently been extensively studied.[172,182-183] Among the monosaccharides tested, D-glucose induced a maximum of 4-fold fluorescence intensity increase of **6R** while only a 2-fold increase was observed with L-glucose (10^{-5}~10^{-1} M, pH 7.77, λ_{ex}: 289 nm, λ_{em}: 358 nm). The situation was reversed with the **6S** form, in which L-glucose induced twice the fluorescence intensity increase than D-glucose. Similar phenomenon was observed with fructose. Mass spectrum results and binding constant calculation supported a 1:1-complex binding pattern. Competition studies showed that D-glucose could be recognized by sensor **6R** in the presence of L-glucose (10^{-3} M). Thus, it was concluded that selective chiral discrimination of monosaccharide enantiomers was achieved successfully in this case.

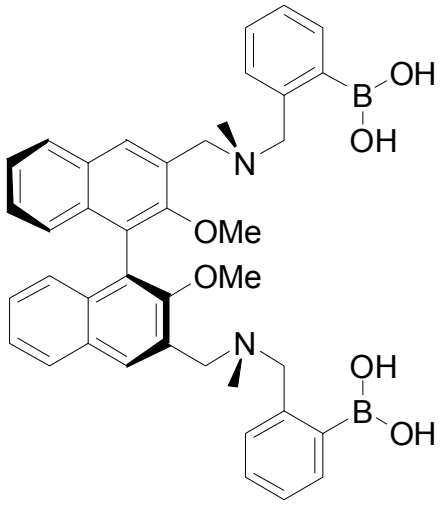

6R or **6S**

Figure 1.4 1,1'-Binaphthyl bisdentate boronic acid as chiral glucose sensor by Shinkai

The Lakowicz group has synthesized a series of *N*-(*o-, m-, p*-boronobenzyl)-6-methoxyquinolinium bromide (*o-, m-, p*-BMOQBA) (**7**, Figure 1.5) for potential tear glucose detection in contact lens.[184-185] Due to electrostatic interactions between the positively charged quaternary nitrogen and the negatively charged boronate ester upon sugar binding, fluorescence was observed to decrease by 12-15% in the presence of 2 mM glucose (λ_{ex}: 345 nm, λ_{em}: 450 nm, pH 7.5). These glucose probes were reported to have good water solubility, high quantum yields (Φ: 0.5), function near physiological pH and show color changes in the visible region. The author suggested that tear glucose (0.5~5 mM in diabetic patients, ~10 fold lower than blood glucose level) sensing would be favored for its non-invasiveness and continuous monitoring compared with traditional blood glucose monitoring methods.

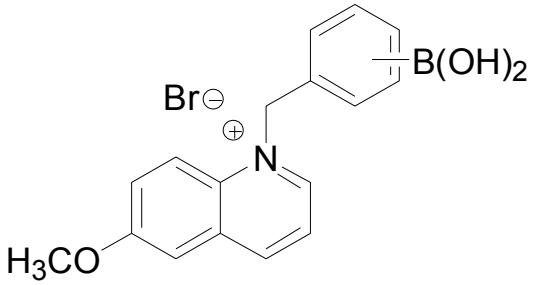

7, BMOQBA

Figure 1.5. *N*-(*o-, m-, p*-boronobenzyl)-6-methoxyquinolinium bromide **7** by Lakowicz

Among some of the computational chemistry-guided carbohydrate sensor design efforts, the most prominent example is the work of Drueckhammer,[186] which took a vector-based approach for the design of boronic acid-based sensors for glucose in its

pyranose form (Scheme 1.4) instead of the furanose form, which is the binding form with many other diboronic acid compounds reported in the literature.[141,180,187-192] The work started with the virtual “reaction” of glucopyranose with two phenylboronic acid moiety at the 1,2- and 4,6- positions. Then the system was subjected to quantum mechanics geometry optimization. The two phenylboronic acid moieties after optimization were considered as vectors to allow for the computational search, using the CAVEAT program, of rigid scaffolds that allow for the proper arrangements and orientation of these two boronic acid vectors for optimal complementarity. Compound **8** was an example candidate sensor for D-glucopyranose. As designed, **8** was able to bind D-glucose with high affinity and binding resulted in a decrease of fluorescence intensity. Indeed, the binding was in the pyranose form as demonstrated by ^{1}H-NMR. The selectivity of the sensor for D-glucose versus other saccharides including D-galactose, D-mannose, and D-fructose was also studied. The sensor showed at least a 400-fold higher affinity for glucose (K_d: 2.5×10^{-5} M) than for the two other saccharides, D-galactose (K_d: 1.0×10^{-2} M) and D-mannose (K_d : 1.6×10^{-2} M). The high selectivity for D-glucose was attributed to the proper scaffold of the sensor, which positioned the two boronic acid moieties complementary to the diol pairs of glucose. Compound **8** represents a very successful example of using *de novo* computational design for the construction of carbohydrate sensors. Very importantly, the same general approach should be applicable to the design of sensors for other saccharides and organic molecules.

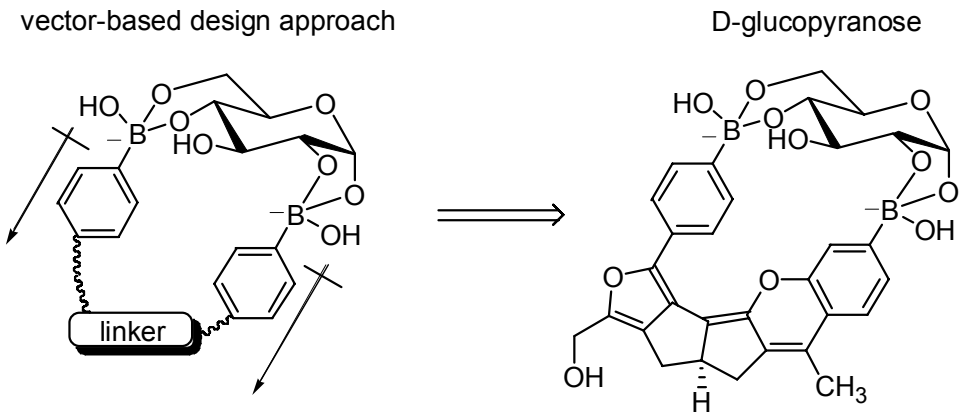

8

Scheme 1.4. Vector-based approach for the design of boronic acid-based sensor **8** for glucose in its pyranose form by Drueckhammer

Different from those carbohydrate sensors with boronic acids directly attached to fluorphores, Singaram and coworkers developed a bimolecular sensing system comprising an anionic fluorphore molecule and a boronic acid modified quencher seperately.[147,193-194] Inspired by the methyl viologen quenching fluorescence of 8-hydroxypyrene-1,3,6-trisulfonic acid trisodium salt (HPTS, Scheme 1.5), Singaram lab firstly developed the system by incorporating two boronic acid moieties into viologen quencher to make the 4,4'-*N,N'*-bis(benzyl-2-boronic acid)-bipyridinium dibromide (4,4'-*o*-BBV, Scheme 1.5) quencher.[193] It was proposed that the fluorescence quenching mechanism was mediated through electron transfer process between anionic HPTS and cationic viologen moiety complexed by electrostatic interactions (Scheme 1.5). Once carbohydrate binds to BBV, the tetrahedral anionic boronate formation will transform the viologen into zwitterionic neutral form, thus diminishing the HPTS-BBV electrostatic

interaction and reducing the fluorescence quenching process. It was reported that addition of glucose (360 mg/dL) could result in two fold fluorescence increase (λ_{ex}: 461.8 nm, λ_{em}: 511nm) of the 4,4'-*o*-BBV/HPTS (3×10^{-4} M/1×10^{-5} M, pH 7.4) solution (Scheme 1.5).[193] Further exploration of the BBV/HPTS was carried out through synthesizing a series of BBV analogues. Among them, 3,3'-*o*-BBV (Scheme 1.5) stands out for its remarkable selectivity for glucose (K_a: 1.9×10^3 M^{-1}) over fructose (K_a: 1.1×10^3 M^{-1}) and galactose (K_a: 1.8×10^2 M^{-1}) in pH 7.4 phosphate buffer.[147] It was suggested that the exceptional selectivity was achieved by binding one glucose molecule with both boronic acids on 3,3'-*o*-BBV in a chelating pattern. Besides, the low affinity of 3,3'-*o*-BBV towards lactate (K_a: 26 M^{-1}) makes it more desirable in clinical glucose detection.

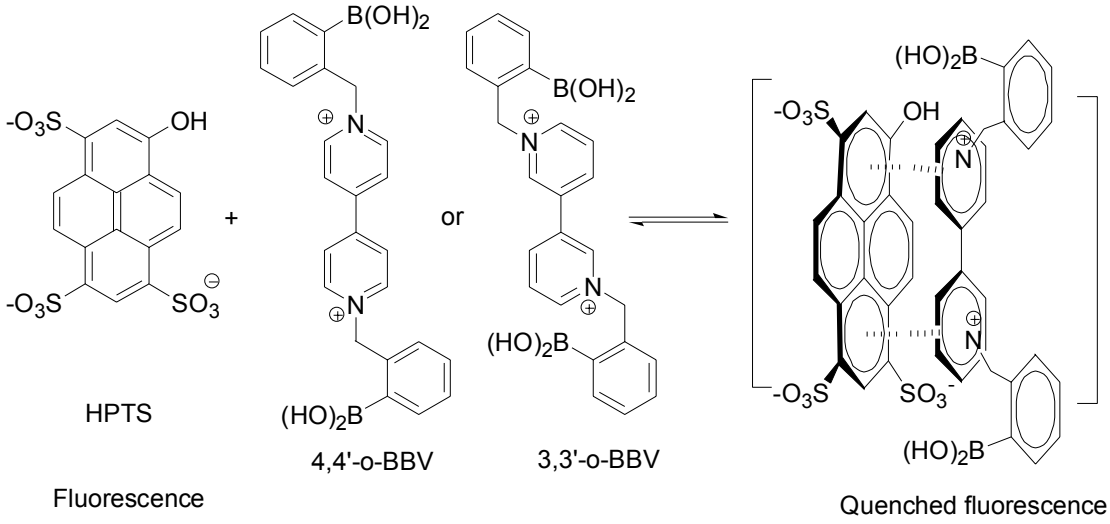

Scheme 1.5 Equilibrium of BBV quenching HPTS fluorescence

Another multiple-component system using boronic acids for carbohydrates detection was the before-metioned ARS system developed by Wang group.[155] In this case, ARS

was utilized as a separate fluorescent reporter and competitively binding toward a boronic acid in presence of carbohydrate analyte (Scheme 1.6). It was proposed that the boronic acid-ARS binding increases the ARS fluorescence intensity through removal of the fluorescence-quenching catechol diol protons. With a good water solubility of ARS (up to 10^{-3} M), addition of various arylboronic acids had induced about 20-80 fold of fluorescence intensity increase of ARS solution, accompanied with a visible color change from deep red to yellow at pH 7.4. Conceivably, carbohydrates competing with ARS for boronic acids could result in fluorescence decrease due to the disruption of ARS-boronic acid complex. It was reported that titrating of fructose into ARS/PBA (10^{-4} M/10^{-3} M) solution could induce 8-fold decrease of fluorescence intensity at 100 mM level. Using the three-component ARS system, the binding constant (K_a) between PBA and sialic acid was determined to be 21 M^{-1} (pH 7.4 in 0.1M phosphate buffer) by the Benesi–Hildebrand method.[195] Thus, it was demonstrated that a general fluorescent assay method has been established to determine the binding constant between a non-fluorescent boronic acid and target carbohydrate.

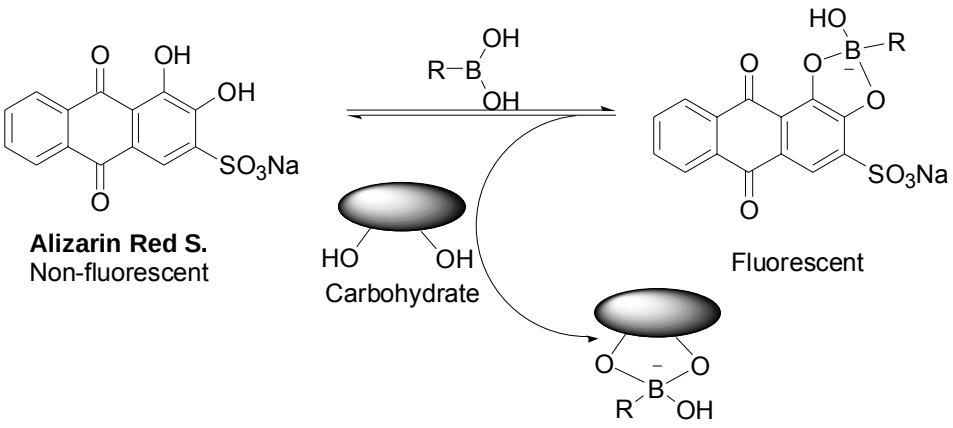

Scheme 1.6 Competitive binding of ARS and carbohydrate toward a boronic acid

Among all those carbohydrate detection by boronic acids in solution, some successful real-world application cases have been reported of using fluorescent boronic acid for cell surface glycan recognition. In the 1970s, Hageman and coworkers observed the interactions between boronic acid and cell surface glycans.[196-198] *m*-Aminobenzylboronic acid at 0.2 mM was found to inhibit sporulation of *Bacillis subtilis* without affecting its vegetative growth.[197] Since the culturing cells were highly clumped at later stage in the presence of a boronic acid and the sporulation inhibition could not be reversed by diluting the inhibitor, it was proposed that *m*-Aminobenzylboronic acid might bind to the cell surface carbohydrate through boronate ester formation. Later on, with fluorescent boronic acid **9** (Figure 1.6), *Bacillis subtilis* was visibly fluorescent labeled and the labeling could be reversed by mannitol solution.[196] In addition, it was found that another synthesized double-headed boronic acid **10** (Figure 1.6) was capable of agglutinating both type O human erythrocytes and sheep erythrocytes in similar

pattern.[196] It was proposed that the double-headed reagent agglutinate cells through cross-linking, acting in a similar way as lectins. All such results suggested that boronic acids can be used to bind cell-surface glycans.

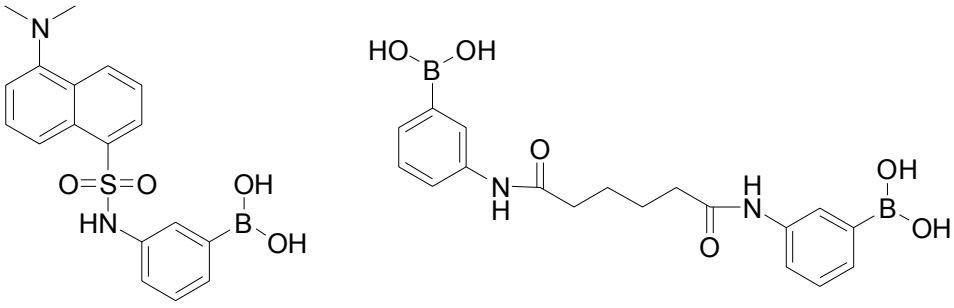

9 **10**

Figure 1.6 Cell surface binding boronic acids by Hageman

Promising cell-surface glycan binding results were reported of a bisboronic acid-based fluorescent sensor for selectively labeling sLe^x-expressing cells (Figure 1.7) by Wang and coworkers.[142,199] The design strategy was based on the idea that with a proper linker, two boronic acid moieties could be appropriately arranged to complement the diol/hydroxyl structures on sLe^x. Shinkai's anthracene-based boronic acid system was chosen as the fluorophore in this case, for it showed significant fluorescence intensity increases upon sugar binding.[161,200] Among all the linkers chosen, *para*-disubstituted phenyl ring **11a** (Figure 1.7) showed the best binding and selectivity for sLe^x. Fluorescent cell labeling studies showed that **11a** selectively labeled sLe^x expressing HEPG2 cells while non-expressing COS7 cells and Lewis Y (Le^y, Figure 1.7) expressing HEP3B cells were not labeled. HEPG2 cells treated with neuraminidase and

fucosidase resulted in significantly decreased labeling, indicating that both the fucose and sialic acid residues were required for **11a** labeling of HEPG2 cells. A control bisboronic acid (**11b**) showed no similar labeling. Small molecule lectin mimics such as **11a** can be very useful for cell-specific delivery of imaging and therapeutic agents.

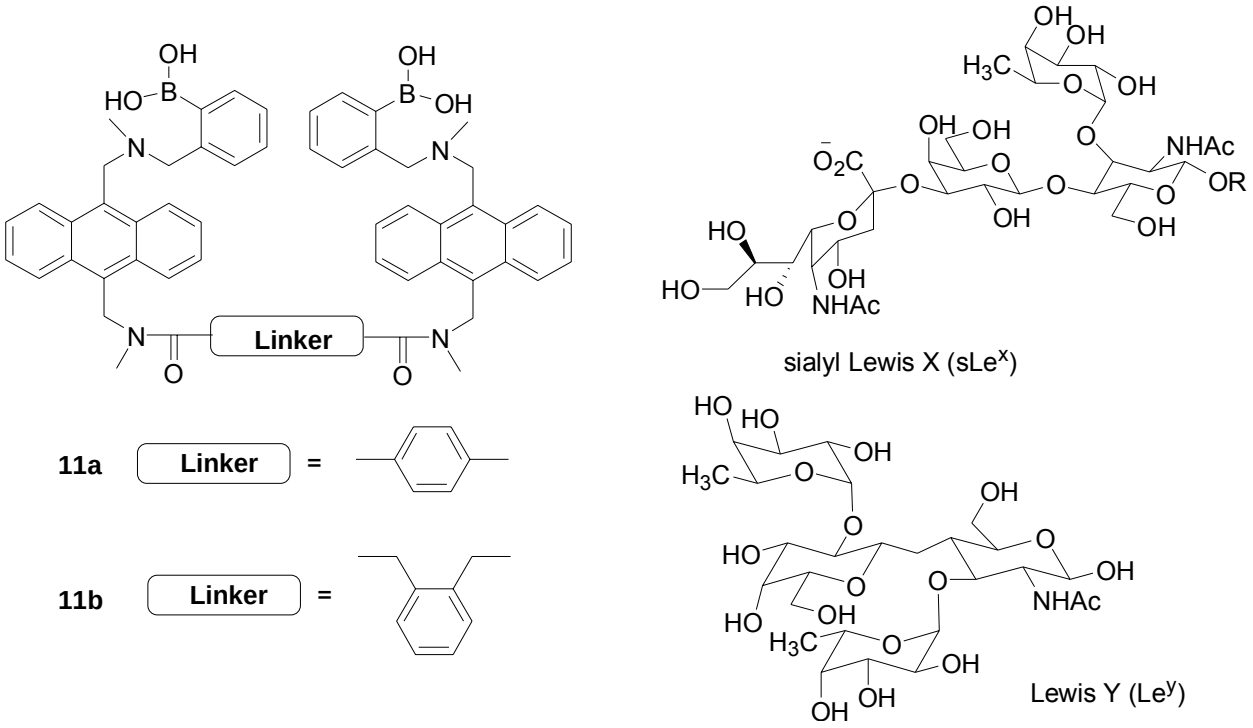

Figure 1.7 Bisboronic acids **11a** and **11b** by Wang for sialic Lewis acids binding

1.2.3 Conclusion

In conclusion, based on the fundamental chemistry knowledge of boronic acids, all the successful cases of carbohydrate detection using small moleculr boronic acids show a promising scenario of further exploring its application. Nevertheless, one of the most important contemporary challenges in using boronic acids for the design of carbohydrate sensors is in the selection of the appropriate scaffold to position the boronic acid and

other functional groups in appropriate places and orientations in order to afford the necessary specificity and affinity. Single boronic acid-diol interaction by itself is too weak to lead to high affinity and selectivity. The situation was improved somehow with bisboronic acid sensors with proper positioning of the bisdentate moieties. However, finding a good sensor is a very chance-dependent case and so far only a limited number of such applications have been reported. Meanwhile, complementing to the rational *de novo* design approach of small molecular boronic acid sensors design, template-directed synthesis and combinatorial library approaches could overcome the problem to some extent, since no detailed structural information of the analytes are required in buiding those polymer-based boronic acid sensors.

1.3 Boronic acid sensors based on non-biopolymers

1.3.1 Brief introduction of polymer-based boronic acid sensors

In general, there are two classes of polymer-based boronic acid sensors, non-biopolymers and biopolymers. Biopolymers like polypeptides and oligonucleotides serving as scaffold for boronic acid positioning are often created through a combinatorial approach to yield a large molecular library with high diversity, which is later screened against carbohydrate analytes to select proper “binders”. In contrast, non-biopolymer-based boronic acid sensors are usually generated through two other strategies. The first one involves self-assembled monolayer (SAM) functionalized with boronic acid moieties as glycan trap. This method is often coupled with highly-sensitive detection techniques such as quartz crystal microbalance (QCM)[201] or surface plasma

resonance (SPR).[202] The second approach to construct carbohydrate sensors/binders is template-directed synthesis such as molecular imprinting technique, which has the desired feature of not requiring prior knowledge of the carbohydrate 3-dimensional structures. Details of each approach are discussed in the following sections.

1.3.2 Self-assembled monolayer (SAM)-based boronic acid sensors

Boronic acid-based SAM was constructed by the Fernandez group as an affinity-trap for glycoprotein horseradish peroxidase (HRP) detection.[201] Gold film surface was first coated with 6,8-dithioctic acid, which was then linked to 3-aminophenyl boronic acid (Figure 1.8). Presumably, in binding the carbohydrate moieties of HRP were brought into the proximity of the boronic acid groups through multiple weak interactions. In QCM tests, addition of glycosylated HRP caused a ~17 Hz frequency decrease while deglycosylated HRP only caused a less than 2.5 Hz decrease. The 7-fold difference indicated that the adsorption on boronic acid-based SAM trap was mediated and differentiated based on the saccharide portion.

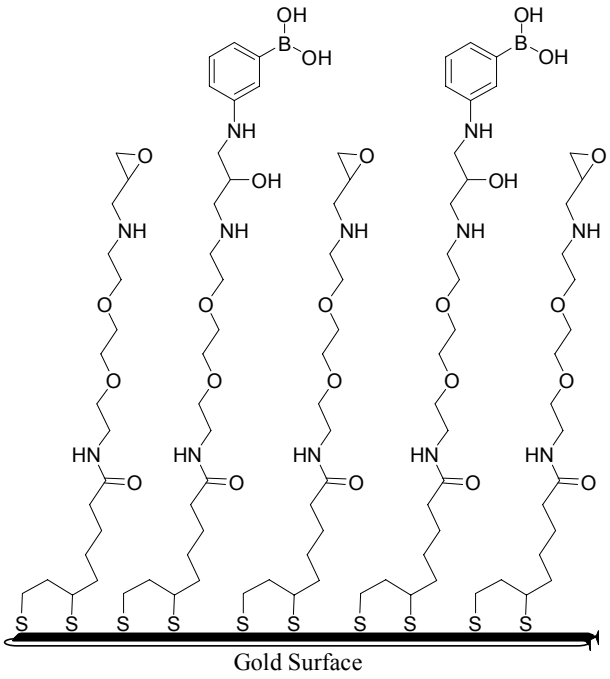

Figure 1.8 Boronic acid-based SAM glycoprotein trap by Fernandez

SPR was used by the Chen group for glycoprotein detection using boronic acid SAM.[202] Glycated hemoglobin HbA1c, formed by non-enzymatic glycation of the hemoglobin β chain with glucose on the *N*-terminal valine, was chosen as the target because its level can be used as a clinical indicator for chronically elevated sugar level in diabetic patients. Gold surface was coated with dithiobis(4-butylamino-m-phenylboronic acid) (DTBA-PBA) SAM. The SPR results showed that the detection limit of HbA1c was 0.01μg/ml and good linear regression was obtained in the concentration range from 0.43 to 3.49 μg/ml (pH 9). Compared with traditional tests,[203-204] this method showed approximately a 1000-fold increase in sensitivity. The SPR sensitivity could be improved another 5-fold by adding a Lewis base when HbA1c concentration was lower than 50 nM.

Thus, both high sensitivity and specificity of HbA1c sensing were achieved using this DTBA-PBA-SAM-SPR method.

1.3.3 Molecular imprinted polymer boronic acid sensors

Among the different template-directed synthesis approaches, molecular imprinting is especially useful in creating receptor sites for organic molecules including carbohydrates. Molecular imprinting is a technique first demonstrated in the late 40's by Dickey.[205] It involves 3 steps including: 1) mixing the template/analyte with the functional monomers and cross linkers at low temperature to allow for complementary intermolecular interactions; 2) polymerization of the monomers and cross linkers under mild conditions; and 3) extraction of the template molecules from the polymers, which leaves behind polymeric sites with memories of the template molecules in terms of size, shape, and functional group orientations (Scheme 1.7). This technique has been used for the preparation of selective recognition sites for a wide variety of molecules.[206-208] Naturally, the same method has been used for the preparation of sensors,[209] including boronic acid-based carbohydrate sensors.

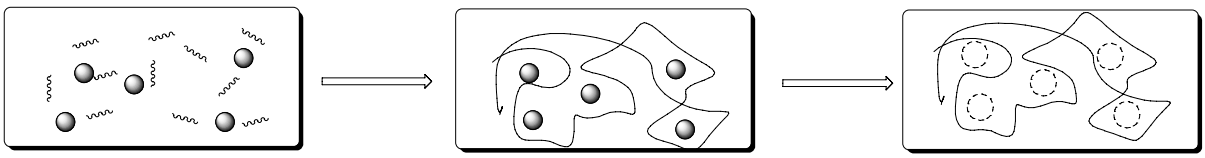

Scheme 1.7 Molecular imprinting process

Wulff first demonstrated the use of boronic acid compounds in molecular imprinting for the construction of polymeric cavities specific for certain saccharides.[210] D-fructose and D-galactose were used as the template compounds. Specifically, these sugars were first conjugated with 2 equivalent of VPB ((4-vinylphenyl)boronic acid), presumably at 2,3;4,5-OH of fructose and 1,2;3,4-OH of galactose, to yield their respective polymerizable monomers. EGDMA (ethylene glycol dimethacrylate) was used as the cross linker. The polymers prepared were shown to have “memories” of the template including stereochemical features. For example, the D-fructose-imprinted polymer could differentiate the D-form from the L-form by a factor of 1.47-1.63. It is interesting to note that the D-fructose- imprinted polymer could also differentiate L-galactose from D-galactose by a factor of 1.17 while D-galactose-imprinted polymer could differentiate L-fructose from D-frucose by a factor of 1.25. It was proposed that the high similarity between D-fructose and L-galactose as well as L-fructose and D-galactose in terms of their spatial hydroxyl group arrangements was responsible for the observed cross reactivities.

Using the same imprinting principle, the Wang lab was the first to synthesize boronic acid-based fluorescent polymers for saccharides as potential fluorescent sensors.[211-212] In such studies, a polymerizable boronic acid monomer (**12**) was prepared (Figure 1.9). The anthracene-based boronic acid unit in **12** is known to increase fluorescent intensity upon sugar binding as reported by the Shinkai lab.[139,213] The monomer was first reacted with D-fructose to form a covalent complex before polymerization in the presence of

EGDMA as the cross linker. In re-binding studies, the fructose-imprinted polymer showed significant fluorescent intensity changes (over 100%) upon fructose addition. This polymer also showed preference for D-fructose over D-glucose and D-mannose, which was at least twice as large as that determined with the control boronic acid alone.

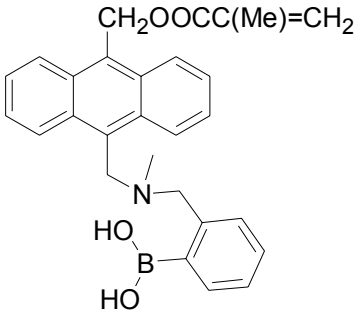

12

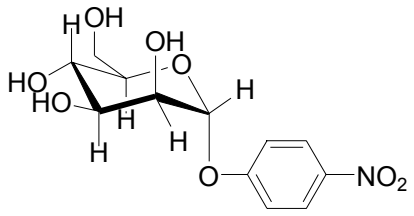

4-nitrophenyl-α-D-mannopyranoside

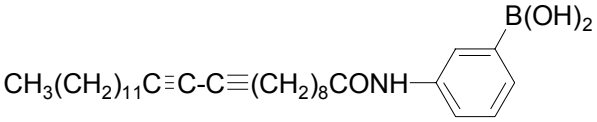

13a

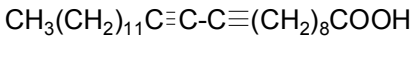

13b

Figure 1.9 Boronic acid monomer **12, 13a,** cross-linker **13b** and 4-nitrophenyl-α̃-D-mannopyranoside

In yet another example, Kurihara and coworkers[214] conducted surface imprinting of 4-nitrophenyl-α-D-mannopyranoside with a polymerizable phenylboronic acid monomer, (3-(10',12'-penta-cosadiynamido)phenylboronic acid) **13a** and cross-linker **13b** (Figure 1.9). 4-Nitrophenyl-α-D-mannopyranoside (Figure 1.9) was used as the template molecule and the 4-nitrophenoxy group can be used to quantify the binding by UV-visible spectroscopy. In re-binding studies using both imprinted and control polymers, about

75% the binding sites of the imprinted surface were occupied by the template, while about 57% of the non-imprinted surface was covered. This implied that the imprinted monolayers had an improved affinity for the template molecule.

Molecular imprinting technique is also used in developing boronic acid-based electrochemical sensors. Usually, thick imprinted polymer layer on the electrode surface is unfavorable since it hinders analytes diffusion and retards polymer-electrode communication. The problem can be partially overcome by utilizing thin layer polymer film electropolymerization on electrodes or on the gate surface of an) device through radical polymerization.[215-217] In such cases, the barrier of analyte diffusion and electrical contact is minimized. In this regard, the Willner group reported the copolymerization of acrylamide-acrylamide- phenylboronic acid on TiO_2 film for imprinting AMP, GMP and CMP.[217] Charging the boronic acid polymer membrane with nucleotides controlled the gate potential of the ISFET to allow for detection of each nucleotide. Similar thin layer boronic acid polymers were constructed by the same group towards various nucleotides and monosaccharides on Au electrodes, piezoelectric Au quartz crystals, or on the gate surface of ISFET device.[215] Faradaic impedance spectroscopy measurement showed enhanced selectivity for the template molecules by increasing the cross-linking degree of the polymer. Most recently, the same group reported fabrication of stereoselective and enantioselective imprinted polymer for monosaccharides such as D-glucose and D-mannose.[216] The co-electropolymerization of phenol with a 3-hydroxyphenyl boronic acid-monosaccharide complex on Au support created a thin film of boronate-conjugated

polyphenol layer coated electrode (**14**, Figure 1.10). Competitive electrochemical assay was carried out by measuring the amperometric responses using ferrocene modified-monosaccharides (**15**, Figure 1.10) as the redox labels to analyze each saccharide's binding affinity. The observed stereoselectivity and enantioselectivity indicated that rather delicate structural contour was constructed around saccharide template with boronic acid and other motifs accommodating the hydroxyl groups in a delicate coordination way.

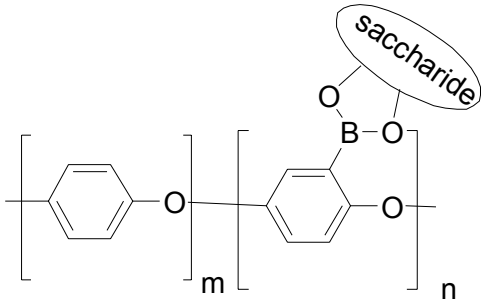

14

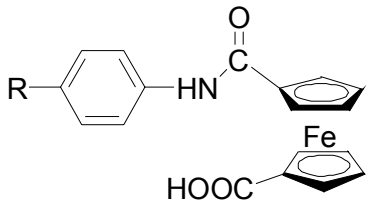

R= D-Glu, D-Man, D-Gal

15

Figure 1.10 Boronic acid-contained polyphenols **14** and ferrocene-monosaccharide redox labels **15**

Flow calorimeter was used by the Scheller group[218] to study the interactions of phenylboronic acid-based polymers imprinted with fructosyl valine (Fru-Val), fructose and pinacol, respectively. Fru-Val is known as the *N*-terminal glycated amino acid on glycosylated hemoglobin (HbA1c) (HbA0 is the non-glycated hemoglobin). The imprinted polymer for Fru-Val was prepared by copolymerizing the complex of Fru-Val and VPB

with cross linker TRIM (trimethylolpropane trimethacrylate). An exothermic peak signal was observed when Fru-Val flew through the imprinted polymer in a thermistor. This was followed by an almost steady state signal. The intensity of the peak signal increased in response to Fru-Val in a concentration- dependent manner (up to 5 mM). Control polymer prepared from the pinacol-VPB complex in the same way didn't give such significant signal changes. The apparent imprinting factor (IF), the ratio of binding with imprinted polymer to that with the control polymer at equilibrium, was determined as 41 by measuring the signal intensity ratios. The temperature increase induced by Fru-Val interactions with imprinted polymer was 2.4-fold higher than that of fructose-imprinted polymer interactions and 270-fold higher than that of Val-imprinted polymer interactions. Thus, a selective Fru-Val MIP sensor was developed and used in calorimeter measurements.

1.3.4 Conclusion

In conclusion, boronic acids have very unique properties and can be used as a key functional group in the construction of polymer-based sensors/binders for carbohydrates or glycans. Non-biopolymer sensors functionalized with boronic acids have been reported through either self-assebling monolayer (SAM) technique or template directed synthesis. Neither of these strategies requires prior knowledge of the analytes' detailed structural information. Which SAM-based boronic acid sensors primarily rely on sensitive detection methods such as SPR or QCM, more detection methods are available for evaluation of molecular imprinted boronic acid polymer sensors such as spectroscopic,

electrochemical and flow calorimetric methods.

1.4 Boronic acid sensors based on biopolymers

1.4.1 Brief introduction of biopolymer-based boronic acid sensors

Though the discussion of template-directed boronic acid-based sensor work has been focused on non-biopolymers, one should not feel restricted by this. Such an approach is in line with dynamic combinatorial library work, which has been proven useful.[219-223] For example, one could envision the linking of two boronic acids through a tether in a library consisting of multiple boronic acids and linker species. Such a library could give a large number of bisboronic acid end products. Using combinatorial chemistry to create a library and then screening the library against the target analytes to select binders, the library synthesized can be either small molecular ligands,[117,224-225] peptide-based boronic acid library (PBLs),[226-230] or nucleic acid-based boronic acid library (NBLs).[231-232] Similar with the non-biopolymer version, the biopolymer-based boronic acid sensors design doesn't need prior knowledge of the structural and conformational information of the carbohydrates either. Besides, the chemical synthetic approaches of biopolymers such as peptides and nucleic acids are very mature and well-established techniques, which provide more convenience and promise in their libraries construction. Furthermore, the biological nature of peptides and nucleic acids also has the implication that such types of boronic acid sensors could possibly be generated through enzymatic approaches *in vitro*[231] or through cellular machinery *in vivo*.[233]

1.4.2 Peptide based boronolectin

Recently, there have been some efforts in developing libraries of peptide-based boronolectins (PBLs), which offer the chance of searching for binders through combinatorial/diversity-based approaches. Along this line, the labs of Anslyn,[226] Hall,[228] Duggan,[229-230] and Lavigne[227] have independently made significant contributions.

In the work from the Anslyn group, arrays of boronic acid derived pentapeptide receptors (**16**, Figure 1.11) were constructed for saccharide sensing.[226] The pentapeptide receptors were selected from a random pool of a synthesized library. The binding affinity of each resin-bound receptor (RBR) was evaluated colorimetrically using an indicator displacement method first developed in the Anslyn lab. In this case, bromopyrogallol red (BPR) was chosen as the indicator and Linear Discriminant Analysis (LDA) was used to process BPR-uptaking data to identify receptor-analyte binding patterns. Collectively, the unique pattern of each PBL receptor in the chemosensor array successfully differentiated monosaccharides from disaccharides, and discriminated isomers within each group. Sucrose and maltose were also differentiated from their low-calorie counterpart (sucralose and maltitol). Furthermore, sucralose was identified successfully in Splenda sweetened tea using the same chemosensor array chip with the LDA data set. It was reported as one of the first assays that supramolecular pattern-based sensors identified a sweetener in a real world beverage sample.

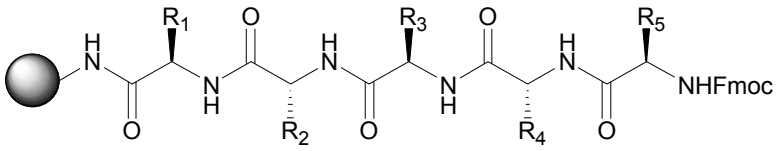

16 R_1-R_5 = side chains of natural amino acids and boronic acid modified side chain

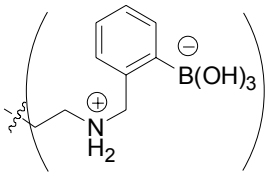

Figure 1.11 PBL library **16** by Anslyn

Hall and coworkers have developed a triamine-derived triboronic acid library[228] using the combinatorial split-and-pool strategy.[234-236] The triamine backbone was synthesized with tripeptides as the starting point, followed by exhaustive reduction of the amide group to amine and functionalization of the amine with phenylboronic acid (**17a**, Figure 1.12). Lewis-b (Le^b) tetrasaccharide, which is a type of cell surface oligosaccharide commonly expressed on bacteria, red blood cells or tumor cells, was chosen as the binding target.[107,237] Though the study did not yield strong binders, this was an example of proof-of-concept that a library of receptors containing more than two boronic acid units was constructed in a controlled manner and individual library members were successfully characterized by HPLC and ESI-MS after cleavage. Thus, it has the potential for future optimization and application in screening against saccharides for high affinity and selectivity recognition. In addition to this example, a resin-to-resin transfer reaction (RRTR) (of arylboronic acid) was developed by the Hall group and could also be used in PBL library construction in the future.[238]

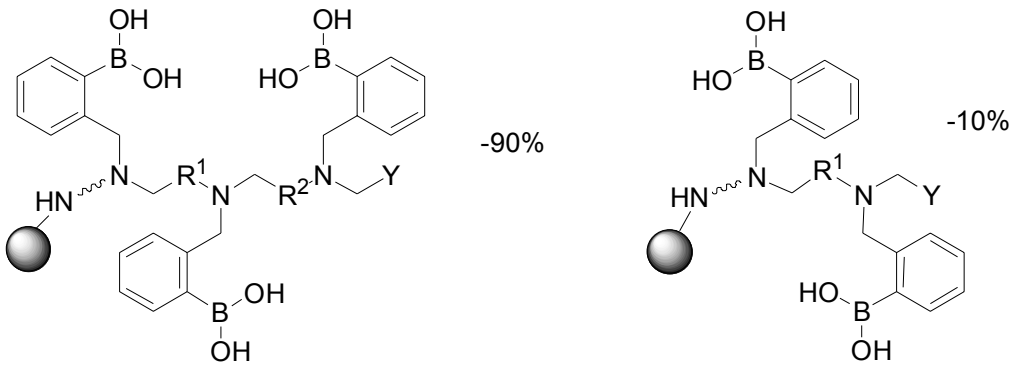

17a (90%) **17b** (10%)

289 members

Figure 1.12 PBL library **17a** and encoding moiety **17b** by Hall

Duggan and co-workers also prepared solid-supported PBL libraries derived from 4-borono-L-phenylalanine (BPA, **18**, Figure 1.13).[229-230] The pentapeptide-based bisboronic acids including a 'lysine series' and an 'arginine series' (Table 1.1) were tested for their affinity toward various monosaccharides using competitive binding assay against Alizarin Red S (50% methanol/50 mM $NaHCO_3$, pH 10.7), first developed by the Wang lab.[163,239] It was hypothesized that the positively charged Lys and Arg residues could enhance boronic acid-diol binding by ion-pairing with negative-charged boronate esters. Test results showed that optimal binding towards fructose and glucose was achieved when two BPA units were adjacent or separated by one amino acid residue; *e.g.*, the tightest D-glucose binding sequence was Arg PBL 1 (K_a: 3641 M^{-1}) and the tightest D-fructose binding sequence was Lys PBL 12 (K_a: 4162 M^{-1}). While Arg PBL 4 and 6 showed an 8.3- and 5.4-fold preference for D-fructose binding, Lys PBL 8 showed a 2.1- fold preference for D-glucose binding. More interestingly, in chiral discrimination

binding studies, Arg PBL 4 displayed an 8.4-fold preference for L-glucose while Lys PBL 12 showed a 4.3-fold preference for D-glucose. Thus, it was clearly demonstrated that affinity and selectivity of PBL binding towards saccharide could be greatly influenced and finely tuned through peptide backbone modifications. The requirement of the PBA residues to be close to each other to achieve high specificity might also suggested that binding was a well coordinated and cooperated process.

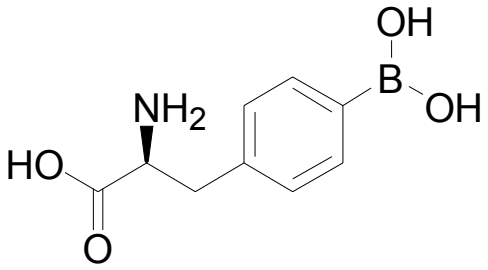

18, *p*-boronophenylalanine

Figure 1.13 Structure of *p*-boronophenylalanine **18**

Table 1.1 Amino acid sequences of Arg series (1-6) and Lys series (7-12) PBLs by Duggan

1	N-Ac-BPA-BPA-Ala-Arg-Arg-AHA-SS
2	N-Ac-BPA-Arg-BPA-Ala-Arg-AHA-SS
3	N-Ac-BPA-Arg-Arg-BPA-Ala-AHA-SS
4	N-Ac-BPA-Arg-Ala-Arg-BPA-AHA-SS
5	N-Ac-Arg-BPA-BPA-Arg-Ala-AHA-SS
6	N-Ac-Arg-BPA-Arg-BPA-Ala-AHA-SS
7	N-Ac-BPA-BPA-Ala-Lys-Lys-AHA-SS

8	N-Ac-BPA-Lys-BPA-Ala-Lys-AHA-SS
9	N-Ac-BPA-Lys-Lys-BPA-Ala-AHA-SS
10	N-Ac-BPA-Lys-Ala-Lys-BPA-AHA-SS
11	N-Ac-Lys-BPA-BPA-Lys-Ala-AHA-SS
12	N-Ac-Lys-BPA-Lys-BPA-Ala-AHA-SS

*AHA=6-aminohexanoic acid, SS= solid support.

Lavigne and coworkers have synthesized a PBL library on aminomethyl PEG-PS resin and demonstrated its applications in cancer related glycoprotein detection.[227] A 12-mer PBL library with a sequence of Cbz-A-$(X)_{10}$-A-resin (A: alanine, X: 2,3-diaminopropanoic acid, 2,4-diaminobutanoic acid, ornithine, lysine, or alanine) was synthesized using the split-and-pool method,[235-236,240-241] and 2-formylphenylboronic acid was coupled to the side chain amine through reductive amination. Fluorescein isothiocyanate (FITC)-labeled glycoproteins, including ovalbumin (Oval), bovine submaxillary mucin (BSM), and porcine stomach mucin (PSM), were incubated with the resin-bound PBL library in the presence of 1% BSA (bovine serum albumin) and 10% glycerol. Using microscopic image screening, beads selective for Oval and BSM, partially cross-reactive for both BSM and PSM, and completely cross-reactive with all glycoproteins were observed. In contrast, non-PBL resin did not bind any glycoprotein and non-glycosylated protein BSA did not significantly bind any beads. Such control

results indicated that the binding process was PBL- and saccharide-dependent. Inclusion of PBL resin beads in microtiter plate arrays generated specific color patterns for binding Oval, BSM and PSM. Thus, although no individual PBL bead was isolated and characterized, the general results described illustrated the potential of this PBL-resin array in future diagnostic applications in selective glycoprotein detection.

Different from the above PBLs synthesized through combinatorial chemistry, Schultz and coworkers developed a method for producing boronate containing protein through site-specific incorporation of genetically encoded BPA (**18**, Figure 1.13) in *E. coli*.[233] An orthogonal tRNA/aminoacyl-tRNA synthetase (aaRS) pair encoding BPA was generated through altering the specificity of *Methanococcus jannaschii* (*Mj*) derived amber suppressor tyrosyl tRNA (*Mj*tRNA$^{Tyr}_{CUA}$)/tyrosyl- tRNA synthetase (*Mj*TyrRS) pair. Expression experiment results showed that protein was only produced in the presence of BPA by *E. coli* with plasmid containing *Mj*tRNA$^{Tyr}_{CUA}$ and evolved BPA-tRNA synthetase. The expressed boronate-containing protein was characterized by ESI-MS. The protein was able to bind polyhydroxyl compounds such as glucamine and sorbitol through boronate ester formation. In fact, it was also proposed that intramolecular serine-boronate crosslink was formed in the protein based on the crystal structure of previously reported original protein and the ESI-MS of the boronate protein. In fact, boronate ester formation of the protein with polyhydroxylated compound was so significant that one-step scarless affinity purification of the boronate protein was achieved with *N*-methylglucamine conjugated resin. Thus, it was proposed that this

technology could be applied in the development of boronate containing antibody for glycoprotein detection or *in vivo* labeling of boronate protein with polyhydroxylated reporters.

1.4.3 Nucleic acid based boronolectin

In the area of nucleic acid-based lectin mimics, there have been extensive activities. For example, the Yu group developed unmodified RNA aptamers for oligosaccharide (sLe^x) detection;[242] the Anslyn group developed unmodified RNA to fine-tune the selectivity of an existing small molecule carbohydrate receptor.[232] The aptamers selection process followed essentially those SELEX (systematic evolution of ligands with exponential enrichment) techniques first developed by the labs of Szostak, Joyce, and Gold.[243-245] Recently, the Wang lab has successfully developed a boronic acid-modified TTP analogue (B-TTP) that can be enzymatically incorporated into DNA sequence, and discussed its potential application for aptamer selection in glycoprotein detection and differentiation.[71,231]

The Anslyn lab[232] used unmodified RNA aptamers to tune the selectivity of a boronic acid-based receptor with great success. For example, bis-boronic acid **19** (Figure 1.14) by itself was known to bind citrate (K_d: 5.5 $\times 10^{-6}$ M^{-1}) slightly better than tartate (K_d: 7.1 $\times 10^{-6}$ M^{-1}). The immobilized bis-boronic acid receptor **20** on glyoxal agarose beads (Figure 1.14) was subjected to an RNA pool (N50) SELEX in the presence of 200 μM tartate. Negative selection was performed on the RNA pool against the immobilized tris-amine beads **21** as blank control (Figure 1.14) before each round of SELEX to

increase the selection specificity. The RNA binding to the complex of receptor-tartate became dominant in the pool from the 7th round. In radio-labeled binding assays, all seven families of the cloned RNA aptamers showed their preference of binding the receptor-tartate complex (from 12 to 25%) to the receptor alone (<7%). One specific sequence was used in the fluorescence binding test of receptor towards analytes. In the presence of this aptamer, the receptor was able to bind tartate with K_d of 2.1 $\times 10^{-4}$ M^{-1} while no binding to citrate was observed (K_d >3 $\times 10^{-3}$ M^{-1}). Thus, the selectivity of the bis-boronic acid was tuned to at least 14-fold higher for binding tartate than citrate in presence of the selected aptamer. In comparison, the receptor had a 1.3-fold higher for citrate than tartate in the absence of aptamer.

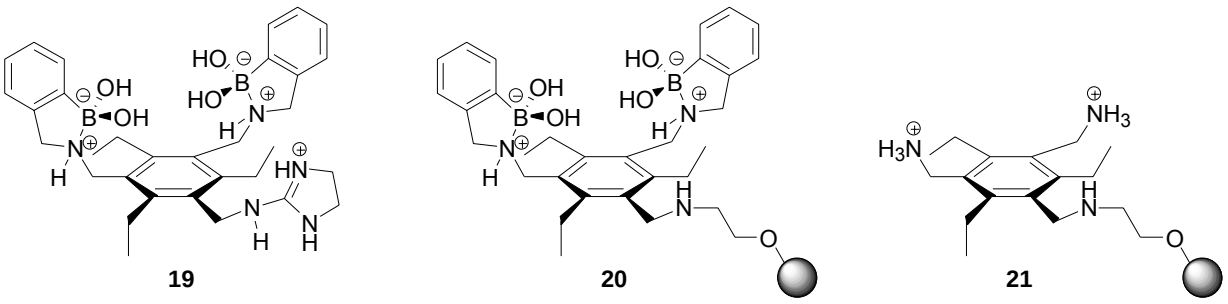

Figure 1.14. Bis-boronic acid **19**, its immobilized form **20** on glyoxal agarose beads and blank control tris-amine beads **21** by Anslyn

Based on the general aptamer selection method developed about 18 years ago by the labs of Szostak, Joyce, and Gold,[243-245] the Wang lab are on the effort of developing a methodology of using boronic acid modified DNA to select aptamers that can recognize

an intact glycoprotein with the ability to differentiate glycosylation variations. This was achieved through the incorporation of a boronic acid modified thymidine moiety (B-TTP, Figure 1.15) into the DNA sequences.[246] Because of the intrinsic affinity of boronic acids for carbohydrates, the hypothesis was that the incorporation of the boronic acid moiety would allow for the aptamer selection process to gravitate toward the “sweet spot” (glycosylation site) and therefore allow for distinction of glycosylation variations. In another word, this method of using boronic acid-modified DNA allows for the selection to go after the “sweet spot.” The boronic acid moiety was functionalized with a terminal azido group and attached to the linear linker at 5-position of thymidine triphosphate via Cu(I)-catalyzed azido-alkyne cyclization (CuAAC) reaction.[247-249] It was demonstrated that B-TTP can be successfully recognized by DNA polymerase as substrate and incorporated into elongating DNA sequence. Both MALDI-MS and gel electrophoresis results support completion of full length DNA polymerization using B-TTP in place of natural TTP in reaction. Further experiment showed that DNA polymerization and amplification using boronic acid-labeled DNA as template was achieved with no noticeable difference from using natural DNA template. Thus, it is not surprising that PCR amplification of DNA using B-TTP was also attained. Among all those observed results, it should be specifically noticed that in one particular experiment, the boronic acid-modified DNA gel-shift band was separated from natural DNA band with the same length and composition in the catechol-modified PAGE result. Since it is commonly known that catechol is capable of forming tight complex with boronic acid,[125-126,250-251] the

gel-shift result serves as a good indication that the diol-binding ability of boronic acid was well retained after being tethered to DNA backbone. Thus, all those preliminary results are good proof-of-concept evidence supporting the feasibility of proposed idea of developing boronic acid-based aptamers, or nucleic acid-based boronlectins (NBLs) in the future.

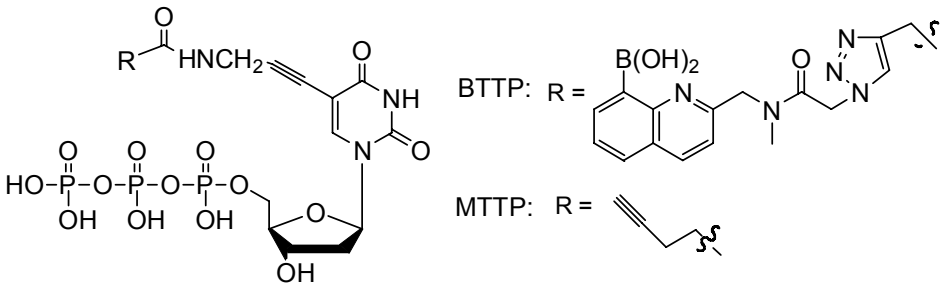

Figure 1.15 Boronic acid modified TTP (B-TTP) by Wang

1.4.4 Conclusion

In general, the biopolymer-based boronic acid sensors are created in a combinatorial approach for either PBLs or NBLs. There have been several array methods for evaluating PBL libraries using colorimetric detection methods, which is similar to the lectin-microarray analysis of glycans.[226-227] However, very limited number of the individual PBL affinity toward carbohydrate analytes was reported. For the one by Duggan, the highest PBL affinity toward carbohydrate was estimated to be around K_a of 4000 M^{-1}, which means most of the PBLs were at K_d of about -mM level binding affinity.[230] It is understandable since none of those constructed PBLs were designed purposely to have the structural conformation complementary to the target carbohydrate

analytes. Thus, colorimetric array methods may be a better method to evaluate PBLs because it's the binding- pattern profiles that serve as the comparing parameters. In contrast, NBLs for carbohydrate recognition are still under a developing stage. As reported, the SELEX technique often generates aptamers of binding affinities that rival antibodies. In one particular case, Yu and coworkers have selected out RNA aptamers against sLex with K_d values around 10^{-9} to 10^{-11} M.[242] Yet, the selected aptamers also showed cross-reactivity issue among Lewis acid group, a similar problem resembling lectins. This could be explained as a result from the nature of their interactions, which were still based on hydrogen bond and hydrophobic interactions. Anslyn and coworkers did an excellent work by combining the power of SELEX and boronic acid-carbohydrate interaction together to address that issue.[232] But in his experiment, the aptamers and boronic acids were still separated molecules working together, and the aptamers were only playing a tuning role in the entire binding process. In that sense, Wang lab is working on recruiting the boronic acid moieties into the nucleic acid molecules for further SELEX procedure.[231] It was proposed that the intrinsic affinity of boronic acids toward carbohydrates would probably lead the selecting process to bias on such interactions to generate more selective aptamers. Thus, efforts of constructing boronic acid-modified nucleic acid aptamers are carried out on this way.

1.5 The objectives and contributions of this dissertation

The objective of this research is to synthesize a new fluorescent B-TTP building block that can be enzymatically incorporated into DNA. Ideally, the boronic acid should show fluorescent intensity increase at a visible wavelength upon glycan binding as the reporting signal. It is critical that the property of fluorescence change for the new B-TTP be maintained even after DNA incorporation. In this case, naphthalimide-based boronic acid (NB) developed by our lab was chosen as the moiety to be linked to TTP, because of its long excitation/emission wavelengths and fluorescence increasing properties. Preliminary studies of several designed and synthesized NB-DNA were carried out to evaluate the fluorescence changes upon model sugar binding. It was proposed that by optimizing the DNA sequence and structure, the DNA-based boronic acid sensors with high affinity and selectivity against specific glycan target could be obtained. The work described in this dissertation consists of the following three key parts:

A. Synthesizing new B-TTP with intrinsic long-wavelength fluorescence

Along the line of trying to develop nucleic acid-based boronolectins, a new B-TTP was synthesized using similar strategy as previous one.[231] The advantage or improvement of the new B-TTP is that the chosen naphthalimide-based boronic acid (NB) fluoresces at long-wavelength and its fluorescence intensity increases upon carbohydrate binding. It was discovered that the fluorescent properties of NB were well retained after tethering to the 5-position of TTP, and the new B-TTP could be recognized by DNA polymerase as a substrate.

B. Fluorescence properties studies of NB- modified DNA sequences

After incorporation of NB-TTP into DNA sequences, fructose as model carbohydrate was added into the DNA solution to study its fluorescence change. It was observed that the fluorescence intensity increased in a concentration-dependent manner. Further experiments involved several bis-boronic acid DNA sequences with different number of bases as a spacer in between. In addition to fructose, three disaccharides were also tested for their effects on changing NB -DNA fluorescence.

C. *In vivo* cell imaging study of NB-TTP

Encouraged by the *in vitro* enzymatic activity of NB-TTP, we were interested in seeing the NB-TTP *in vivo* activities in cell cultures, which can be observed under fluorescent microscope. In this work, it was surprising to see that NB-TTP not only was capable of getting through cell membrane into cytoplasma, but also showed significant accumulation in the cell nucleus. The result could be very useful for developing fluorescent cell nucleus-labeling agents, or even mapping glycan distribution in living cells.

2. MATERIALS AND METHODS

.

2.1 Synthesis of napthalimide-based boronic acid modified TTP (NB-TTP)

Unless otherwise noted, starting materials and solvents were purchased from Aldrich and Acros, and used without purification. ^{1}H and ^{13}C NMR spectra were recorded on a Bruker 400 MHz spectrophotometer in a deuterated solvent with TMS (δ = 0.00 ppm) or NMR solvent as the internal reference unless otherwise specified. ^{31}P NMR was recorded using 85% H_3PO_4 as an external reference (in an insert). HPLC purification was carried out with a Zobax C18 reversed-phase column (9.4 mm×25 cm). Fluorescence spectra were recorded on a Shimadzu RF-5301 PC spectrofluorometer. Absorption spectra were recorded on a Shimadzu UV-1700 UV/Vis spectrophotometer. Quartz cuvettes were used in all fluorescence and UV studies. All pH values were determined by a UB-10 Ultra basic benchtopp H meter (Denver Instruments). For all reactions, analytical grade solvents were used. Anhydrous solvents were used for all moisture-sensitive reactions.

4-Aminomethylbenzyl alcohol (2):

4-(Hydroxymethyl)benzonitrile (1.0 g, 7.5 mmol) dissolved in dry THF (20 ml) was added slowly into a suspension of $LiAlH_4$ (866 mg, 22.8 mmol) in THF(20 ml) at RT. Foaming with bubble formation was observed while stirring. The light yellow-green suspension was refluxed under N_2 overnight. After cooling down to RT, MeOH (5 ml) was

added to the suspension to quench the reaction. The suspension generated foams while being stirred and cooled in an ice-bath. When no more bubble formation was observed, NaOH (20%, 15 ml) solution was added into the suspension. The solution became colorless while white precipitate was observed. The solution was concentrated *in vaccuo* and the residue was suction-filtered. The solid was repeatedly washed with CH_2Cl_2. The filtrate was combined and washed with H_2O. The organic phase was separated and concentrated on a rotavap. White solid was obtained as product (1.0 g, 98% yield). The product underwent prolonged drying *in vaccuo* to remove residue solvent before the next step reaction.

^{1}H-NMR ($CDCl_3$): δ7.31 (m, 4H), 4.67(s, 2H), 3.85 (s, 2H), 1.76 (s broad, 3H)

^{13}C-NMR ($CDCl_3$): δ142.7, 139.9, 127.5, 127.5, 65.2, 46.4

4-Boc-aminomethylbenzyl alcohol (3):

Into the solution of 4-aminomethylbenzyl alcohol (444 mg, 3.2 mmol) and triethylamine (0.47 ml, 3.3 mmol) in dry THF (5 ml) was added di-*t*-butyl dicarbonate (750 mg, 3.4 mmol) in dry THF (3 ml) dropwise. The mixture was stirred at RT overnight and then concentrated on a rotavap. The residue was dissolved in ethyl acetate (20 ml). The solution was sequentially washed with $NaHSO_4$ solution (5%, × 1), saturated $NaHCO_3$ solution (× 1) and brine (× 1), and then dried over $MgSO_4$. Filtration and solvent evaporation yielded a white powder product (720 mg, 94% yield).

^{1}H-NMR ($CDCl_3$): δ7.27 (m, 4H), 4.92 (s broad, 1H), 4.65 (s, 2H), 4.27 (d, 2H), 2.22 (s broad, 1H), 1.45 (s, 9H)

^{13}C-NMR ($CDCl_3$): δ156.1, 140.3, 138.4, 127.8, 127.4, 79.7, 65.1, 44.6, 28.6

(4-Boc-aminomethylbenzyl) methansulfonate (4):

Into the solution of 4-Boc-aminomethylbenzyl alcohol (700 mg, 3.0 mmol) and triethylamine (0.86 ml, 6.2 mmol) in dry THF (12 ml) in an ice bath, MsCl (0.38 ml, 4.9 mmol) was added dropwise. The mixture was stirred for 1 h in an ice bath. The solution was concentrated on a rotavap and the residue was dissolved in 25 ml of ethyl acetate. The solution was sequentially washed with $NaHSO_4$ solution (5%, × 1), saturated $NaHCO_3$ solution (× 1) and brine (× 1), and then dried over $MgSO_4$. After filtration and solvent evaporation, a colorless oil product was obtained (896 mg, 96% yield), which turned into white solid after prolonged drying *in vacuo.*

^{1}H-NMR ($CDCl_3$): δ7.35 (m, 4H), 5.22 (s, 2H), 4.95 (s broad, 1H), 4.33 (d, 2H), 2.91 (s, 3H), 1.46 (s, 9H)

^{13}C-NMR ($CDCl_3$): δ156.1, 140.7, 132.5, 129.4 128.0, 79.9 71.4, 44.4, 38.5, 28.6

4-Amino-*N*-(4'-boc-aminomethylbenzyl)naphthalimide (5):

4-Amino-naphthalimide (820 mg, 3.85 mmol) in dry DMF (20 ml) was treated with 2 M NaOMe in MeOH (3 ml) until it became a homogenous solution with a deep red color (took several minutes). (4-Boc-aminomethylbenzyl) methansulfonate (1.21 g, 3.85 mmol) was then added. The solution was stirred for 3 h and then quenched by adding H_2O (100 ml). The suspension was extracted with ethyl acetate (100 ml, × 2). The organic extractions were combined and concentrated into 100 ml. The solution was washed with H_2O (25 ml, × 3) and dried over $MgSO_4$. The removal of solvent on a rotavap gave an

orange powder product (1.5 g, 90% yield).

^{1}H-NMR (D_6-DMSO): δ8.63 (d, 1H, *J* = 7.6 Hz), 8.44 (dd, 1H, J_1 = 7.2 Hz, J_2 = 0.8 Hz), 8.21 (d, 1H, *J* = 9.2 Hz), 7.66 (t, 1H, *J* = 8.0 Hz,), 7.49 (s broad, 2H), 7.20 (m, 4H), 6.86 (d, 1H, *J* = 8.4 Hz), 5.19 (s, 2H), 4.06 (d, 2H, *J* = 6 Hz), 1.366 (s, 9H)

^{13}C-NMR (D_6-DMSO): δ163.8, 162.9, 155.7, 152.9, 138.8, 136.4, 134.2, 131.2, 129.8, 129.5, 127.4, 126.9, 124.0, 121.7, 119.4, 108.2, 107.3, 77.7, 43.1, 42.2, 28.2.

MS (ESI-) : *m/z* (%) = 430.3 (100) $[M-H]^-$.

Exact mass: $C_{25}H_{24}N_3O_4$ calc. 430.1767; found 430.1778

4-(2-Bromobenzyl)amino-*N*-(4'-boc-aminomethylbenzyl)naphthalimide (6):

4-Amino-*N*-(4'-Boc-aminomethylbenzyl)naphthalimide (**5**) (1.50 g, 3.49 mmol) and sodium hydride (60% dispersed in mineral oil, 306 mg, 7.66 mmol) were mixed in dry DMF (20 ml). The mixture was stirred for 5 min and then 2-bromobenzyl bromide (870 mg, 3.49 mmol) was added. The mixture was stirred for 3 h before quenching with water (150 ml). The suspension was extracted with ethyl acetate (25 ml, × 3). The organic extractions were combined and washed with water (50 ml). After separation, the organic solvent was removed on a rotavap and the residue was purified on a silica gel column (ethyl acetate/hexane, 1:4). A yellow powder product (840 mg, 40% yield) was obtained.

^{1}H-NMR (D_6-DMSO): δ8.58 (d, 1H, *J* = 7.2 Hz), 8.43 (d, 1H, *J* = 8.4 Hz), 8.13 (d, 1H, *J* = 8.4 Hz), 7.64~7.61 (m, 2H), 7.49 (d, 2H, *J* = 8.0 Hz), 7.37 (dd, 1H, J_1 = 7.6 Hz, J_2 = 1.6 Hz), 7.30~7.28 (m, 1H), 7.27~7.18 (m, 2H), 6.68 (d, 1H, *J* = 8.4 Hz), 5.78 (s, 1H), 5.33 (s, 2H), 4.75 (s, 1H), 4.69 (d, 2H, *J* = 5.6 Hz), 4.24 (d, 2H, *J* = 5.6 Hz), 1.43 (s, 9H)

^{13}C-NMR (D_6-DMSO): δ164.8, 164.2, 156.0, 149.1, 138.0, 137.2, 136.1, 134.7, 133.5, 131.6, 130.0, 129.8, 129.5, 129.3, 128.1, 127.8, 126.2, 125.2, 123.8, 123.4, 120.6, 111.3, 105.3, 79.6, 48.3, 44.7, 43.2, 28.6

MS (ESI+): *m/z* (%) = 600.5 (100) $[M+H]^+$.

Exact mass: $C_{32}H_{31}BrN_3O_4$ calc. 600.1498; found 600.1504

4-(2-Dihydroxylboryl-benzyl)amino-*N*-(4'-boc-aminomethylbenzyl)naphthalimide (**7**):

4-(2-Bromobenzyl)amino-*N*-(4'-boc-aminomethylbenzyl)naphthalimide (**6**) (391 mg, 0.65 mmol), $PdCl_2$(dppf) (160 mg, 0.20 mmol), bis(neopentyl glycolato)diboron (368 mg, 1.63 mmol) and KOAc (198 mg, 2.02 mmol) were mixed in a dry flask under N_2. Anhydrous DMSO (5 ml) was injected into the mixture. The solution was heated at 80~85 ℃ under N_2 for 5 h. Then the solution was cooled down to RT. Water (25 ml) was then added to quench the reaction. The solution was extracted with ethyl acetate (25ml, × 2). The extractions were combined, washed with water (25ml, × 2) and concentrated on a rotavap. The residue was purified on a silica gel column, and the crude product was eluted out by ethyl acetate/MeOH = 10:1. The crude product was further purified on two 20 × 20 cm preparatory TLC plates (ethyl acetate/MeOH = 5:1). The orange fluorescent band (R_f = 0.1~0.5) was cut out and extracted with MeOH. Orange color solid product was obtained (167 mg, 45% yield).

^{1}H-NMR (MeOD): δ8.22 (d, 1H, *J* = 8.0 Hz), 8.04 (d, 1H, *J* = 8.8 Hz), 7.58 (d, 1H, *J* = 7.2 Hz), 7.42 (d, 2H, *J* = 7.6 Hz), 7.33~7.25 (m, 4H), 7.19~7.16 (m, 3H), 6.17 (d, 1H, *J* = 8.4

Hz), 5.30 (s, 2H), 4.55 (s, 2H), 4.15 (s, 2H), 1.42 (s, 9H)

^{13}C-NMR (MeOD): δ167.8, 166.2, 164.7, 158.7, 141.6, 139.5, 138.9, 133.6, 130.9, 129.4, 129.1, 129.0, 128.8, 128.3, 127.5, 126.4, 119.6, 104.0, 101.8, 80.3, 47.7, 45.0, 43.8, 30.9, 28.9

MS (ESI-) : *m/z* (%) = 564.3 (100) $[M-H]^-$.

Exact mass: $C_{32}H_{31}BN_3O_6$ calc. 564.2306; found 564.2310

4-(2-Dihydroxylboryl-benzyl)amino-*N*-(4'-aminomethylbenzyl) naphthalimide (8):

4-(2-Dihydroxylboryl-benzyl)amino-*N*-(4'-Boc-aminomethylbenzyl)naphthalimide (**7**) (390 mg, 0.69 mmol) was suspended in CH_2Cl_2 (12 ml) and TFA (1.2 ml, 15.6 mmol) was added in one-shot. The mixture was stirred at RT for 0.5 h and then concentrated on a rotavap. The residue was washed with a saturated K_2CO_3 solution. Then the residue was dissolved in methanol and loaded on two 20 × 20 cm preparatory TLC plates. 100% ethyl acetate was used to develop first. Later, ethyl acetate/MeOH (5:1) was used to develop the plate. The orange fluorescent band (R_f = 0.2~0.3) was cut out and extracted with MeOH. An orange color solid product was obtained (210 mg, 66% yield).

^{1}H-NMR (MeOD): δ8.21 (d, 1H, *J* = 6.8 Hz), 8.03 (t, 1H, *J* = 4 Hz), 7.58 (d, 1H, *J* = 7.2 Hz), 7.44~7.37 (m, 4H), 7.29~7.25 (m, 4H), 7.17 (t, 1H, *J* = 7.2 Hz), 6.16 (d, 1H, *J* = 8.8 Hz), 5.32 (s, 2H), 4.55 (s, 2H), 3.86 (s, 2H),

^{13}C-NMR (MeOD): δ167.8, 166.1, 141.6, 140.2, 138.8, 133.6, 130.9, 129.4, 129.3, 129.2, 128.9, 127.5, 126.3, 119.4, 103.8, 101.8, 47.9, 45.5, 43.8

MS (ESI-): *m/z* (%) = 492.3 (100) $[M-H-2H_2O+2MeOH]^-$, 478.3 (70) $[M-H-H_2O+MeOH]^-$,

464.3 (50) $[M-H]^-$.

Exact mass: $C_{27}H_{23}BN_3O_4$ calc. 464.1782; found 464.1796

4-(2-Dihydroxylboryl-benzyl)amino-*N*-(4'-azidoacetyl-aminomethyl-benzyl)naphthalimide (9):

4-(2-Dihydroxylboryl-benzyl)amino-*N*-(4'-aminomethylbenzyl)naphthalimide (**8**) (210 mg, 0.45 mmol), EDCI (170 mg, 0.90 mmol), and azidoacetic acid (91 mg, 0.90 mmol) were mixed in anhydrous DMF (10 ml). The mixture was stirred at RT under N_2 for 1 h. The solution was concentrated by oil pump at 35 °C. The residue was rinsed with H_2O and then saturated K_2CO_3 solution. After that, the residue dissolved in ethanol was loaded on to two 20 × 20 cm preparatory TLC plates and 100% ethyl acetate was used to develop first. Later, ethyl acetate/MeOH (10:1) was used to develop the plate. The orange fluorescent band (R_f = 0.2~0.3) was cut out and extracted with MeOH. An orange color solid product was obtained (241 mg, 98% yield).

^{1}H-NMR (MeOD): δ8.23 (d, 1H, *J* = 7.2 Hz), 8.06 (d, 1H, *J* = 8.4 Hz), 7.59 (d, 1H, *J* = 6.8 Hz), 7.42 (d, 2H, *J* = 7.6 Hz), 7.33 (d, 2H, *J* = 8.0 Hz), 7.27 (t, 2H, *J* = 7.6 Hz), 7.21~7.17 (m, 3H), 6.19 (d, 1H, *J* = 8.8 Hz), 5.30 (s, 2H), 4.55 (s, 2H), 4.34 (s, 2H), 3.88 (s, 2H)

^{13}C-NMR (MeOD): δ170.1, 167.8, 164.6, 141.5, 139.3, 138.9, 138.2, 133.6, 130.9, 129.4, 129.2, 128.9, 128.8, 127.6, 126.5, 119.8, 104.3, 101.8, 53.1, 47.5, 44.2, 44.0, 43.8, 30.9, 18.5

MS (ESI-): *m/z* (%) = 547.3 (100) $[M-H]^-$, 561.3 (50) $[M-H-H_2O+MeOH]^-$.

Exact mass: $C_{29}H_{24}BN_6O_5$ calc. 464.1782; found 464.1796

The M-TTP was synthesized following previously published procedure (Scheme 3.2).[231]

5-[3-(Trifluoroacetamido)-propynyl]-2'-deoxyuridine (10):

5-Iodo-2'-deoxy uridine (354 mg, 1.0mmol) was dissolved in degassed dry DMF (10 mL). Copper (I) iodide (38 mg, 0.2 mmol), freshly distilled triethylamine (0.28 mL, 2.0 mmol) and freshly distilled *N*-propynyltrifluoroacetamide (453 mg, 3.0 mmol) were added later. The mixture was stirred for 30min in dark under N_2 protection until everything dissolved. Tetrakis(triphenylphosphine) palladium (0) (116 mg, 0.10 mmol) was added and the mixture was stirred overnight in dark under N_2 protection at r.t.. Then solvent was removed and the residue was purified with a silica gel column (dichloromethylene: methanol=15:1) to give white solid product (320 mg, 85%)

^{1}H-NMR (DMSO): δ 2.12 (2H, m), 3.59 (2H, m), 3.79 (1H, d), 4.23 (3H, d), 5.09 (1H, t), 5.25 (1H, d), 6.10 (1H, t), 8.19 (1H, s), 10.07 (1H, s)

5-[3-Amino-propynyl]-2'-deoxyuridine (11)

Compound **10** (250 mg, 0.64 mmol) was dissolved in ammonium hydroxide (5 ml) and stirred overnight. The solution was concentrated in vacuo and residual water was removed by oil pump for 24h to give product as deep yellow oil (180 mg, 100%)

^{1}H-NMR (DMSO): δ 2.14 (2H, m), 3.59 (3H, m), 3.82 (1H, m), 3.92 (2H, s), 4.24 (1H, m), 5.20 (2H, br), 6.10 (1H, t), 8.25 (1H, s)

5-[3-(4-Pentynoic amido)-propynyl]-2'-deoxyuridine (12)

Compound **11** (180 mg, 0.64 mol) was dissolved in dry DMF (5 ml). 4-Pentynoic acid (68mg, 0.69mmol) and PyBop (515 mg, 0.99 mmol) were added into the solution under ice bath cooling. The mixture was stirred overnight at r.t.. The solvent was removed at 78 °C *in vacuo* and the residue was purified with silica gel chromatography (dichloromethylene: methanol=15:1) to give pure product as white solid (89 mg, 37%): ^{1}H-NMR (DMSO): δ 2.11 (2H, dd), 2.28-2.39 (4H, m), 3.53-3.63 (2H, m), 3.79 (1H, quart), 4.10 (2H, d), 4.22 (1H, m), 5.10 (1H, t), 5.25 (1H, d), 6.11 (1H, t), 8.17 (1H, s), 8.43 (1H, t)

M-TTP:

All liquid reagents and solvents were freshly distilled to be anhydrous. Compound **12** (0.15 g, 0.4 mmol) and proton sponge (0.102 g, 0.48 mmol) were dried *in vacuo* over P_2O_5 overnight and then dissolved in anhydrous trimethylphosphate (0.6 ml) under nitrogen. Then the mixture was cooled in an ice bath and $POCl_3$ (44 μL, 0.5 mmol) was added dropwise via a syringe with stirring. The reaction mixture was stirred on ice for 2 h and then bis-tri-n-butylammonium pyrophosphate (0.98 g) dissolved in DMF (1.6 ml) and tri-n-butylamine (0.6 ml) was added in one portion. The mixture was stirred at room temperature for 10 min and then triethylammonium bicarbonate solution (0.1 M, pH8, 10 ml) was added. The reaction mixture was stirred at room temperature for an additional hour and concentrated on a rotavap equipped with an oil pump. The residue was purified with a DEAE-Sephadex A-25 column using a linear gradient concentration (0-0.6 M) of

NH_4HCO_3 aqueous buffer solution. Monitored with the UV 260nm absorbance, the product was eluted out by 0.12–0.15 M NH_4HCO_3 fraction. The elution was collected and lyophilized to give the final product as a white powder (161 mg, 60%).

^{31}P-NMR (D_2O, internal standard: 85% H_3PO_4): δ -5.34(γ P), -10.14(α P), -18.60(β P)

^{1}H-NMR (D_2O): δ 7.99 (s, 1H), 6.30 (t, 1H), 4.58 (m, 1H), 4.21 (m, 5H), 2.51 (m, 4H), 2.37 (m, 3H)

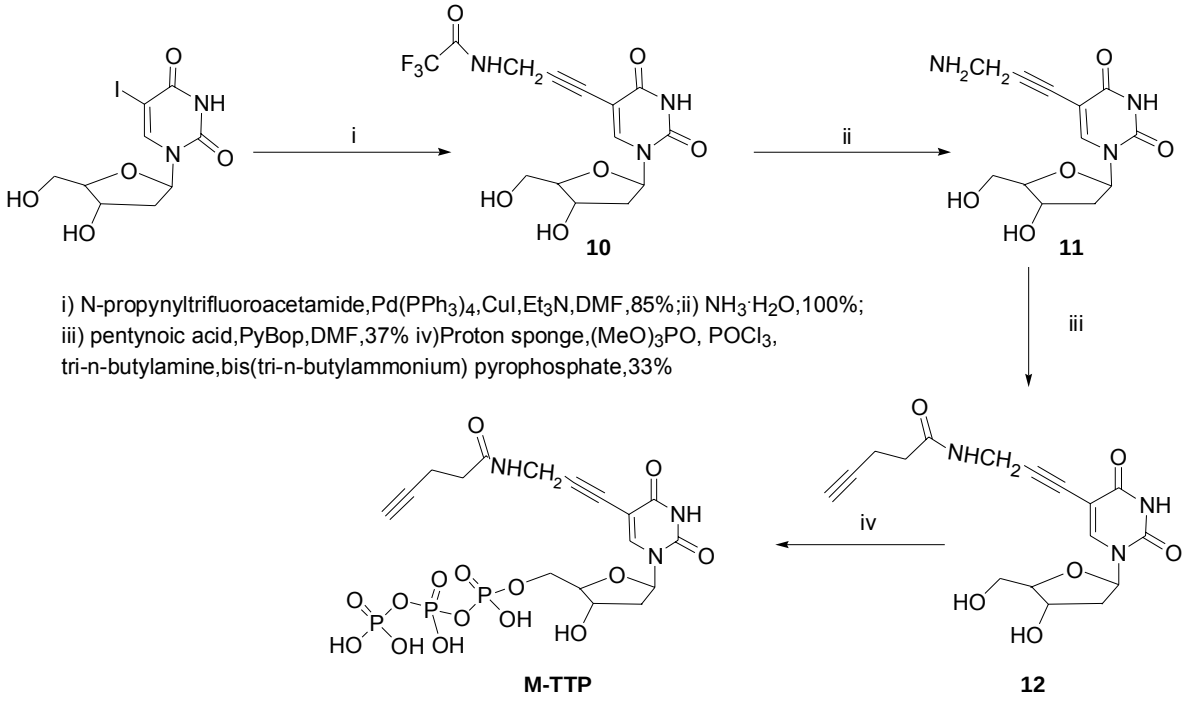

Scheme 2.1 Synthesis route of M-TTP

NB-TTP:

4-(2-dihydroxylboryl-benzyl)amino-*N*-(4'-azidoacetyl-aminomethylbenzyl)naphthalimide (**7**) (10 mg, 0.018 mmol) and M-TTP (10 mg, 0.017 mmol) were mixed in a flask under N_2. MeOH/H_2O (1:1, 200 μl) was injected into the flask later to suspend the mixture with

stirring. TBTA (1.7 mg, 0.0033 mmol) and CuBr solution (0.24 mg, 0.0017 mmol) in 50 µl DMF were added later. The reaction mixture was sonicated for several minutes and then stirred at RT under N_2 for 5 h. The reaction was quenched by adding 1 ml of H_2O and then centrifuged at 13.5k rpm for 15 min. The aqueous supernatant was collected and the residue was repeatedly extracted with 100 mM NH_4HCO_3 buffer pH 8.0 until the extraction was no longer deep orange. The aqueous extractions were combined and purified by HPLC. The collected fraction was lyophilized into orange color powder. The product was washed with MeOH and ice-cold water to remove residual starting material. Further purification of NB-TTP was achieved by MeOH precipitation of the saturated aqueous solution. A bright red-orange colored powder was obtained as pure product (5 mg, 25% yield)

^{11}B-NMR (D_2O, internal standard: 15% BF_3 in ether): δ29.9

^{31}P-NMR (D_2O, internal standard: 85% H_3PO_4): δ-5.41 (γ P), -10.31(α P), -18.60(β P)

^{1}H-NMR (D_2O/MeOD = 2:1, Watergate solvent suppression): δ8.17 (d, 1H, *J* = 7.6 Hz), 7.91 (d, 1H, *J* = 9.2 Hz), 7.7~7.5 (m, 2H), 7.1~7.5 (m, 9H), 6.07 (d, 1H, *J* = 9.2 Hz), 5.95 (t, 1H), 5.25 (s, 1H), 4.3~4.0 (m, 3H), 2.94 (t, 2H) , 2.47 (t, 2H), 2.16 (t, 2H)

MS (ESI-): *m/z* 1032.3 (100) $[M\text{-}H\text{-}2H_2O\text{-}HPO_3]^-$, 1112.3 (20) $[M\text{-}H\text{-}2H_2O]^-$, 1134.3 $[M\text{-}H\text{-}3H_2O\text{+}MeOH]^-$, 1054.3 $[M\text{-}H\text{-}3H_2O\text{+}MeOH\text{-}HPO_3]^-$

MS (MALDI linear mode): *m/z* 1112.57 (100) $[M\text{-}H\text{-}2H_2O]^-$, 1032.97 (45) $[M\text{-}H\text{-}2H_2O\text{-}HPO_3]^-$

Exact mass: $[M\text{-}H\text{-}2H_2O]^-$ $C_{46}H_{42}BN_9O_{18}P_3$ calc. 1112.1954; found 1112.1940.

2.2 Photo stability test of boronic acid 9:

Solution of boronic acid **9** (1×10^{-6} M) in 0.1 M phosphate buffer at pH 7.4 was prepared. Using the Time Course function of Shimadzu RF-5301 PC spectrofluorometer, excitation wavelength was fixed at 490 nm. Both excitation and emission slits were set at 5 nm. The fluorescence intensity measurements were taken every 0.3 s at two wavelengths (540 and 570 nm) and the fluorescence was monitored for 3600 s [Figure 2.1 (a)]. The entire fluorescence spectrum was scanned at the end point [Figure 2.1 (b)] It can be seen that the fluorescence intensity was constant at both tested emission wavelength (540 and 570 nm) and the fluorescence profiles overlap very well after constant irradiation for 1 h and 2 h.

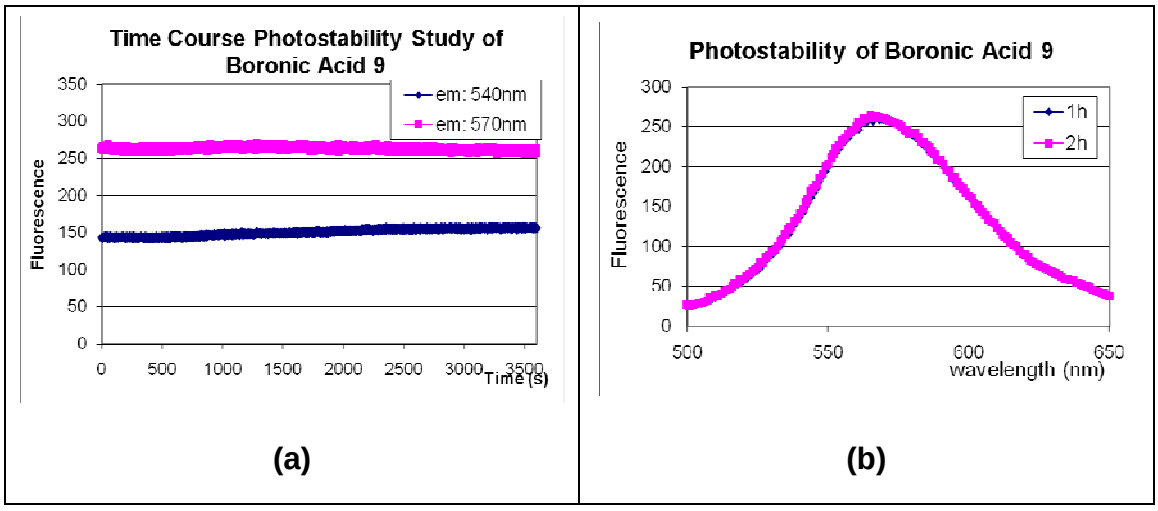

Figure 2.1 Photostablity studies of boronic acid **9** in 0.1 M phosphate buffer at pH 7.4

2.3 Mass spectrometry

ESI-MS work was performed using a Waters Micromass Q-TOF micro instrument. Data were acquired in either a positive and negative ion mode by syringe pump infusion of the sample solutions at a flow rate of 7 μL/min. The MALDI mass spectrometry analysis was performed on an Applied Biosystems 4800 plus MALDI TOF/TOF analyzer mass spectrometer (Framingham, MA). This instrument is equipped with a Diode-pumped Nd:YAG laser at 355-nm. The mass spectra were acquired as an average of 3 shots with the same laser intensity attenuator setting (4002 arbitrary unit) for all samples. All spectra were recorded on a biomass spectrometer in linear-negativemode with delayed extraction. 3-Hydroxypicolinic acid (3-HPA)/diammonium citrate (9:1) in water was used as the matrix. A 10:1 matrix:sample mixture was prepared, applied to the sample plate as 1 μL drops, and allowed to air dry before analysis. 25 kV acceleration voltage was used. A mass range of 1000–10000 was scanned. Each spectrum was summed frommultiple spectra at different spots. Proteins, such as insulin, thioredoxin, and apomyoglobin, were used as external standards. This work was performed by at the Mass Spectrometry Facilities of Georgia State University.

2.4 High Performance Liquid Chromatography (HPLC) for NB-TTP purification

The aqueous extractions of crude NB-TTP product with 100 mM NH_4HCO_3 buffer pH 8.0 were combined and purified by HPLC (Zobax C18 RP preparatory column, Shimadzu LC-10AT VP system). Elution condition: 100 mM NH_4HCO_3 buffer pH 8.0 /CH_3CN (3 ml/min), 0–10 min (CH_3CN 10%), 10–30 min (CH_3CN, 10-100%), 30–40 min (CH_3CN,

100%), 40–45 min (CH_3CN, 100-10%), 45–55 min (CH_3CN, 10%). R_t = 17.5-22.5 min. The collected fraction was lyophilized into orange color powder. The product was washed with MeOH to remove residual starting material and extracted again with 100 mM NH_4HCO_3 buffer. The extraction was lyophilized again to give the pure product.

2.5 NB-TTP Fluorescence binding tests

Solutions of NB-TTP (1×10^{-6} M) and NB-TTP (1×10^{-6} M) with D-fructose (0.1 M) were prepared in 0.1 M phosphate buffer at pH 7.4, respectively. These two solutions were mixed in various ratios to give the desired D-fructose concentrations (10^{-3} to 0.1 M). 3 ml of each mixed solution was used to test the fluorescence intensity several minutes after mixing. Eight points were collected for the calculation of the apparent binding constant K_a assuming a 1:1 complex formation mechanism. These studies were run in triplicate.

The binding constants were determined using the following equation:

$$I_0/(I-I_0)=(\varepsilon_B/\varepsilon_{B-S}K_a)*1/[\text{fructose}]+ \varepsilon_B/\varepsilon_{B-S}$$

where I_0 is fluorescence intensity of NB-TTP solution; I is NB-TTP fluorescence intensity upon adding sugar, ε_B is fluorescence correlation factor of NB-TTP; ε_B-s is the fluorescence correlation factor of NB-TTP-fructose complex; K_a is the binding constant; [fructose] is the sugar concentration.

2.6 Primer extension using the Klenow fragment for MALDI-TOF-MS studies

14-nt Primer (16 μM), 21-nt template (6.8 μM), Klenow (0.1 units/μl), TTP (0.3 mM) or NB-TTP (0.3 mM), and three other dNTPs (0.3 mM each) in total volume of 100 μl were incubated at 37 °C for an hour. The prepared DNA was purified using Microcon YM-3

centrifugal filter (Millipore Corp.) to remove dNTPs and other low molecular weight molecules. The harvested DNA was further purified by 5 M NH_4OAc/ethanol precipitation (three times) as a way to replace metal ions with ammonium as the phosphate counterions.[252] The DNA pellet was dissolved in 10 µl for MALDI-TOF-MS analysis. The oxidative deborylated NB-DNA sample was prepared by adding 0.25 µl of H_2O_2 solution (100 mM) into 5 µl of NB- DNA solution. MALDI mass spectral results were obtained using insulin as the internal standard.

2.7 PAGE analysis of primer extension

A mixture of 14-nt primer DNA (50 µM), T4 polynucleotide kinase (0.5 units/µl, Biolabs, Inc.) and γ-^{32}P-ATP (0.6 µl, from Perkin-Elmer Corp.) in 12 µl T4 kinase buffer solution was incubated at 37 °C for 1 h. The ^{32}P-labeled DNA was purified using Microcon YM-3 centrifugal filter (Millipore Corp.) to remove low molecular weight molecules. Using a similar primer extension protocol as previously described, the ^{32}P-labeled primer alone, reaction mixture without enzyme, reaction mixture without dNTPs, reaction mixture with both enzyme and natural dNTPs and reaction mixture with NB-TTP, the other 3 dNTPs and enzyme were incubated at 37 °C for 1 h. The reactions were quenched with 2× DNA loading dye. 3 ul of samples from each reaction were taken and run on 15% PAGE at 300V for 3 h. Later, the gel was fixed and dried. Film was developed after autoradiography with the dried gel for overnight.

2.8 NB -DNA fluorescence binding tests

2.8.1 Double stranded NB- DNA binding tests

Primer (7 μM), Template 0~7 (7 μM), Klenow (0.1 units/μl), NB-TTP (125 μM), and three other dNTPs (0.3 mM each) in total volume of 200 μl were incubated at 37 °C for an hour. After purification of the DNA through membrane filtration and NH_4OAc/ethanol precipitation three times, the orange-colored DNA pellet was supposed to be quantitatively precipitated out,[252] and dissolved in 50 μl of H_2O. 45 μl of the NB- dsDNA solution was diluted by 4.5 ml 0.1 M phosphate buffer (pH 7.4) to make theoretical concentration of 0.5 μM solution. D-fructose was added into the DNA solution with concentration increasing from 10^{-3} to 0.1 M. 1 ml of solution was used to test the fluorescence intensity more than 5 minutes after mixing. Each test was triplicated.

2.8.2 Single stranded NB- DNA binding tests

Primer (21 μM), Template 0~7 (7 μM), Klenow (0.1 units/μl), NB-TTP (125 μM), and three other dNTPs (0.3 mM each) in total volume of 200 μl were incubated at 37 °C for an hour. After purification of the DNA through membrane filtration and NH_4OAc/ethanol precipitation three times, the orange-color DNA pellet was dissolved in 50 μl of H_2O. 45 μl of the NB- ssDNA solution was heated at 90 ^{o}C for 1 min, then quickly cooled down in ice bath and diluted by 2.5 ml 0.1 M phosphate buffer (pH 7.4) to make theoretical concentration of 0.56 μM solution. 0.5 ml of each NB- ssDNA solution was mixed with 0.5 ml of phosphate buffer (blank), 0.5 ml of D-fructose phosphate buffer solution (0.2 M), 0.5 ml of D-lactose phosphate buffer solution (0.2 M), 0.5 ml of D-maltose phosphate

buffer solution (0.2 M), and 0.5 ml of D-sucrose phosphate buffer solution (0.2 M) solution respectively. 1 ml of each NB-ssDNA/sugar solution was tested the fluorescence intensity more than 5 minutes after mixing. The fluorescence intensity was divided by that of the blank to calculate the increasing fold. Each test was triplicated.

2.9 HeLa cell sub-culture and fluorescence imaging study

2.9.1 HeLa cells sub-culture

The cells have to be sub-cultured or passaged as part of maintenance to prevent over growth of the cells. The process is common for any adherent cell line.[253] A sterile flask was taken, added with 19.5 ml of fresh medium (DMEM + 10% Normal FBS + 1% Penicillin/Streptomycin) and incubated in a CO_2 incubator at 37 ^oC, 5% CO_2 and 90% relative humidity.

T-75 flask with 80-85% confluent culture was taken out from the CO_2 incubator and the spent medium was removed. The cells were washed for 2 min with10ml of DPBS twice. 2-3 ml of trypsin (0.25%, from Mediatech, Inc) was add to the flask and incubated for 2 min in a CO_2 incubator at 37^oC, 5% CO_2 and 90% relative humidity. After 2-3 mins, the flask was removed from the incubator and 4ml of fresh medium was added to neutralize the effect of trypsin. The suspension was mixed gently to break the clumps. 0.5ml of the suspension was drawn and added into the flask with pre-warmed fresh medium. The flask was kept for incubation in a CO_2 incubator at 37 ^oC, 5% CO_2 and 90% relative humidity.

2.9.2 HeLa cells fluorescence imaging study

A T-75 flask of 80% confluent HeLa cell line was treated with 3 ml of trypsin (0.25%, from Mediatech, Inc). Cover slips were sterilized by treatment with 70% ethanol and then exposed to UV light in the laminar airflow. The sterilized cover slips were carefully placed into the 24-well plate and 500uL of cell suspension was added onto the cover slip in each well. The plate was left in the incubator at 37 ^{o}C, 5% CO_2 and 86% humidity until the cell line reached 50-60% confluence (approximately 24hr).

After incubation, test fluorescence compound dissolved in growth medium was added to the cells in the 24-well plate at required concentrations. The plate was left in the incubator at 37 ^{o}C, 5% CO_2 and 86% humidity. After incubation for 24 hr, medium from each well was removed and the cells were gently washed with 500 ul PBS twice. 200 ul of ice-cold methanol was added to each well and incubated at r.t. for 5 mins. Then methanol was removed and the cells were washed again with 500 ul PBS twice.

The cover slips were carefully removed from the wells using a forceps and placed an inverted position on slides with the cells side facing the slide. The coverslips were dried with Kimwipes and the edges were sealed using clear nail polish. The slides with coverslips on top were inverted and observed under a Zeiss Axiovert 400M inverted epifluorescence microscope using the 40X oil lens with Immersol 518F oil. The filter cubes were switched to FITC (495/520) channel and the images were captured using AxioVision Rel 4.6 program.

2.9.3 HeLa cells crude protein and genomic DNA extraction:

The procedures were following the technical manual of Wizard genomic DNA purification kit by Promega Corporation. The cultured cells were first trypsinized and transferred to a 1.5ml microcentrifuge tube. The cells were pelleted by centrifuging at 13,000 × *g* for 10 sec. The supernatant was removed. The pellet was washed with 200 μL PBS and centrifuged again. The pellet was added with 600 μL of Nucleic Lysis Solution and pipette until no visible cell clumps remain. 3 μL of RNase Solution was added into the lysate solution and mixed by inverting the tube 2-5 times. The mixture was incubated at 37 °C for 30 min and then cooled down to r.t. 200 μL of Protein Precipitation Solution was added into the mixture and the mixture was vortexed vigorously for 20 sec. The sample was chilled on ice for 5 min. The protein was precipitated by centrifuging at 13,000 × *g* for 4 min. The tight white pellet was collected at crude protein extraction. It was dissolved in 1 mL of PBS and directly subjected for fluorescence test.

The supernatant was transferred to a clean 1.5 mL microcentrifuge tube containing 600 μL of isopropanol. The solution was gently inverted until white thread-like strands of DNA form a visible mass. The suspension was centrifuged at 13,000 × *g* for 1 min and the supernatant was removed. The DNA white pellet was added with 600 μL of 70% ethanol. The mixture was gently inverted several times to wash the DNA and then centrifuged at 13,000 × *g* for 1 min. The supernatant was removed and the pellet was

air-dried for 15 min. The DNA was rehydrated by incubating with 100 μL of DNA Rehydration Solution at 65 °C for 60 min. The solution was diluted by PBS into 1 mL solution and subjected for fluorescence test.

2.9.4 Isolation of HeLa cell nuclei

The procedure was following the method described by Gonzalez-Lazaro.[254] The cultured HeLa cells were trypsinized and washed with PBS. The cell pellet was suspended in 1 mL of solution 1 (0.32 M sucrose, 0.002 M $MgCl_2$, 0.001 M K_2HPO_4, pH 6.8) and centrifuged at 1000 × *g* for 7 min. The supernatant was removed and the pellet was resuspended in 1 mL of solution 2 (0.01 M NaCl, 0.001 M K_2HPO_4, pH 6.8) and incubated at 4 °C for 15 min. The cells were then centrifuged at 800 × *g* for 10 min. The supernatant was removed and the pellet was suspended in 1 mL of solution 3 (0.32 M sucrose, 0.001 M $MgCl_2$, 0.3% Triton X-100, 0.001 M K_2HPO_4, pH 6.2-6.4). The cells were lysed through a 22-gauge needle (10 passes). The partially lysed cells were then centrifuged at 800 × *g* for 10 min and the supernatant was discarded. The pellet was suspended in 1 mL of solution 3 and lysed through a 22-gauge needle (10 passes) again. The lysed cells were centrifuged and the pellet was washed with solution 1. All instrument and solutions were pre-cooled at 4 °C before usage and the experiment was carried out at r.t. as quick as possible.

3. SYNTHESIS AND ENZYMATIC STUDIES OF NAPHTLIMIDE-BASED BORONIC ACID-CONJUGATED TTP (NB-TTP)

3.1 Introduction

Our lab has had a long-standing interest in using the boronic acid moiety, which is known to interact with diols/carbohydrates, fluoride, cyanide, and other nucleophiles/Lewis bases,[122,200] as a recognition group for sensing and other applications.[123] Recently, we have reported the synthesis of a boronic acid-modified thymidine triphosphate (B-TTP),[231] its enzymatic incorporation into DNA, and discussed the feasibility of using it in DNA aptamer selection. Along this line, we desire to incorporate a fluorescent boronic acid into DNA that has the following properties: (1) the excitation and emission wavelengths are longer than the λ_{max} of nucleobases; (2) shows fluorescent property changes upon carbohydrate binding; (3) is stable under PCR conditions; (4) is stable under copper-mediated “click” conditions with DNA;[255-256] and (5) is relatively easy to synthesize.

To synthesize another B-TTP with improved features such as intrinsic fluorescence emission at long-wavelength, 4-amino-1,4-naphthalimide (Nap) was chosen as the fluorophore after careful consideration and evaluation. Before, Heagy and coworkers reported a series of 1,4-naphthalimide based *N*-phenylboronic acids.[177] They were promising in the sense of their long wavelength emission (550 nm) and good water solubility, but were limited in applications because their fluorescence decreases upon

sugar binding. Mohr and coworkers developed one 1,4-naphthalimide based carbohydrate sensor with a terminal boronic acid at the 4-amino position linked through an aliphatic chain.[257] The designed 1, 5-relationship of the boronic acid with the nitrogen at the aliphatic linker was proposed to interact through B-N bond formation to modulate the PET (photoinduced electron transfer) system that influence the fluorescence properties.[139] An alternative hydrolysis mechanism was also proposed to explain the same phenomenon by the Wang group.[172] The Mohr boronic acid sensor showed a maximum of 130% fluorescence intensity increase upon D-fructose addition (λ_{ex}: 410 nm, λ_{em}: 530 nm, pH 7.15). Recently, a systematic study of novel 4-amino-1,4-naphthalimide-derived phenylboronic acids was carried out by our group. A comprehensive mechanistic investigation of the fluorescence changing was also performed.[170,258] In this case, boronic acid was directly functionalized in 1,5-relationship with the nitrogen of the 4-aniline group (Figure 3.1). Sensor **1a** showed 2.5-fold and 1.1-fold fluorescence intensity increase upon fructose and glucose binding, respectively (λ_{ex}: 493 nm, λ_{em}: 570 nm, 0.1% MeOH in 0.1M phosphate buffer, pH 7.4).[258] Interestingly, sensors **1b-1c** with modification at the *para*- position by different electron-withdrawing or electron-donating groups didn't result in much changes in carbohydrate binding constants and fluorescence intensity increases. However, correlation of the boronic acid p*K*a values and binding indicated a general Hammett correlation trend with different substituents.[170] It was proposed that an excited-state internal charge-transfer (ICT) mechanism was responsible for the fluorescence intensity

increase accompanying decreased solvent polarity, increased pH value or upon carbohydrate binding. It was suggested that through stabilization of the excited-state charge separation by the negatively charged boronate, bathochromic shift of the UV λ_{max} value with increased absorption intensity could at least partially contribute to the increased fluorescence emission intensity. In addition, the carbohydrate-boronate ester formation would limit the rotation around C-N bond due to steric hinderance, which could lead to a higher fluorescence quantum yield and thus enhanced fluorescence intensity. Also, the boronate ester formation could increase the B-N distance, which would lessen the stabilization effect of boronate on the excited-state charge–transfer species, and caused the hypsochromic shift of both the UV λ_{max} value and fluorescence emission wavelength upon carbohydrate addition. The increased B-N distances upon carbohydrate binding were supported by molecular modeling calculations using density function theory (DFT) in a polarizable continuum model (PCM).

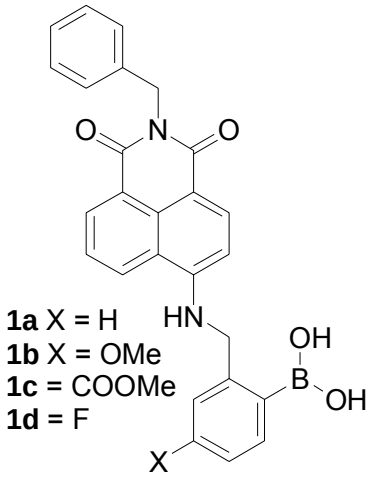

Figure 3.1 4-Amino-1,4-naphthalimide-derived phenylboronic acids by Wang

Through tethering the boronic acid sensor **1a** to the 5-position of TTP, it is expected that the fluorescent TTP analogue could yield DNA aptamers with not only high affinity and selectivity against carbohydrate analytes, but also fluorescence changes in the visible range as reporting signals.

3.2 Results and discussion

3.2.1 Synthesis of NB-TTP

The NB-TTP design strategy (Figure 3.2) was similar as the previous one,[231] by choosing 4-amino-1,4-naphthlimide (Nap) as the fluorphore, benzyl boronic acid as the carbohydrate-binding moiety, and a terminal alkyne at TTP 5-position (M-TTP, Figure 1.15) for linkage. The final coupling step was designed through Cu(I)-catalyzed alkyne-azide cyclization (CuAAC),[247,249,259] which is a commonly used and efficient way of linking a large fluorophore group to biomolecules.

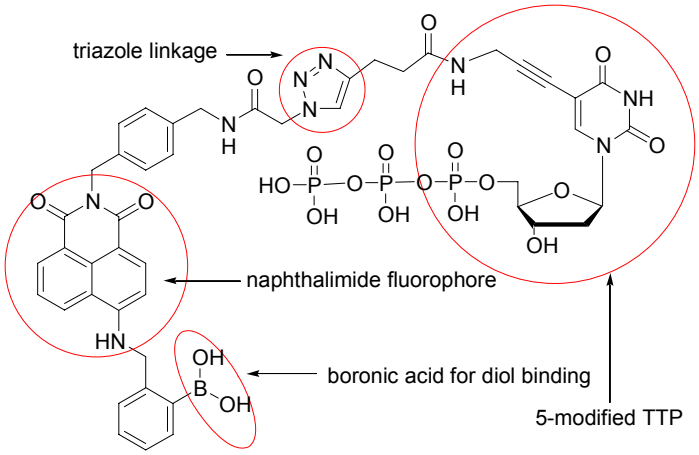

Figure 3.2 NB-TTP design strategy

The naphthlimide-based boronic acid (NB) **9** was synthesized in eight consecutive

steps starting from reduction of 4-(hydroxymethyl)benzonitrile with $LiAlH_4$, followed by Boc- protection of the -NH_2 group and methansulfonation of the –OH group to give **4**. Alkylation of 4-amino-naphthalimide with **4** and 2-bromobenzyl bromide sequentially yields the aromatic bromide **6**(aNap), which was subjected to Pd(II) catalyzed borylation in the subsequent step. The obtained boronic acid **7** (NB**7**) was deprotected of the Boc-group using TFA and then coupled with azidoacetic acid through EDCI to give boronic acid **9** with a terminal azide linker (Scheme 3.1).

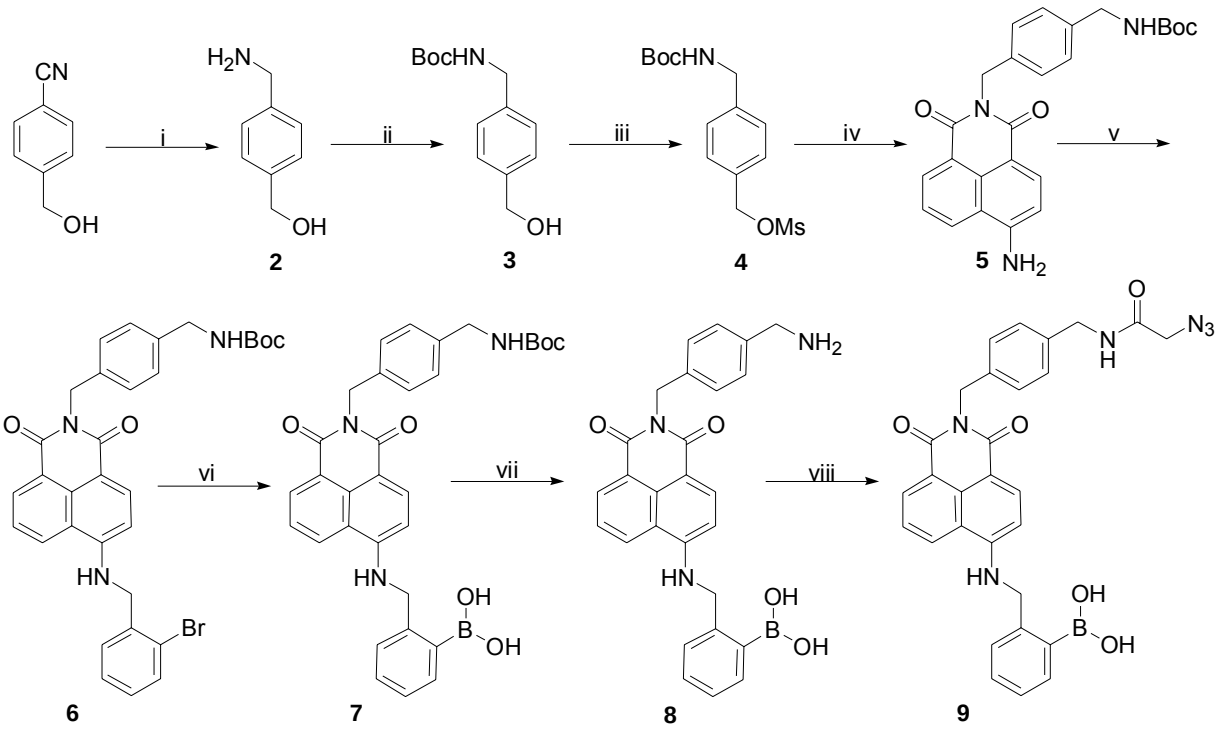

i) $LiAlH_4$, THF reflux, 98%; ii) di-*t*-butyl dicarbonate, Et_3N, THF, 94%; iii) MsCl, Et_3N, THF, 96%; iv) NaOMe, 4-amino-naphthalimide, DMF, 90%; v)NaH, 2-bromo-benzyl bromide, DMF, 40%; vi) Bis(neopentyl glycolato) diboron, $PdCl_2$(dppf), KOAc, DMSO, 45%; vii) TFA, CH_2Cl_2, 66%; viii) azidoacetic acid, EDCI, DMF, 98%

Scheme 3.1 Synthesis route of naphthalimide-based boronic acid (NB)**9**

During the experiment, it was observed in Step *vii* and *viii* that low yields were achieved with large amount of insoluble solid. Normally, both Boc- deprotection by TFA and EDCI coupled amide formation should give close to quantitative yield. Later treatment of the solid with saturated K_2CO_3 solution made it soluble in MeOH. It was revealed by ^{1}H-NMR their identity as the boronic acids **8** and **9**, respectively. Thus, the solubility of 4-amino derived phenylboronic acids of naphthlimide was greatly affected by pH. Acidic condition created by TFA or azidoacetic acid could significantly decrease the boronic acid solubility.

Before coupling boronic acid **9** with M-TTP, we performed a photostability test of it because photo bleaching is a common problem faced by many fluorophores.[260-261] It can be seen that the fluorescence intensity was constant at both tested emission wavelength (540 and 570 nm) and the fluorescence profiles overlap very well after constant irradiation for 1 h and 2 h (Figure 2.1). Thus, photo stability should not be a major issue in this case, which further improves the chance of success for this type of boronic acid.

In the coupling step, TBTA (*tris*-(benzyltriazolylmethyl)amine) was added as a Cu(I) ligand to accelerate the reaction rate and also protect the product from metal-catalyzed degradation (Scheme 3.2).[255,262-264] Due to the poor solubility of boronic acid under acidic condition, extraction of NB-TTP from reaction mixture was achieved using basic 0.1M NH_4HCO_3 buffer (pH 8.0). After HPLC purification of the buffer extraction, the lyophilized NB-TTP product was washed with MeOH and ice-cold water to remove the residual

amount of starting material **9**. Characterization of NB-TTP with ^{1}H-NMR in pure D_2O was not successful due to the continuous peaks in aromatic region (δ: 7-9 ppm) which were indistinct. The reason was assumed to be due to the naphthlimide aromatic stacking (π-π stacking) in aqueous environment. High quality of ^{1}H-NMR spectrum data were obtained by dissolving NB-TTP in a mixed solvent of D_2O/MeOD (2:1) with Watergate solvent suppression method. Surprisingly, NB-TTP had very low solubility in water despite of its highly hydrophilic triphosphate moiety. Using UV absorbance method, it was determined that the NB-TTP saturated aqueous solution had a concentration of lower than 170 μM. This is also good evidence to support the theory of naphthlimide stacking in aqueous solution. However, it was also observed that in the presence of MeOH the water solubility of NB-TTP was further decreased. In fact, dissolving NB-TTP in water followed by MeOH precipitation served as an excellent way for its purification. Thus, NB-TTP behaved as an amphiphilic molecule with one end of hydrophobic fluorophore and the other end of hydrophilic nucleoside triphosphate. In practice, vigorous shaking of the NB-TTP aqueous solution resulted in foaming similar to soaps or other detergent solutions. The identity of NB-TTP was also confirmed with mass spectrometry. With a calculated $[M-H]^{-1}$ of 1149.65, *m/z*: 1112.2 was obtained as the major peak in negative mode of ESI-MS, which corresponded to the fragment ion of $[M-H-2H_2O]^{-}$. While it is normal for boronic acid or nucleoside triphosphate to lose one molecule of H_2O in mass spectrum, it is not surprising to see two molecules of H_2O were lost in a boronic acid- nucleoside triphosphate conjugate molecule.

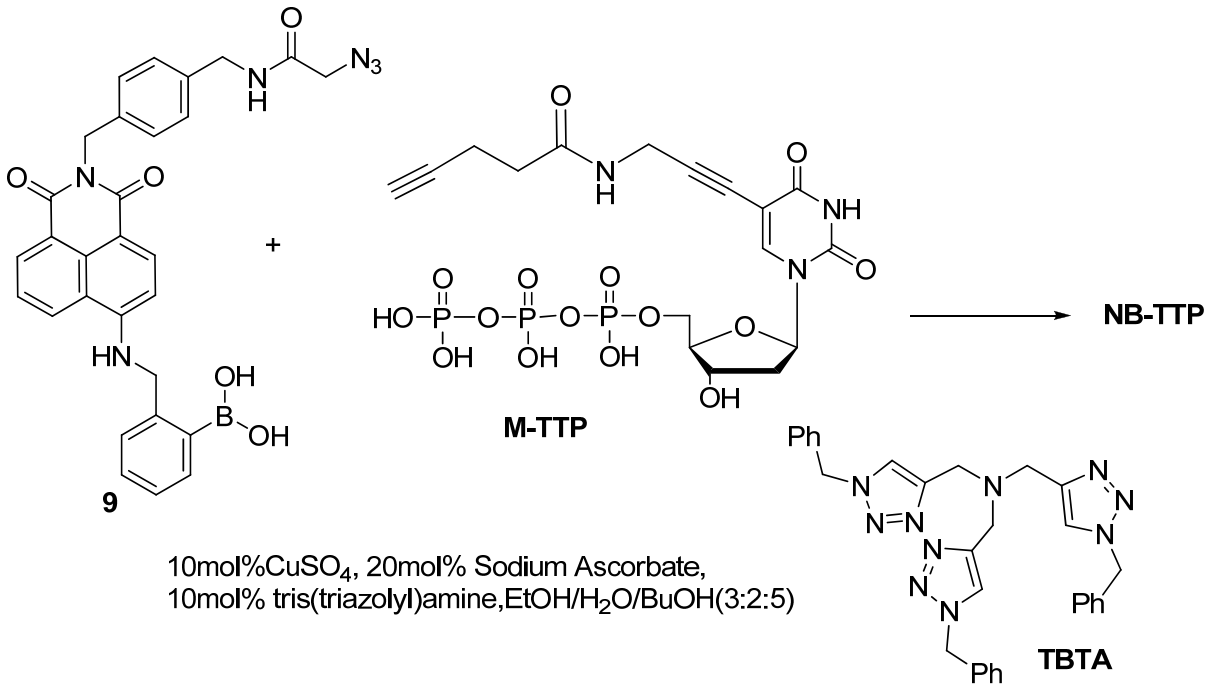

Scheme 3.2 Synthesis of NB-TTP using CuAAC

Since the newly designed NB-TTP was featured with its unique fluorescence properties change upon carbohydrate binding, fructose was chosen as the model molecule for validation test before its incorporation into DNA sequences. Hence, as shown in Figure 3.3 (a), the fluorescence intensity of NB-TTP increased upon D-fructose addition in a concentration dependent fashion (λ_{ex}: 490 nm, λ_{em}: 540 nm). Thus, the binding constant K_a was calculated using the equation described in Section 2.5 in Chapter 2.[265] The K_a was determined to be 73 ± 5 M^{-1} from triplicate experiments. Such results demonstrate that even after conjugation with a nucleobase (thymidine), the naphthalimide-based boronic acid (NB) maintains its ability to change fluorescent

properties upon sugar binding.

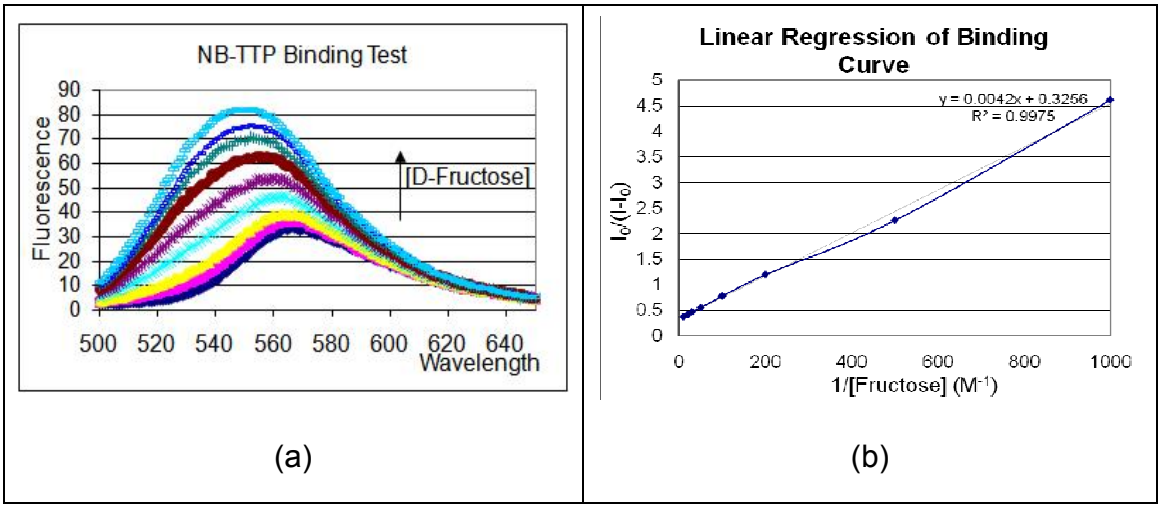

Figure 3.3 Fluorescent binding tests of NB-TTP with D-fructose (λ_{ex}: 490 nm) in 0.1M phosphate buffer (pH 7.4)

3.2.2 Enzymatic studies of NB-TTP

Next we studied whether this NB-TTP can be incorporated into DNA in an enzyme-catalyzed reaction. In this study, NB-TTP was incorporated into a DNA sequence of 14-nt primer (5'-TAGCGGGTTGCTGG-3', calc. MW: 4350.8) complemented with a 21-nt template (5'-GGTTCCACCAGCAACCCGCTA-3', calc. MW: 6336.2) through Klenow Fragment catalyzed primer extension. The primer and template sequences were designed in such a way that the first base to be incorporated is a T, which led to a "none-or-all" case in the extension. The results were analyzed by both MALDI mass spectrometry and gel electrophoresis methods.

In the control reaction, full extension of the primer using natural dNTPs yielded a DNA

with *m/z*: 6520.4 (calculated $[M+H]^+$: 6519.3) as the major product peak in MALDI-MS (Figure 3.4). The minor peak of *m/z*: 6850.6 could have resulted from a non-specific extension with an extra nucleotide. In the NB-TTP (replacing TTP) reaction, primer extension yielded a DNA with *m/z*: 7142.8 as the major product peak (Figure 3.5). Since the calculated $[M+H]^+$ is 7186.5, it is reasonable to assign the detected peak as the deborylated NB-DNA sequence (calc. $[M+H-HBO_2]^+$: 7142.5). In order to further determine whether the deborylation happened during primer extension reaction or during ionization in MALDI-MS, another sample of NB-TTP extension DNA sequence treated with H_2O_2 was analyzed under same condition. In this case, a new peak of *m/z*: 7160.6 was observed (Figure 3.6), which is assigned as the oxidative deborylated NB-DNA sequence (calc. $[M+H-HBO]^+$: 7158.5). Thus, it was concluded that the boronic acid of NB-TTP was intact after incorporation into the DNA sequence and deborylation happened during the ionization process, which is very common with arylboronic acids.

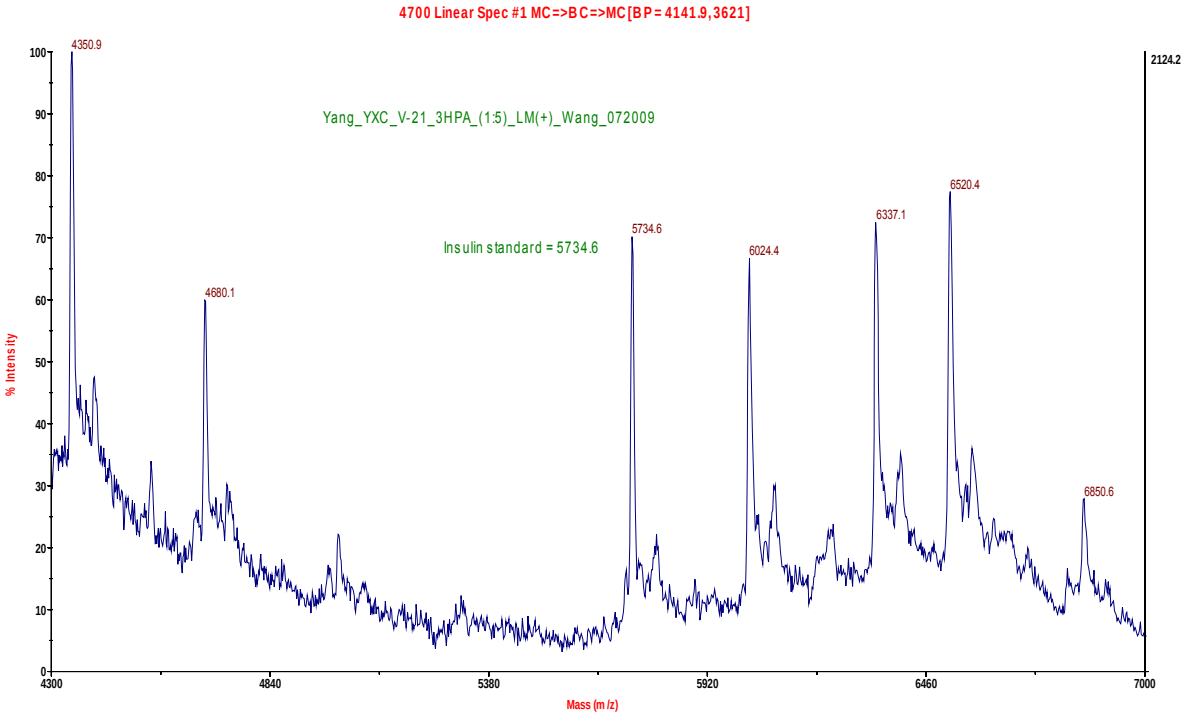

Figure 3.4 MALDI-TOF-MS of primer extension using natural TTP

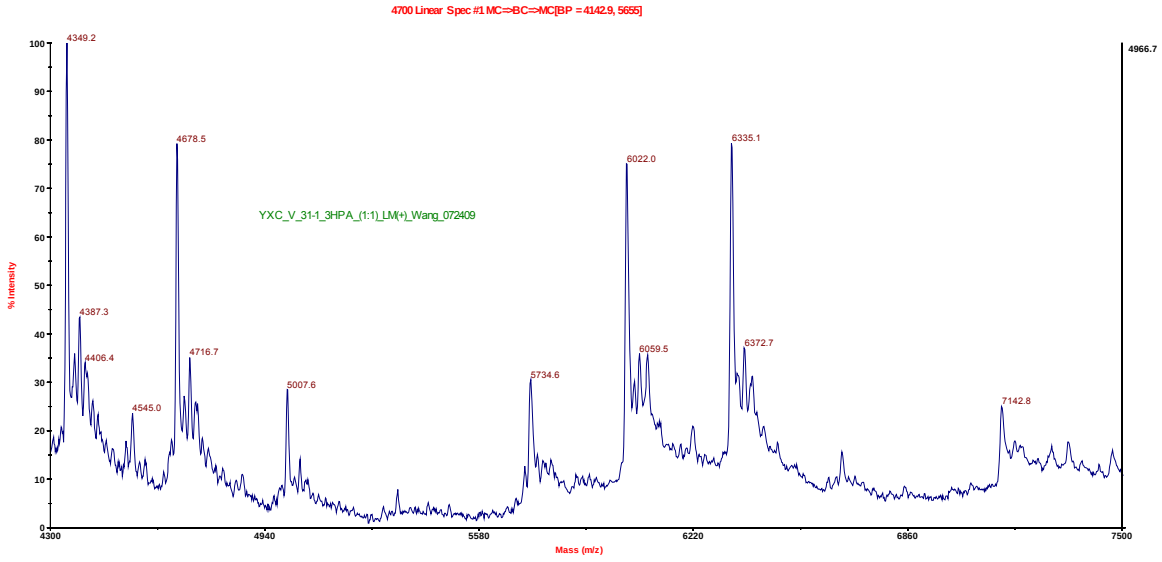

Figure 3.5 MALDI-TOF-MS of primer extension using NB-TTP

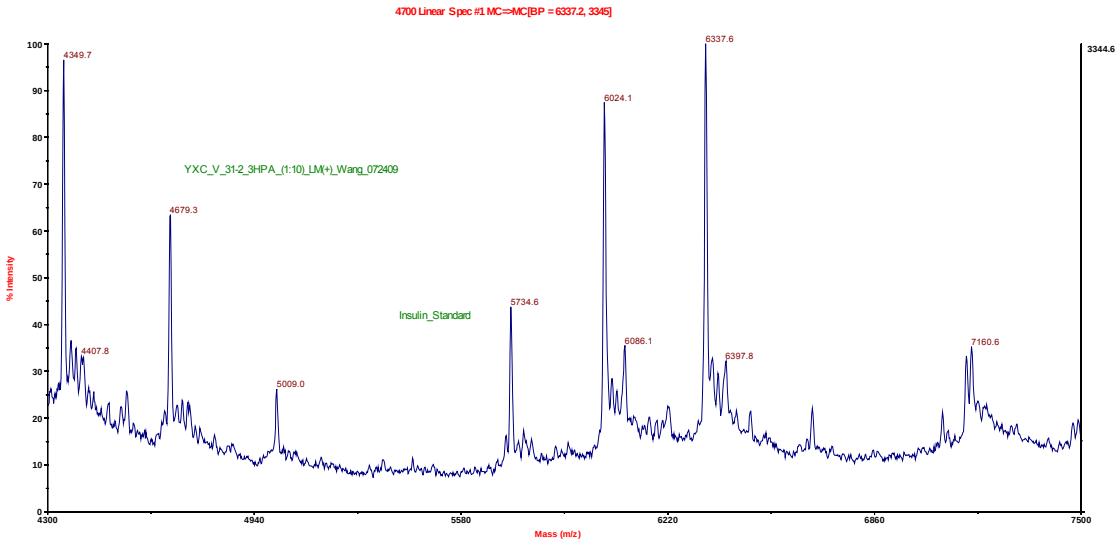

Figure 3.6 MALDI-TOF-MS of primer extension using NB-TTP, followed by treatment with H_2O_2

The DNA from primer extension using NB-TTP was also studied using gel electrophoresis. The 14-nt primer was labeled with ^{32}P at the 5'-end using γ-^{32}P-ATP and T4 kinase (Figure 3.7, Lane 1). Negative control reactions without the Klenow fragment (Figure 3.7, Lane 2) and without dNTPs (Figure 3.7, Lane 3) showed no full length DNA sequence. On the other hand, positive control reactions in the presence of both the enzyme and natural dNTPs (Figure 3.7, Lane 4) showed full length DNA. The shorter length of DNA in the Lane 3 without dNTPs could result from the 3'→5' exonuclease activity of Klenow fragment.[266] Primer extension using NB-TTP and three other natural dNTPs gave a full length of DNA sequence (Figure 3.7, Lane 5). Its smear band could be due to the interaction of the boronic acid moiety with the gel matrix or the DNA conformation disrupted by the large naphthalimide moiety. Thus, both mass spectrometry and gel electrophoresis results indicated that NB-TTP was recognized by

DNA polymerase as a substrate and incorporated into DNA.

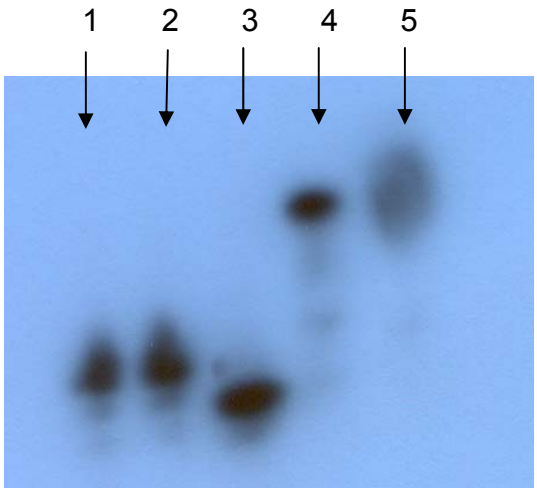

Figure 3.7 Primer extension analyzed on 15% PAGE:

1) primer only; 2) reaction without enzyme; 3) reaction without dNTPs; 4) reaction with natural dNTPs; 5) reaction with NB-TTP and other dNTPs

3.3 Conclusion

In conclusion, we have successfully synthesized a naphthalimide-based boronic acid modified TTP (NB-TTP) in totally 13 steps. The chosen boronic acid moiety displayed long-wavelength fluorescence emission, good photo stability, and fluorescent properties changes upon carbohydrate binding. The features were retained after conjugating the boronic acid to TTP moiety. Enzymatic studies of the NB-TTP showed that it can be successfully recognized by DNA polymerase such as the Klenow fragment as the substrate. The NB-TTP incorporated DNA sequences were analyzed by both mass spectrometry and gel electrophoresis methods, which both gave positive results that supported each other.

4. FLURESCENCE PROPERTY STUDIES OF NB-TTP-MODIFIED DNA

4.1 Introduction.

In addition to their critical roles in storing genomic information, DNA molecules are also very important in the development of aptamers,[267-269] nanoelectronic assemblies,[270] nanosensors,[271] nanoclusters,[272-273] nanocomputing,[274-275] and DNA rotary machine,[276] to name a few.[277] DNA functionalization brings in additional properties for broadened applications. For example, gold-nanoparticle functionalized DNA assemblies have been used in sensor development with extraordinary sensitivity;[278] and side-chain functionalized DNA has been used in aptamer selection with improved affinity and properties.[279-283]

Boronic acid-modified DNA may have applications in carbohydrate and glycoprotein sensing as well as the construction of other DNA assemblies with unique properties. For example, nucleic acid and peptide-templated multi-boronic acid compounds are artificial lectin mimics;[227,230,284-285] boronic acid-containing compounds have been used in the preparation of polymers with reversible properties;[286-289] boronic acid-modified proteins can be used as lectin mimics with improved affinity and for protein purification;[233] and boronic acid-containing polymers have been used for the development of glucose-sensitive insulin release systems.[290-291] Among them, boronic acid sensors with both nucleic acid- and peptide-backbone structure were created in a combinatorial fashion as described in introduction part. The difference between them lies in that nucleic

acid-base boronolectins (NBLs) are selected from a random pool of molecular library, while peptide-based boronolectins (PBLs) are constructed in a pattern-based detection array method that mimics mammalian olfactory sensing system. It is almost certain that the biomolecular backbone structure and the boronic acid positioning would affect or even determine the glycan binding affinity and selectivity. Therefore, fundamental studies of such in NBLs are quite important. However, so far no such studies have been reported, probably because that the selection nature of the SELEX method doesn't require too much detailed structural information. However, for the purpose of rational construction of NBLs with intrinsic fluorescence, such information could be very critical. For example, due to the self-quenching of fluorophores and possible destabilization of sensor-target complex by fluorophores, increasing the labeling density on nucleic acid backbone doesn't necessarily lead to higher fluorescence intensity and binding affinity.[292-295]

4.2 Results and discussion

4.2.1 Double stranded NB-DNA binding tests

After incorporating NB-TTP into the DNA sequence, we were interested in studying whether sugar addition to the DNA solution would still cause fluorescence property changes. Since dNTPs and oligonucleotides are known to quench fluorescence,[296-298] the retention of NB-TTP's fluorescent property in DNA was uncertain. The DNA was synthesized in the same method of using Klenow fragment. For every full-length double stranded DNA, only one NB-TTP was incorporated for 14nt-primer extension with the 21-nt template. After purification with membrane filtration and ethanol precipitation, the

NB-DNA was dissolved in 0.1M phosphate buffer (pH 7.4) to make a 5 μM solution, which was based on the theoretical yield of DNA synthesis. Fructose concentration was increased from 1 to 100 mM. The fluorescence intensity of NB-DNA increased by about 1.5-fold upon fructose addition (λ_{ex}: 490 nm, λ_{em}: 540 nm) (Figure 4.1). Hence, it showed that even after incorporation into DNA sequence, the boronic acid fluorescence properties were still well retained. This is the very first example of side-chain functionalized DNA showing intrinsic fluorescent property changes upon sugar binding. Similar modified DNA will be very useful in the synthesis of DNA molecules/assemblies for various applications including sensing of carbohydrates, glycolipids, and glycoproteins.

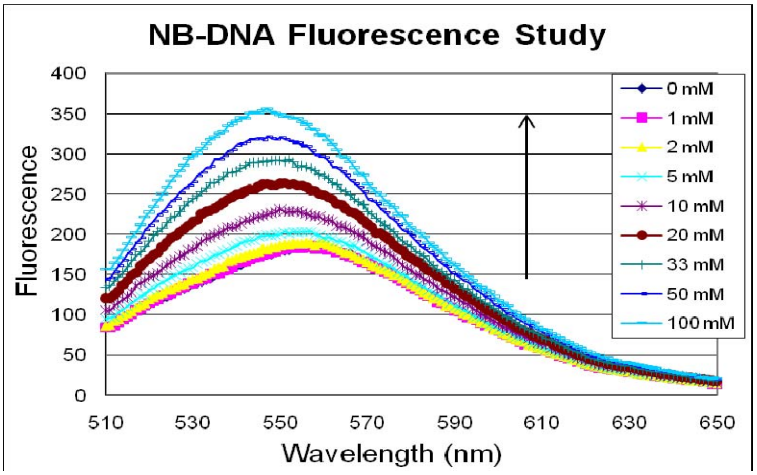

Figure 4.1 Fluorescent binding tests of NB-DNA (0.5 μM) with D-fructose in 0.1M phosphate buffer (pH 7.4)

Based on preliminary NB-DNA fluorescence binding studies, more DNA sequences are designed to further analyze factors affecting DNA fluorescent properties. To minimize

the changes of the DNA sequences, Templates 1-7 were designed in a way of having two adenosine on the 5'-end end separated by 0-6 bases while the rest of bases were kept the same (Table 4.1). The 21nt-template used for previous enzymatic studies were designated as Template 0 for control. Thus, for primer extensions, two NB-TTPs would be incorporated to the 14nt-primer with 0 to 6 bases of distance spacing. After that, the double stranded bisboronic acid NB-DNA would be tested of its fluorescence properties with the model carbohydrate fructose.

Primer	3'-GGTCGTTGGGCGAT-5'
Template 0	5'-GGTTCCACCAGCAACCCGCTA-3'
Template 1	5'-GGTTCCAACCAGCAACCCGCTA-3'
Template 2	5'-GGTTCACACCAGCAACCCGCTA-3'
Template 3	5'-GGTTACCACCAGCAACCCGCTA-3'
Template 4	5'-GGTATCCACCAGCAACCCGCTA-3'
Template 5	5'-GGATTCCACCAGCAACCCGCTA-3'
Template 6	5'-GAGTTCCACCAGCAACCCGCTA-3'
Template 7	5'-AGGTTCCACCAGCAACCCGCTA-3'

Table 4.1 Designed DNA template sequences for primer extension reactions

Before the carbohydrate-binding test, it was necessary to verify the NB-TTP enzymatic incorporation efficiency again. Even thought previous chapter has already demonstrated that single NB-TTP could be successfully incorporated through enzymatic DNA polymerization, the bulkiness of the first incorporated naphthalimide moiety on DNA could impose a possible steric hinderance to the incorporation of the second NB-TTP. Fortunately, from the gel electrophoresis results, it can be seen that full-length extensions were achieved with all the DNA templates as the major bands for each lane

(Figure 4.2). Interestingly, the positive control using a NB-TTP/natural TTP mixture showed two fully extended DNA bands with Template 1(Figure 4.2, Lane 3). Due to the larger molecular weight of NB-TTP than that of TTP, the faster moving band could be assigned as full-length DNA of incorporation of two TTP while the slower moving band could be full-length DNA with the incorporation of at least one NB-TTP. The smear of the full length NB-DNA bands (Figure 4.2, Lane 4-10) were probably due to the interactions of boronic acid with gel matrix or the DNA conformation disrupted by the large naphthlimide moiety, which corresponded well with previous enzymatic study PAGE results (Figure 3.8).

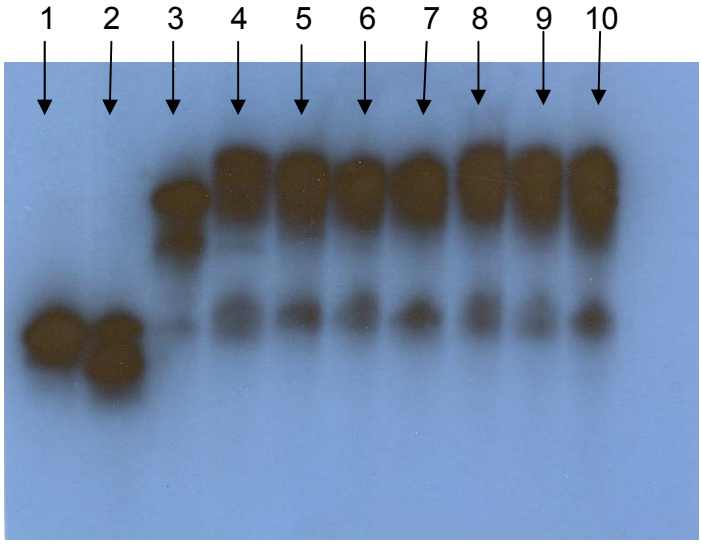

Figure 4.2 15% PAGE analysis of primer extensions with Templates 1-7

1) primer only; 2) reaction without dNTPs; 3) Template 1 extension with NB-TTP +TTP; 4) Template 1 extension with NB-TTP; 5) Template 2 extension with NB-TTP; 6) Template 3 extension with NB-TTP; 7) Template 4 extension with NB-TTP; 8) Template 5 extension with NB-TTP; 9) Template 6 extension with NB-TTP; 10) Template 7 extension with

NB-TTP

The same model carbohydrate, fructose, was chosen as the model for the fluorescent property tests. Double stranded NB-DNA (NB-dsDNA) sequences were generated through primer extension reactions with primer/template ratio of 1:1 and no heat denaturation before the binding tests. Template 0 was used as the control sequence. Fluorescence intensity increases of the various NB-dsDNA sequences upon addition of 0.1 M fructose examined. From the testing results (Figure 4.3), it could be seen that DNA 5 showed significantly higher fluorescence intensity increase than the control (DNA 0), while DNA 7 showed lower fluorescence increase than the control. Meanwhile, the comparison of any other two DNA sequences showed no significant differences due to the relatively large experimental errors. Therefore, it indicates at least to some extent that the number of boronic acids, the distance spacing between them and the DNA sequence do contribute to difference observed in binding. However, those DNA sequences were not purposely designed to have significant intrinsic difference in fructose binding pattern. This is only a preliminary proof-of-concept experiment study.

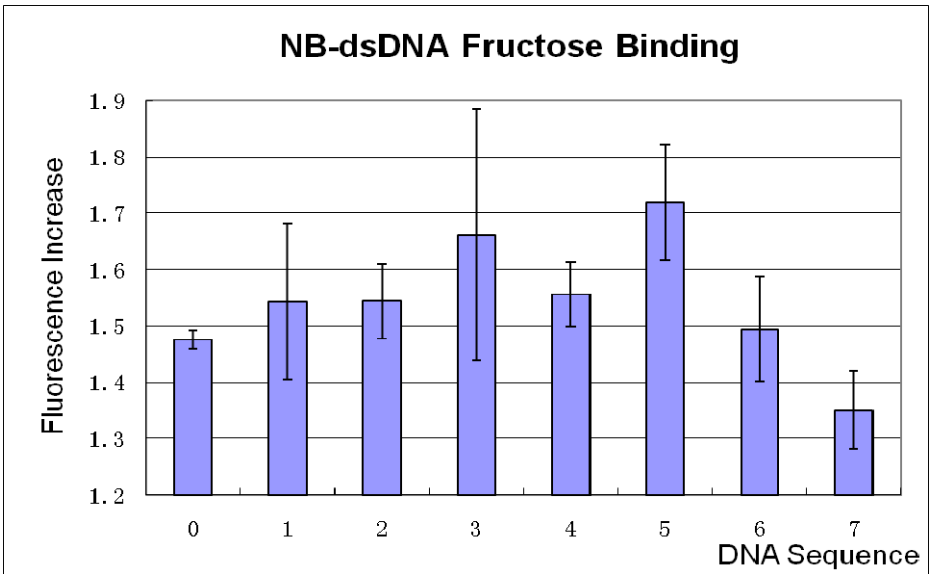

Figure 4.3 Fluorescent binding tests of NB-dsDNA (Template 0~7) with D-fructose (λ_{ex}: 490 nm) in 0.1M phosphate buffer (pH 7.4)

4.2.2 Single stranded NB-DNA binding tests

For the sequence-dependent fluorescence studies of the single stranded DNA, three disaccharides, lactose, maltose and sucrose were chosen as the model carbohydrates. Single stranded NB -DNA (NB-ssDNA) was created through primer/template ratio of 3:1 and heat denaturation before binding. It was expected that the bis-boronic acid on DNA backbone would have more discrimination towards disaccharides with relatively larger molecule and the ssDNA could provide more flexibility in the recognition process. The test results (Figure 4.4) showed that DNA 1 and DNA 5 have significant preference of lactose to maltose and sucrose while others didn't. In addition, DNA 5 still showed higher

fluorescence intensity increase upon fructose binding than DNA 0 and DNA 7, which was similar to the result of dsDNA binding tests (Figure 4.3). Thus, even though the differences between the signal intensity increase are relatively small (<30%), they were indeed reproducible results. Of course, the nature of boronic acid itself still played the major role in carbohydrate recognization in this case, as compared to the effect of DNA sequences.

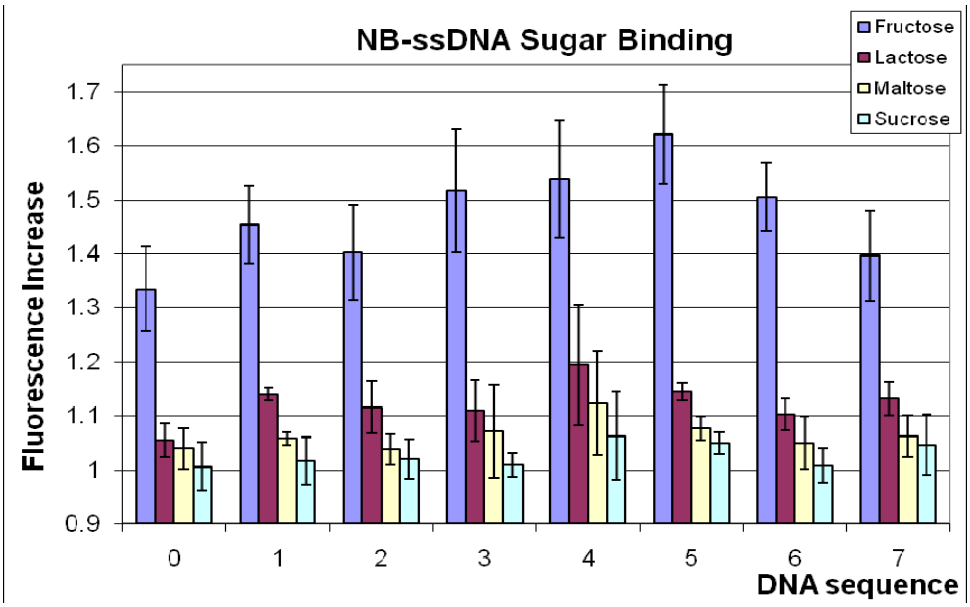

Figure 4.4 Fluorescent binding tests of NB-ssDNA with carbohydrates (λ_{ex}: 490 nm) in 0.1M phosphate buffer (pH 7.4)

4.2.3 Optical Properties Comparison Between Naphthalimide (Nap), aNap, NB, NB-TTP, NB- dsDNA and NB-ssDNA

Throughout the whole process of systematic modification of the fluorphore 4-amino-1,8-naphthalimide (Nap), the optical properties of Nap has been changed along

each modification step (*e.g.* λ_{max} and Abs of UV absorbance, λ_{max} and emission intensity of fluorescence). Thus, it would be necessary to evaluation the optical effect of each modification step. Thus, alkylated 4-amino-1,8-naphthalimide (**6,** aNap), NB (**7**), NB-TTP, NB-dsDNA0, NB-TTP-dsDNA5 and NB-TTP-ssDNA5 were chosen to evaluate the effect of alkylation, borylation, TTP conjugation, DNA incorporation, on the optical properties of Nap (Table 4.2).

	Nap	aNap (**6**)	NB(**7**)	NB-TTP	NB-dsDNA0	NB-dsDNA5	NB-ssDNA5
UV λ_{max}	434±1	445±1	490±1	495±1	473±1	468±1	470±1
UV Abs at λ_{max}	0.022±0.001	0.013±0.001	0.020±0.001	0.028±0.001	0.012±0.001	0.019±0.001	0.019±0.001
Fluorescence λ_{max}	541±1	529±2	574±1	572±1	531±3	535±1	533±2
Fluorescence Intensity at λ_{max}	480±6	186±4	235±8	478±11	878±102	610±23	852±58
Integrated Fluorescence Intensity	35241±387	13128±156	16838±537	36693±786	71971±7430	54586±2035	72029±4917
Quantum yield (Φ)	0.013±0.004	0.008±0.003	0.007±0.002	0.011±0.003	0.049±0.015	0.023±0.007	0.031±0.009

Table 4.2 Optical effect of Nap modifications

(Experiments in triplicate were conducted in 0.1M phosphate buffer pH 7.4, with 0.01% DMSO (for Nap and aNap), or 0.01% MeOH (for NB(**7**)); [Nap] = [aNap] = [NB] = [NB-TTP] = 2 μM; NB-DNA was prepared in the same way as for binding tests, theoretical [NB-dsDNA0] = [NB-dsDNA5] =[NB-ssDNA5] = 1.4 μM)

From the results listed in Table 4.2, it can be seen that the magnitude of the intensity increase of both UV absorbance (2-fold) and fluorescence (3-fold) were decreased after alkylation of Nap. Besides, alkylation of Nap resulted in a red-shift by about 10 nm in its UV λ_{max} and a blue-shift by about 10 nm in fluorescence λ_{max}. In contrast, the borylation of aNap increased both the UV (1.5-fold) and fluorescence (1.3-fold) intensities, while at the same time resulted a λ_{max} red-shifted of about 40 nm in both UV and fluorescence, Conjugation of NB to TTP moiety didn't affect UV significantly, but increased the fluorescence intensity by about 2-fold. Such results indicated that increasing hydrophobicity (alkylation) of Nap could lead to a decrease in both UV and fluorescence intensities, while increasing hydrophilicity (borylation and TTP conjugation) could lead to UV and fluorescence intensity increases (Fig 4.5).

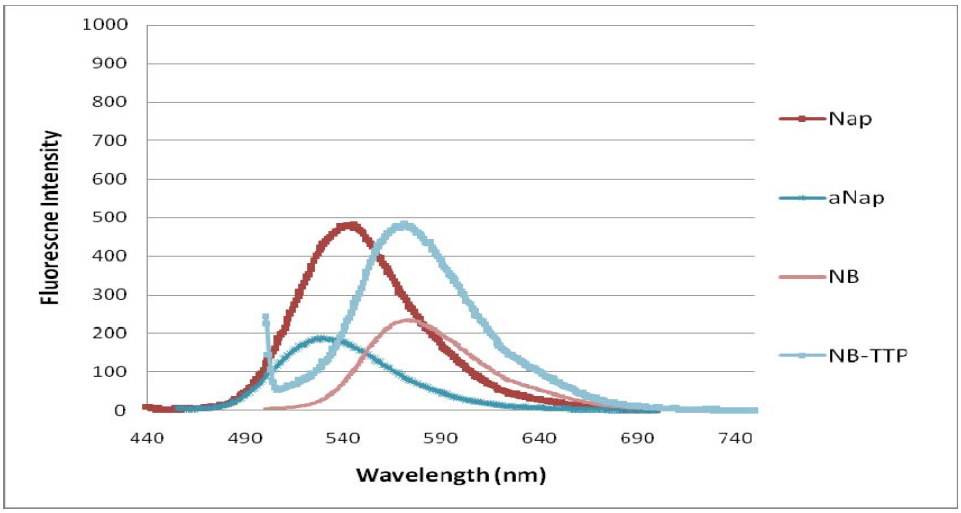

Figure 4.5 Fluorescent profiles of Nap, aNap, NB and NB-TTP at 2 μM in 0.1 M phosphate buffer pH 7.4 with 0.01% DMSO (for Nap and aNap) or 0.01% MeOH (for NB(**7**))

After chemical modification, the optical effect of DNA incorporation of NB-TTP was studied. Using DNA sequence 0 with only one T incorporation, it was surprising that the fluorescent intensity of NB-TTP increased by more than 2-fold after DNA incoporation. This could be partially due to the further increased hydrophilicity of NB. Both UV and fluorescence λ_{max} blue-shifted (20 nm for UV, 40 nm for fluorescence) after DNA incorporation. It should also be noted that the quantum yield of NB-TTP also increased by more than 3-fold after incorporation into dsDNA0. However, NB-TTP incorporation into DNA sequence 5 with incorporation of two T bases didn't increase the fluorescent intensity further. Instead, it was decreased by 1.25-fold as compared to that of NB-dsDNA0. This phenomenon was probably due to the self-quenching effect of the two neighboring NB moieties on the same dsDNA sequence. This assumption was further supported by the fact that the fluorescent intensity of NB-ssDNA5 was 0.4-fold higher than NB-dsDNA5, probably because of decreased self-quenching effect on more flexible ssDNA backbone. The fluorescent profile comparison of NB-TTP DNA incorporation is shown in Fig 4.6.

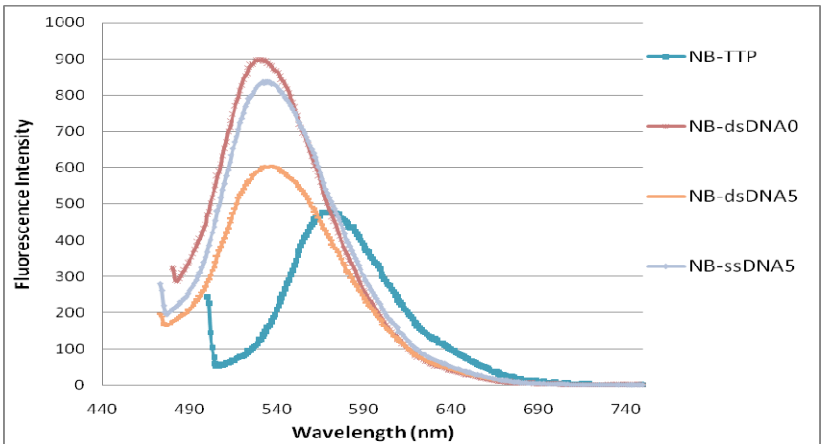

Figure 4.6 Fluorescent profiles of NB-TTP (2 μM), NB-dsDNA0, NB-dsDNA5 and NB-ssDNA5 (1.4 μM) in 0.1 M phosphate buffer pH 7.4

In all, the effect of chemical modification on fluorphore Nap was tested and evaluated. The general trend is that increasing hydrophobicity of Nap would decrease its fluorescent intensity, while increasing its hydrophilicity would increase its fluorescent intensity. The self-quenching effect of two neighboring NB on the same DNA backbone was observed, and the effect could be partially decreased by melting dsDNA into ssDNA.

4.3 Conclusion

In conclusion, the enzymatic activity of NB-TTP as DNA polymerase substrate has been further confirmed by gel electrophoresis. Even for two NB-TTPs to be continuously incorporated, full-length DNA polymerization was obtained. Furthermore, fluorescent binding studies indicated that binding affinity or selectivity of DNA-based boronic acid sensors toward carbohydrates could indeed be affected by the number of boronic acid

moieties, the spacing between them and DNA sequence to certain extent. Furthermore, the spectroscopic effects of chemical modification on Nap and DNA incorporation of NB-TTP were also evaluated. It was proposed that hydrophobicity/hydrophilicity change of Nap could be the reason of the fluorescence wavelength shift and intensity change. The self-quenching effect of two NB moieties on the same DNA backbone was also observed and such effect could be partially alleviated by dissociating dsDNA into ssDNA. Again, the initial DNA sequence (14nt-primer/21-nt template) was almost a random choice and modified with minimal changes to have two NB-TTPs incorporated. These preliminary proof-of-concept studies could provide valuable and insightful information for future rational design of nucleic acid-based boronolectins (NBLs) with intrinsic fluorescence change towards carbohydrates, glycoprotiens or glycolipids.

5. CELL IMAGING STUDIES USING NB-TTP

5.1 Introduction

Inspired by the Hageman's boronic acid-cell surface labeling studies[196-198] and encouraged by our group's success in developing fluorescent diboronic acids recognizing sialic acid on tumor cell membrane,[142,199] further work to explore the potential applications of the synthesized NB-TTP was undertaken. There are several considerable advantages of utilizing NB-TTP to label cells. First, the long excitation and emission wavelengths (λ_{ex}: 490nm, λ_{em}: 540 nm) of NB-TTP fluorophore avoid the potential problems of photodamages and high background noises commonly caused by ultraviolet (UV: 200-400 nm) illumination.[299-300] Besides, NB-TTP also has very close excitation/emmission wavelengths to FITC filter set (495 nm/520 nm), which makes cell labeling easily observable under fluorescent microscope. Second, napthalimide-based compounds have previously been tested in cancer[301-304] and virus infection[305-307] therapy, and cell-imaging study,[308-312] but none of those had boronic acid moieties attached to. The success of incorporating boronic acid into cells could provide valuable information for other therapeutical research such as living cell glycan detection[308] or boron-neutron capture therapy (BNCT).[162,313-315] Third, with the TTP-moiety attached to the fluorophore, we expected that there be the possibility of the DNA duplication machinery of dividing cells to incorporate NB-TTP into their genomic sequences, since it is known that NB-TTP is recognized as DNA polymerase substrate in *in vitro* studies.

However, there are also several issues that need to be taken into consideration

before NB-TTP cell labeling experiments. Since the triphosphate group of NB-TTP is negatively charged under physiological pH condition, the cell permeability of NB-TTP could be a hurdle. Also, the cytotoxicity of NB-TTP is unknown, given the large planar structure of the napthalimide moiety is found in anti-cancer reagents.[301,303-304] Three possible scenarios were expected of the labeling studies: 1) NB-TTP could not enter into the cell, but stay outside and label the cell-surface glycans with the boronic acid moiety; 2) NB-TTP could enter into the cell cytoplasma due to its amphiphilic nature, but could not pass the nuclear membrane; 3) NB-TTP could diffuse across both the cellular and nuclear membrane, and even accumulate inside the nucleus either through incorporation into genomic DNA , intercalation between DNA base through stacking, or simply staining chromatin proteins like histone through ionic interactions. All those possible results could provide valuable information for further experimental design. In this chapter, HeLa cells were chosen as the labeling target of NB-TTP. Nap and boronic acid **9** (Scheme 3.1), with no TTP moiety, was used as the control labeling compound.

5.2 Results and discussion

Nap, NB**9** and NB-TTP at various concentrations (50, 25, 12.5, 6.25, 0 μM) were added into cell culture medium containing HeLa cells in a 24-well plate with coverslips. Coverslips from the wells were taken at different time intervals (2, 5, 9, 17, 24 h), fixed to slides and observed under the Zeiss Axiovert 400M inverted epifluorescence microscope using FITC filter. From the cell imaging pictures taken (Table 5.1), it was observed that

shortly after 2 h of incubation, all compounds (Nap, NB**9** and NB-TTP successfully labelled HeLa cells. As expected, Nap labeled HeLa in a whole-cell pattern with intense fluorescence. This might be because of that Nap has smaller molecular weight and high hydrophobicity, which makes it capable of quick diffusing through cellular and nuclear membrane into cytoplasma and nuclear area. A comparison of labeling results between 50 μM (Table 5.1 c and e) and 25 μM (Table 5.1 d and f) suggested a concentration-dependent staining pattern. At this stage, however, no clear distinction of the labeling style between control (NB**9**) and NB-TTP could be seen since both compounds stained the cells in a homogeneous way and the fluorescence intensities in cytoplasm and in nucleus were comparable. After 5 h of incubation, no significant change of Nap labeling pattern has been observed, but NB**9** seems to accumulate in cytoplasm more than in nucleus (Table 5.2 c and d) while NB-TTP still labeled cells in a non-selective way (Table 5.2 e and f). After 9 and 17 h, it was clear that the NB**9** was significantly more localized in the cytoplasm (Table 5.3 c; Table 5.4 c) while the nucleus showed much lower fluorescence staining. In contrast, NB-TTP showed much more accumulation in the nucleus area with some punctuate-labeling pattern (Table 5.3 e; Table 5.4 e). Similar punctuate-labeling pattern was observed with Nap labeling consistantly (Table 5.1-5.5 a and b). From the imaging results after 24 h incubation, it could be seen that NB-TTP still labeled the cell nucleus with higher fluorescence intensity (Table 5.5 b) while control compound showed few surviving cells (Table 5.5 e). Besides, it also indicated that NB-TTP was stable enough to last for at least 24 h under

cell incubation condition with persistent staining pattern.

Table 5.1 HeLa cell imaging 2 h after incubation
[exposure time 2.54s with FITC filter 495/520]

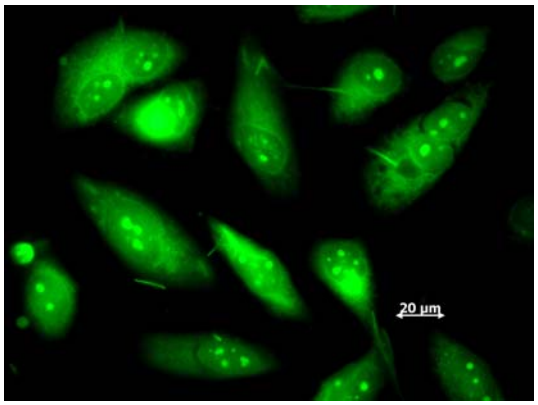

(a) Nap 50 µM

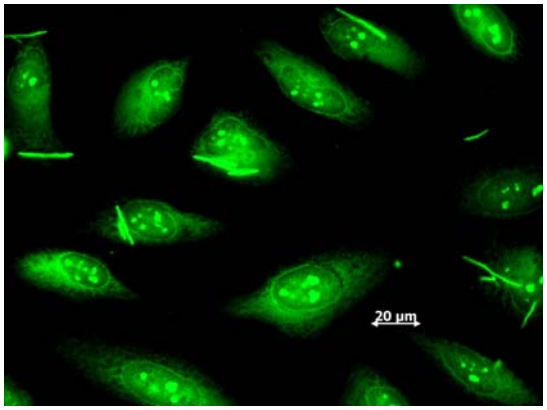

(b) Nap 25 µM

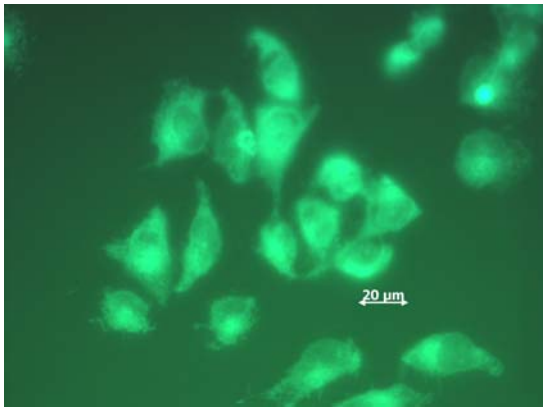

(c) NB**9** 50 µM

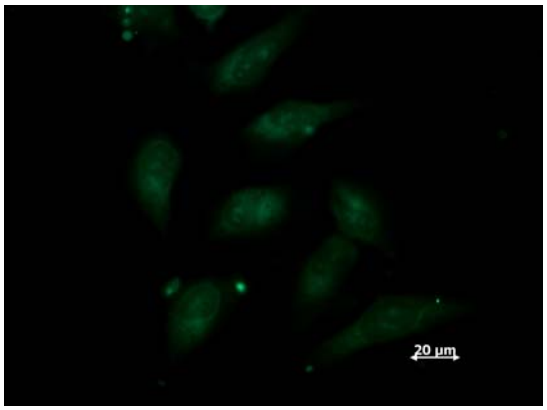

(d) NB**9** 25 µM

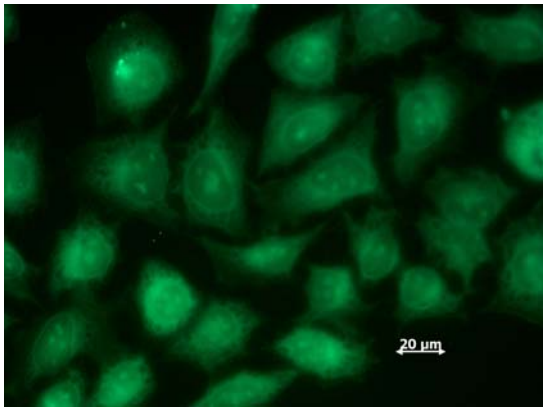

(e) NB-TTP 50 µM

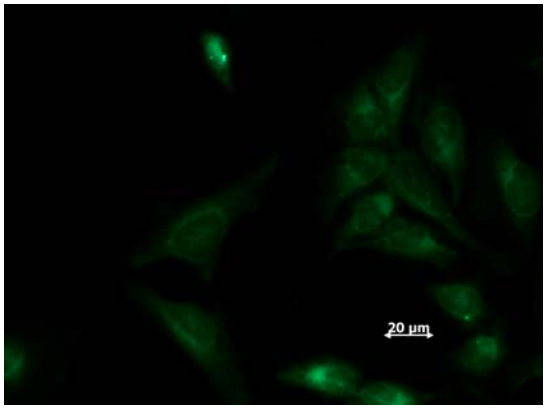

(f) NB-TTP 25 µM

Table 5.2 HeLa cell imaging 5 h after incubation
[exposure time 2.54s with FITC filter 495/520]

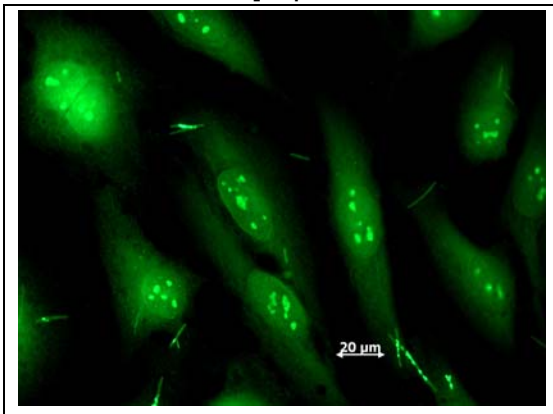

(a) Nap 50 µM

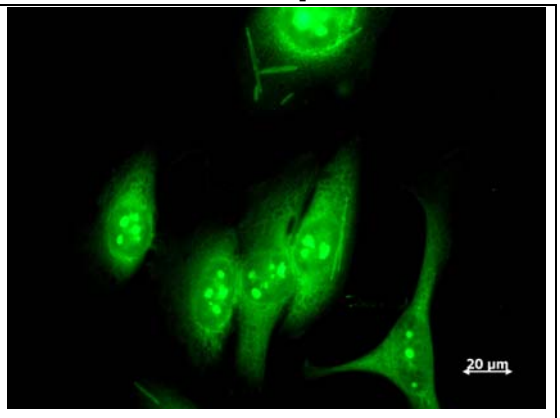

(b) Nap 25 µM

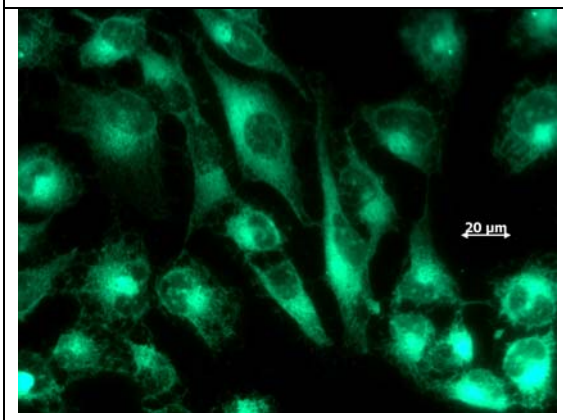

(c) NB**9** 50 µM

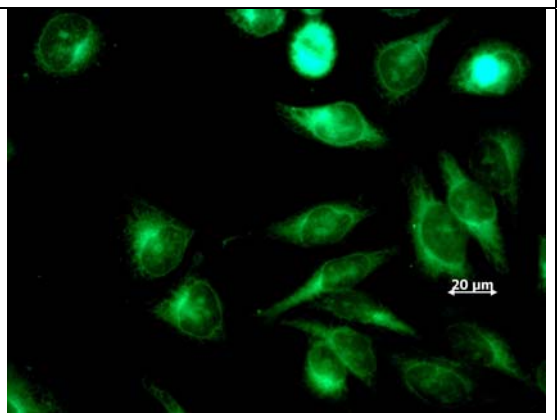

(d) NB**9** 25 µM

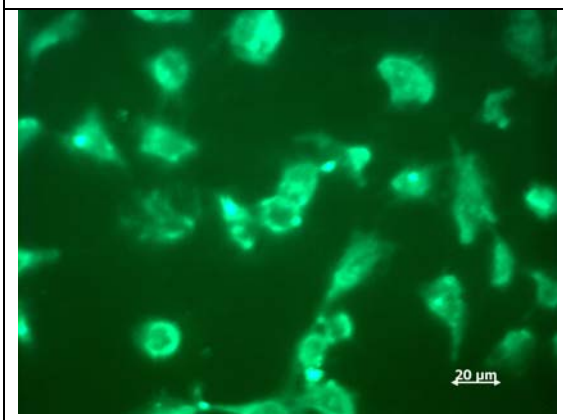

(e) NB-TTP 50 µM

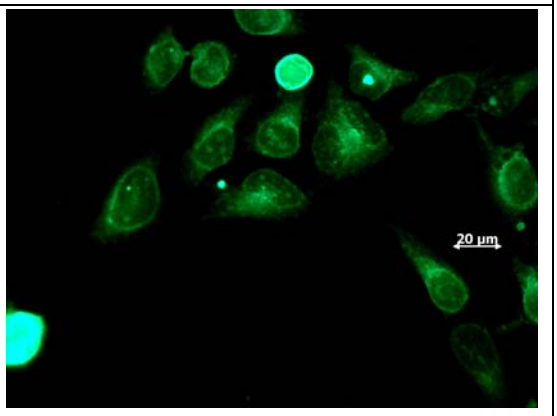

(f) NB-TTP 25 µM

Table 5.3 HeLa cell imaging 9 h after incubation
[exposure time 2.54s with FITC filter 495/520]

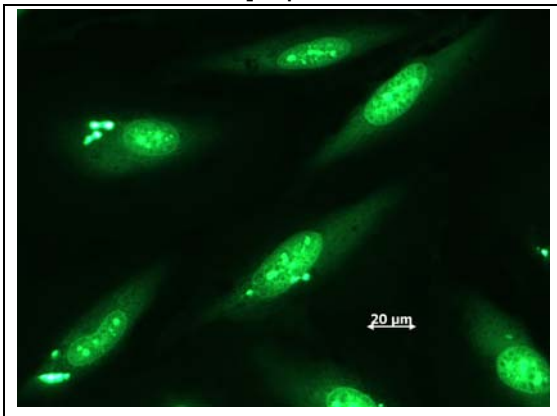

(a) Nap 50 µM

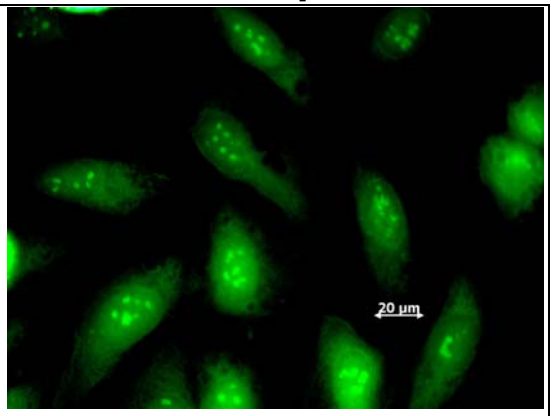

(b) Nap 25 µM

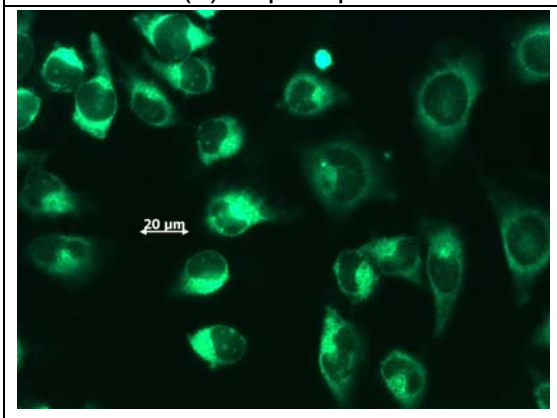

(c) NB**9** 50 µM

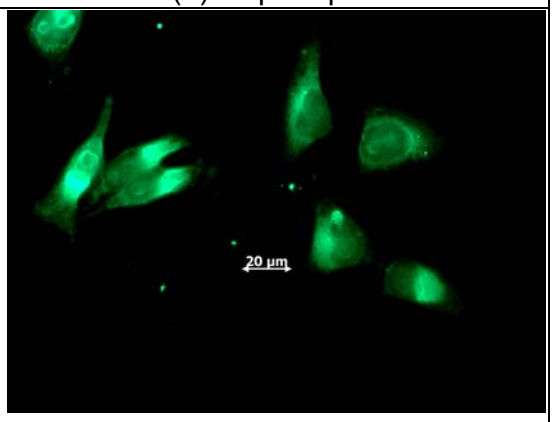

(d) NB**9** 25 µM

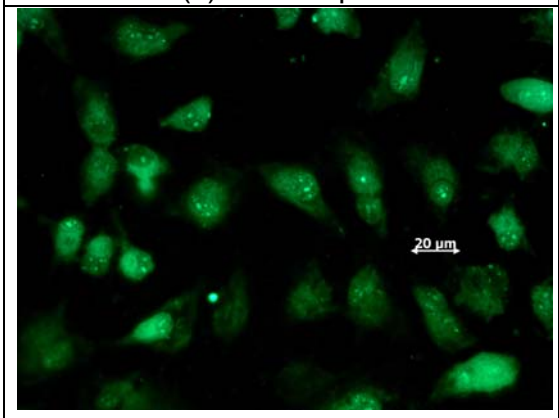

(e) NB-TTP 50 µM

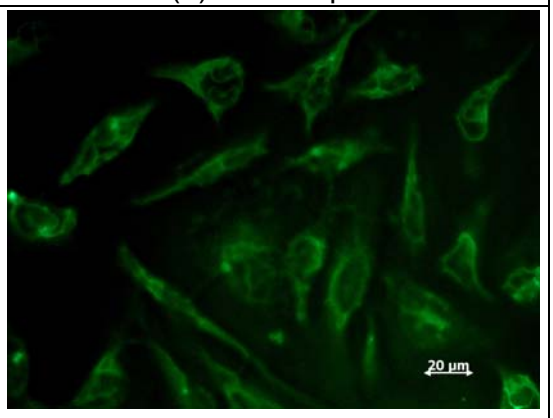

(f) NB-TTP 25 µM

Table 5.4 HeLa cell imaging 17 h after incubation
[exposure time 2.54s with FITC filter 495/520]

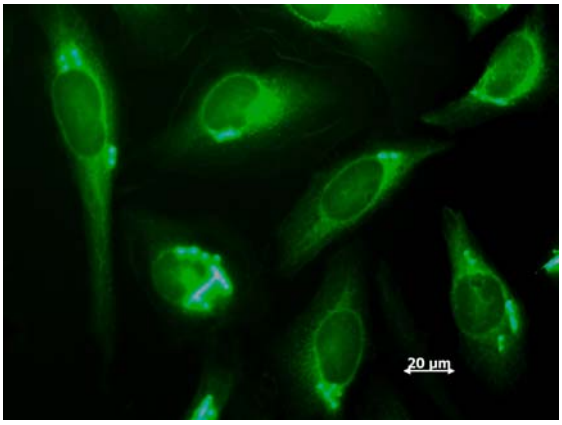

(a) Nap 50 µM

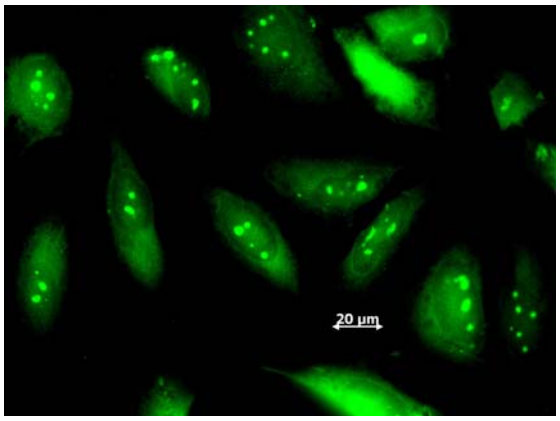

(b) Nap 25 µM

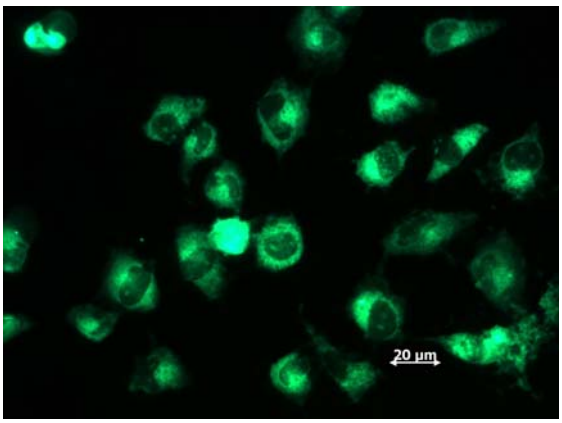

(c) NB**9** 50 µM

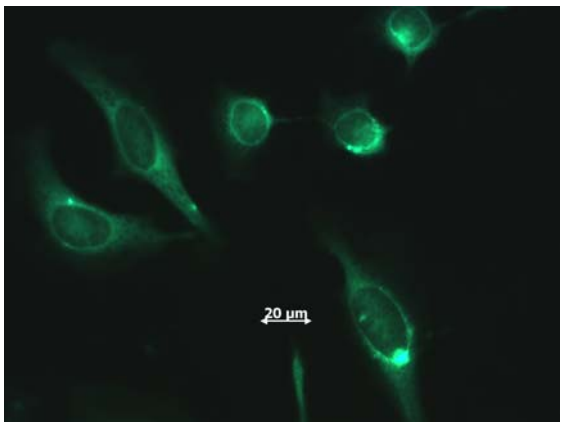

(d) NB**9** 25 µM

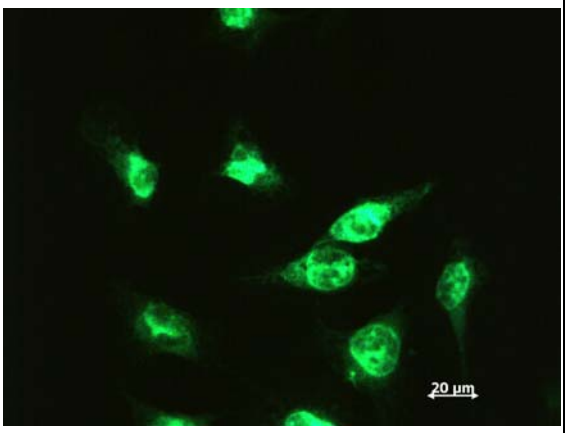

(e) NB-TTP 50 µM

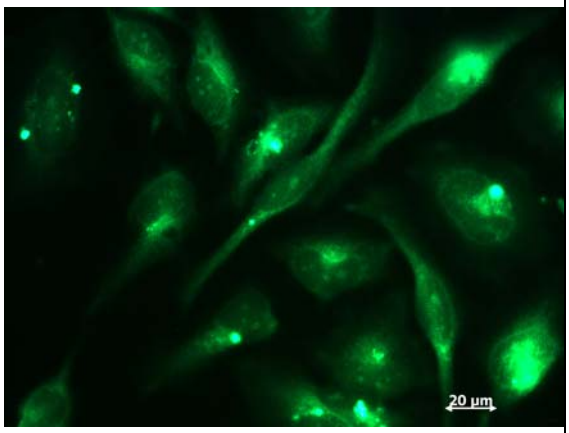

(f) NB-TTP 25 µM

Table 5.5 HeLa cell imaging 24 h after incubation
[exposure time 2.54s with FITC filter 495/520]

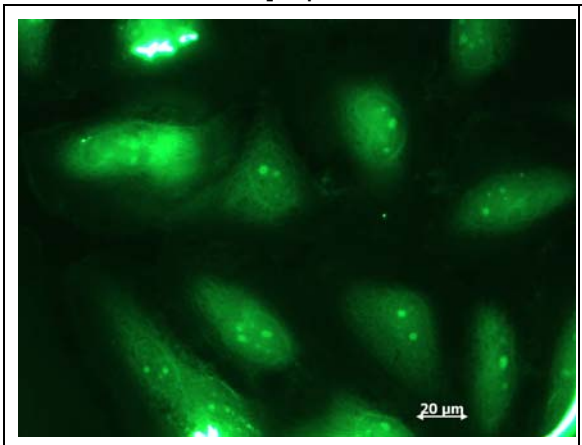

(a) Nap 50 µM

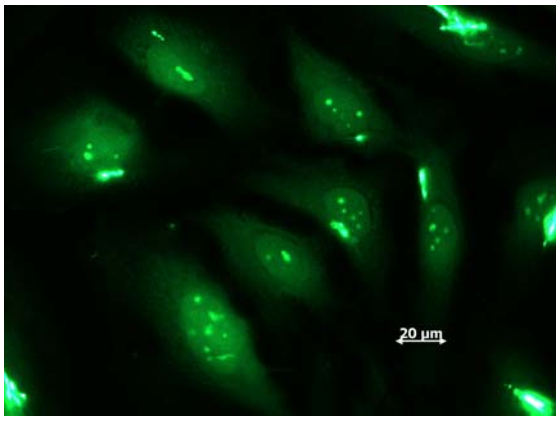

(b) Nap 25 µM

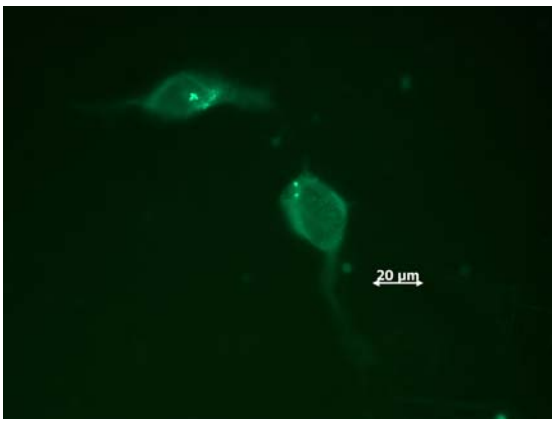

(c) NB**9** 50 µM

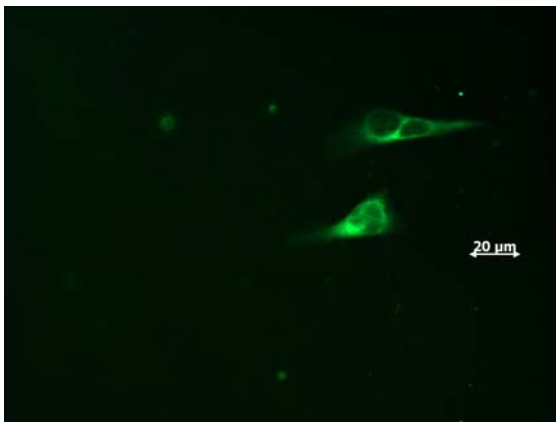

(d) NB**9** 25 µM

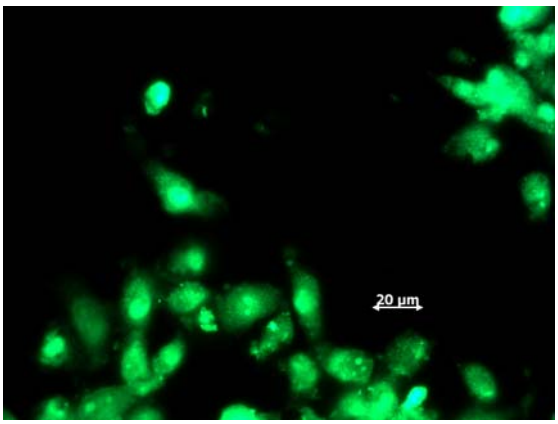

(e) NB-TTP 50 µM

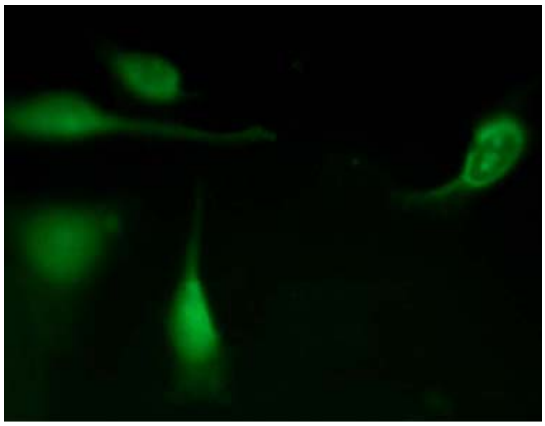

(f) NB-TTP 25 µM

As an overview of the cell imaging profiles of Nap, NB**9** and NB-TTP, it can be concluded that labeling was a concentration- and time-dependent process for NB**9** and NB-TTP, while Nap showed quick and consistant labeling pattern with no significant difference between two used concentrations. Initially, good membrane permeability of Nap allowed it to diffuse into the cell cytoplasm and nucleus area quickly and uniformly. For the less hydrophobic NB**9** and NB-TTP, their permeability and diffusion rate was much slower than Nap. Thus, it took longer time for NB**9** and NB-TTP to develop each labeling-pattern. Since the triphosphate group of NB-TTP is highly hydrophilic, the napthalimide moiety probably contributes significant hydrophobicity to grant the amphiphilic molecule enough lipid solubility. As the incubation time increased, NB-TTP showed a better preference for cell nucleus accumulation while control was primarily localized at cytoplasm area. Since the major difference between NB-TTP and control is the thymidine triphosphate moiety, one plausible way to explain the labeling behavior difference could be the selective incorporation of NB-TTP as a TTP analogue by DNA duplication machinery during the cell mitosis process. However, further experiment shows that the extracted genomic DNA from NB-TTP-labeled HeLa cell had little fluorescence (Figure 5.1 a) compared with the crude protein precipitation fraction (Figure 5.1 b). The NB**9**-labeled cell fractions showed similar result. Thus, the HeLa nucleus could be stained through other mechanisms, *e.g.* ionic interactions between negatively charged NB-TTP with positively charged histones, which could also explain the punctuate-labeling pattern in some labeled cells (Table 5.3 e). Because the NB-TTP

penetration into the nucleus was not a major problem, there could be an enhanced chance for NB-TTP incorporation into genomic DNA by suppressing the natural TTP level, such as addition of thymidylate synthase inhibitor, *e.g.* Raltitrexed. To further confirm that NB-TTP indeed labeled the cell nucleus, HeLa cell nuclei isolation was performed according to published protocol.[254] Obviously, bright rounded nucleus could be seen from the NB-TTP-labeled cells extraction (Figure 5.2 b), while the control-labeled cells didn't show such (Figure 5.2 a).

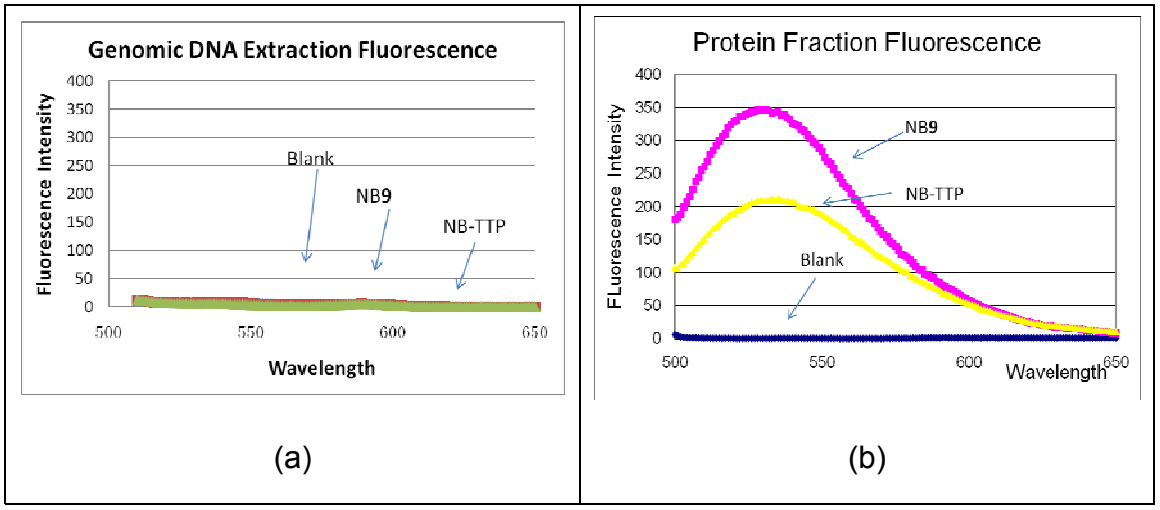

Figure 5.1 Fluorescence measurement of HeLa cell lyses fractions

(λ_{ex}: 490 nm, in 0.1 M pH 8.0 phosphate buffer)

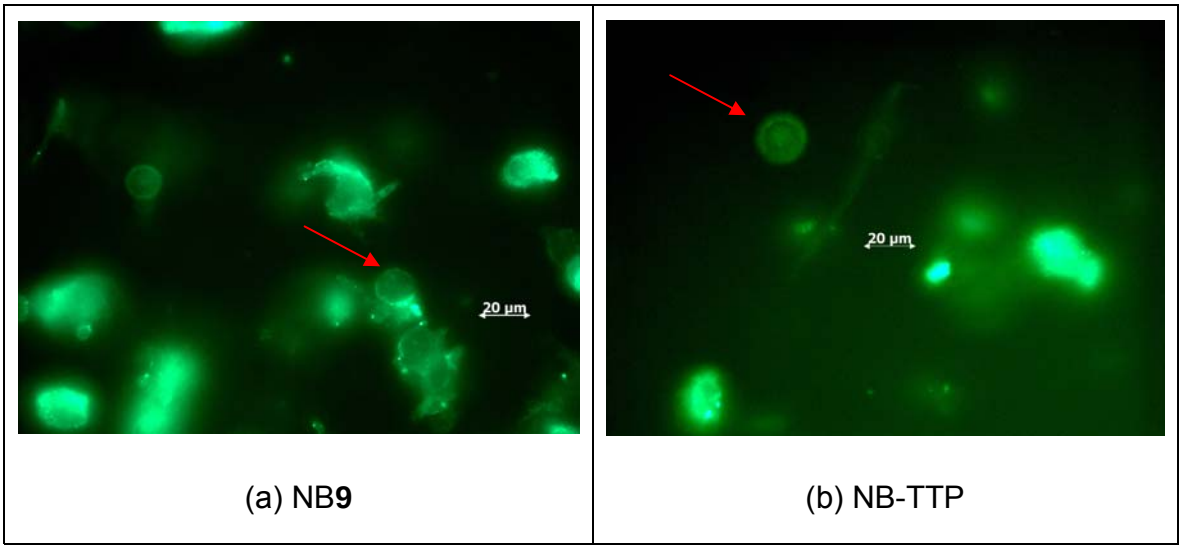

(a) NB**9** (b) NB-TTP

Figure 5.2 HeLa cell nuclei isolation [exposure time: 2.54s with FITC filter 495/520]

5.3 Conclusion

In conclusion, the synthesized NB-TTP has been found to be cell nucleus- labeling fluorescent reagent with good cell-membrane permeability. Compared with the control (boronic acid **9**), NB-TTP showed significant accumulation inside cell nucleus area. The HeLa cell culture was consistently stained by NB-TTP up to 50 µM for at least 24 h. Even though the detailed labeling mechanism was still unclear, the experiment served as a good starting point for the design and synthesis of cell imaging reagent using a similar strategy. Furthermore, the successful demonstration of the feasibility of incorporating boronic acid into living cells may even provide some insight into *in vivo* carbohydrate detection and distribution study in the future.

6. MAJOR FINDINGS, SIGNIFICANCES, POTENTIAL APPLICATIONS AND FURTHER IMPROVEMENTS

The major contribution of the work in this dissertation was the successful synthesis of a naphthalimide-based boronic acid-modified TTP (NB-TTP). The challenges in the multiple synthetic steps lay in the instability of the boronic acid (towards light, air, heat, pH and metal ions) and the triphosphate product (towards heat and pH). In addition, the high polarity of both boronic acid and triphosphate compounds made them very hard to purify. It was only through careful handling of all materials and design of the synthetic strategy, together with condition optimization after trial and error that the desired final product (NB-TTP) was obtained. It was accomplished in a total of 13 steps to yield the final product of MW > 1kD.

The signicance of NB-TTP was its intrinsic longwavelength fluorescence intensity increase upon carbohydrate binding. It was surprising to find that after conjugation of NB towards TTP and incorporation of NB-TTP into DNA sequence, the fluorescence intensity and quantum yield of NB was further increased, rather than being quenched. The binding studies of NB-DNA with fructose indicated that it is the very first example of modified DNA showing intrinsic fluorescent changes upon sugar binding and such changes do not rely on FRET. Thus, it was forseeable that NB-based fluorescent DNA sensors could be developed through appropriately selected DNA sequences or scaffolds with high affinity and selectivity towards specific glycan. The beauty of this new type of sensor is that the binding signal is increased fluorescenct intensity at a visible

wavelength, which made observation and recording convenient.

Besides its potential application in DNA-based sensor development, NB-TTP might also be used in fluorescent cell imaging. From the HeLa cell imaging results, it seemed that the boronic acid moiety of NB prevent it from entering the nuclear area as comared with Nap. In contrast, NB-TTP showed significant accumulation in cell nucleus. The cell lysis fractionation results suggested that the labeling pattern of NB-TTP was not resulting from genomic DNA incorporation, which might be due to the large molecular size and cytotoxic effect of NB. Despite of that, it certainly opened the door of the possibility that by choosing a smaller boronic acid moiety with less cytotoxic effect, a new B-TTP may function as the probe for changes in the nuclear environment, nuclear imaging, and cell division genomic DNA tracing.

In all, the work accomplished was a systematic preliminary study of fluorescent boronic acid modified nucleic acid's potential applications. Further exploration in this field might require more efforts in developing an improved version of NB-TTP, which should demonstrate better water solubility, higher fluorescence intensity, higher quantum yield, more obivious fluorescence changes upon analyte binding, *etc*. In order to do that, careful selection of a new boronic acid moiety is required. This boronic acid should meet the previously described criteria. The same rule also applies to cell imaging applications of boronic acid-modified nucleic acid.

PUBLICATIONS AND MANUSCRIPTS IN PREPARATION

1. **Yang, X.;** Dai, C.; Calderon-Molina, A. D. ; Wang, B.*, “Boronic Acid-modified DNA that Changes Fluorescent Properties upon Carbohydrate Binding”, *Chem Commun.*, **2010**, *46*, 1073-1075
2. **Yang, X.;** Shan, J.; Cheng, Y.; Wang, B.*, “Synthetic Lectin Mimics-Artificial Carbohydrate Receptors” in Carbohydrate Recognition: Biological Problems, Methods, and Potential Applications, Wang, B. and Boons, G-J, Editors, **2010**, invited book chapter accepted
3. Cheng, Y.; Shan, J.; **Yang, X.;** Wang, B.*, “Covalent Interactions in Chemosensor Design” in Chemosensors: Principles, Strategies, and Applications, Wang, B. and Anslyn, E.A., Editors, **2010**, invited book chapter accepted
4. **Yang, X.;** Jin, S.; Cheng, Y.; Wang, B.*, “Boronic Acid-based Chemosensors” in “*Artificial Receptors for Chemical Sensors*” by WILEY-VCH; Ed.: Mirsky, V.M. and Yatsimirsky, A.K., **2009**, invited book chapter accepted
5. Wang, B.;* Li, M.; Lin, N.; Huang, Z.; **Yang, X.**; Zheng, S.; Cheng, Y. “Methods of Preparation of Nucleotides and Aptamers Containing Boronic Acid Groups and Uses Thereof”, patent filed on July 17, **2008**
6. Zheng, S.; Kaur, G.; Wang, H.; Li, M.; Macnaughtan, M.; **Yang, X.;** Reid, S.; Wang, B. Ke, H.; Prestgard, J. “Design, Synthesis, and Structure-Activity Relationship, Molecular Modeling, and NMR Studies of a Series of Phenyl Alkyl

Ketones as Highly Potent and Selective Phosphodiesterase-4 Inhibitors" *J. Med. Chem.,* **2008**, *51*, 7673-7688

APPENDIX: POWERPOINT SLIDES OF DISSERTATION DEFENSE

Georgia State University

Design and Synthesis of Boronic Acid-modified Nucleotides for Fluorescent Sensing and Cell Imaging

Xiaochuan Yang
Advisor: Prof. Binghe Wang
Department of Chemistry

Outline

Introduction
- Applications of boronic acids
- Boronic acid-modified nucleotides

Organic synthesis
- Design and retrosynthetic analysis of NB-TTP
- Synthesis of naphthalimdie-based boronic acid (NB) moiety
- Synthesis of M-TTP and NB-TTP

Enzymatic incorporation studies
- PAGE
- MALDI-MS

Fluorescence tests
- NB-TTP-DNA fluorescent binding studies
- HeLa cell imaging studies

Introduction

--- Applications of Boronic Acids

- Organic: cross-coupling reagents, chiral auxiliaries
- Analytical: sensors for carbohydrates, catechols
- Medicinal: protease inhibitors, quorum sensing inhibitors, cell surface glycan imaging, Boron Neutron Capture Therapy (BNCT)

Introduction

--- Boronic Acid-modified Nucleotides

Potential Applications

1. Glycan Sensors
- DNA as scaffold with 3D conformation
- Boronic acids as recognition moieties

2. Cell Imaging
- Fluorescent probes for nuclear labeling
- Tools of studies for genomic DNA tracing, ROS sensing, cellular glycan mapping, BNCT

Introduction

--- Boronic Acid-modified Nucleotides

QB-TTP (quinoline-based boronic acid-modified TTP):

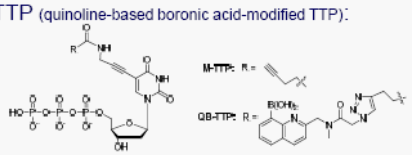

- Can be recognized by DNA polymerase
- Can interact with catechol moiety
- Cannot change fluorescence upon carbohydrate addition

Lin, N.; Yan, J.; Huang, Z.; Altier, C.; Li, M.; Carrasco, N.; Suyemoto, M.; Johnston, L.; Wang, S.; Wang, Q.; Fang, H.; Caton-Williams, J.; Wang, B. *Nucleic Acids Res.* **2007**, *35*, 1222-1229

Design Strategy of New Boronic Acid-modified Nucleotides

- Have longer $\lambda_{ex}/\lambda_{em}$ than those of nucleobases
- Change fluorescence upon binding
- Exhibit high stability under excitation
- Be relatively easy to synthesize

Design Strategy of New Boronic Acid-modified Nucleotides

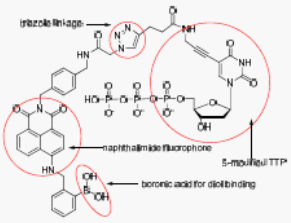

Naphthalimide-based boronic acid-modified TTP (NB-TTP)

Naphthalimide-based Boronic Acids (NB)

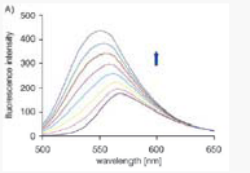

Fluorescence response of NB (10^{-5} M, λ_{ex} = 493 nm) to D-fructose (0 - 500 mM) in PBS (0.1 M, pH 7.4, 1% MeOH)

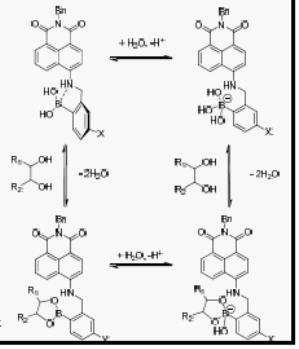

Jin, S.; Wang, J. F.; Li, M. Y.; Wang, B. H;. *Chem.-Eur. J.*, **2008**, *14*, 2795-2804.

Retrosynthetic Analysis

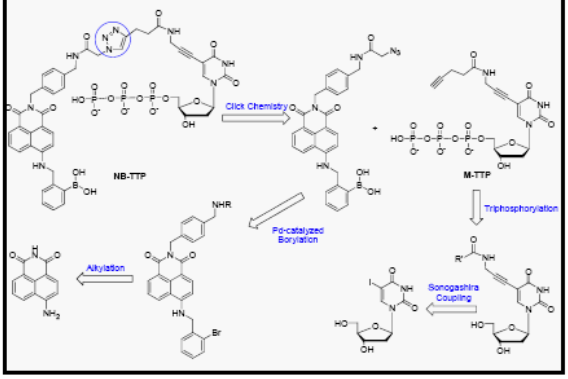

Synthesis of Boronic Acid (NB) Moiety

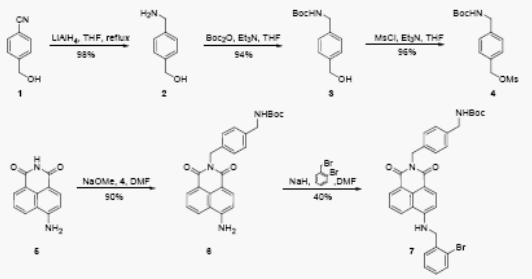

Wagner, A.; Breipohl, G.; Heitsch, H.; Gerhards, H.; Noelken, G.; Wirth, K.; Schoelkens, B.; Hoechst, A. G., Ed.; Ger. Offen.: German, 1997, DE 96-19603767, CAN 127:205472, p 28.
Wang, J. F.; Jin, S.; Akay, S.; Wang, B. H. *Eur. J. Org. Chem.* **2007**, 2091-2099.

Synthesis of Boronic Acid (NB) Moiety

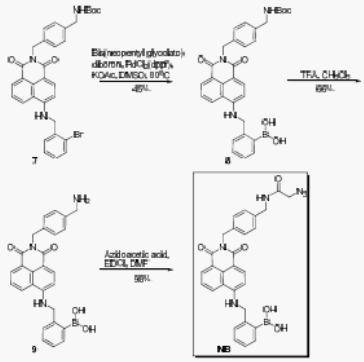

Photostability Studies of NB

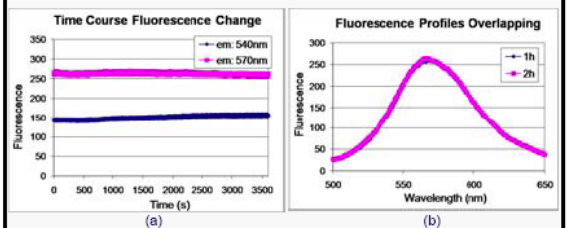

Fluorescence response of NB (1 μM) in PBS (0.1 M, pH 7.4) under continuous irradiation (λ_{ex}: 490 nm)

Synthesis of M-TTP

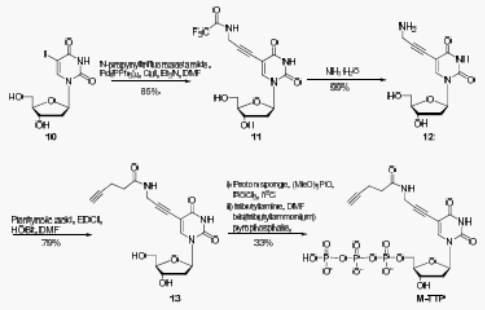

Lin, N.; Yan, J.; Huang, Z.; Altier, C.; Li, M.; Carrasco, N.; Suyemoto, M.; Johnston, L.; Wang, S.; Wang, Q.; Fang, H.; Caton-Williams, J.; Wang, B. *Nucleic Acids Res.* **2007**, *35*, 1222-1229

Synthesis of NB-TTP

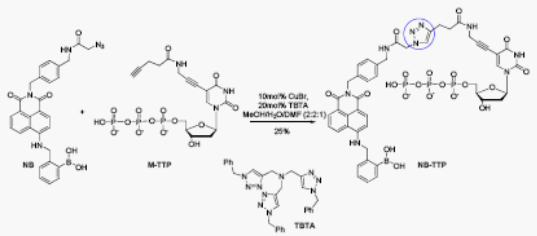

Chan, T. R.; Hilgraf, R.; Sharpless, K. B.; Fokin, V. V. *Org. Lett.* **2004**, *6*, 2853-2855.

NB-TTP ^{31}P-NMR:

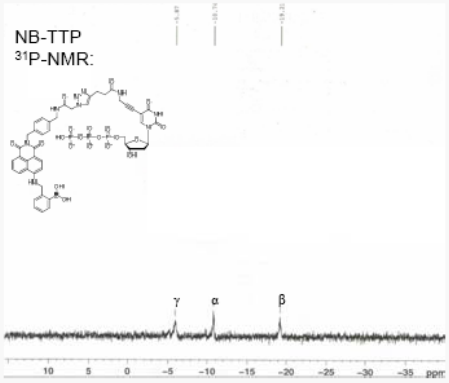

Burgess,K.; Cook, D.;*Chem. Rev.* **2000**,*100*, 2047-2059

NB-TTP Fluorescence Binding Studies

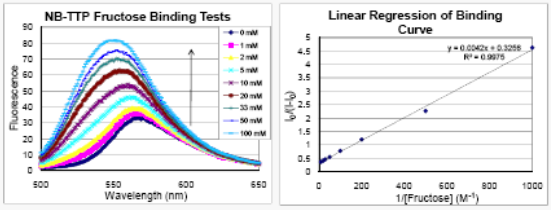

(a) (b)

Fluorescence response of NB-TTP (10^{-5} M, λ_{ex}: 490 nm) to D-fructose in PBS (0.1 M pH 7.4)
Binding constant equation: $I_0/(I-I_0) = (\varepsilon_B/\varepsilon_{B-S}K_a) \times 1/[\text{sugar}] + \varepsilon_B/\varepsilon_{B-S}$
K_a = intercept/slope = 73 ± 5 M^{-1}

Connors, K. A. *Binding Constants: The Measurement of Molecular Complex Stability; 1st ed.; John Wiley & Sons, Inc. 1987.*

Incorporation of NB-TTP by Klenow Fragment

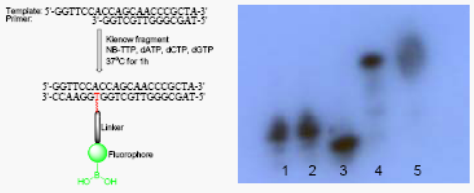

Primer extension analyzed on 15% PAGE:
1) primer only; 2) reaction without enzyme; 3) reaction without dNTPs;
4) reaction with natural dNTPs; 5) reaction with NB-TTP and other dNTPs

Incorporation of NB-TTP by Klenow Fragment

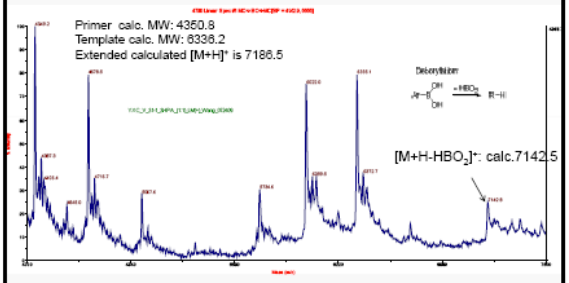

MALDI-TOF-MS of primer extension using NB-TTP

Incorporation of NB-TTP by Klenow Fragment

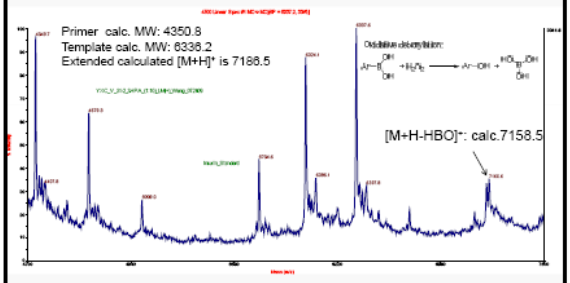

MALDI-TOF-MS of primer extension using NB-TTP, followed by treatment with H_2O_2

NB-TTP-DNA Fluorescence Study

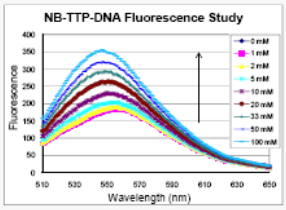

Fluorescence response of NB-TTP-DNA (0.5 μM, λ_{ex}: 490 nm) to D-fructose in PBS (0.1 M, pH 7.4)

Designed Sequences for NB-TTP-DNA Construction

Primer	3'-GGTCGTTGGGCGAT-5'
Template 0	5'-GGTTCCACCAGCAACCCGCTA-3'
Template 1	5'-GGTTCCAACCAGCAACCCGCTA-3'
Template 2	5'-GGTTCACACCAGCAACCCGCTA-3'
Template 3	5'-GGTTACCACCAGCAACCCGCTA-3'
Template 4	5'-GGTATCCACCAGCAACCCGCTA-3'
Template 5	5'-GGATTCCACCAGCAACCCGCTA-3'
Template 6	5'-GAGTTCCACCAGCAACCCGCTA-3'
Template 7	5'-AGGTTCCACCAGCAACCCGCTA-3'

Incorporation of NB-TTP by Klenow Fragment

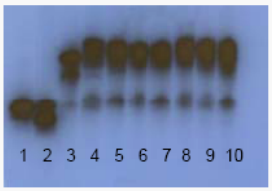

15% PAGE analysis of primer extensions with Templates 1-7
1) primer only; 2) reaction without dNTPs; 3) Template 1 extension with NB-TTP +TTP;
4) Template 1 extension with NB-TTP; 5) Template 2 extension with NB-TTP;
6) Template 3 extension with NB-TTP; 7) Template 4 extension with NB-TTP;
8) Template 5 extension with NB-TTP; 9) Template 6 extension with NB-TTP;
10) Template 7 extension with NB-TTP

Fluorescent Binding Tests of NB-TTP-DNA

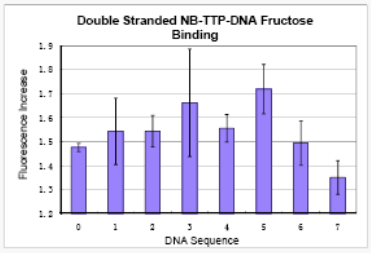

Fluorescence response of double stranded NB-TTP-DNA (Template 0~7, 0.5 μM) to 0.1 M D-fructose (λ_{ex}: 490 nm)

Fluorescent Binding Tests of NB-TTP-DNA

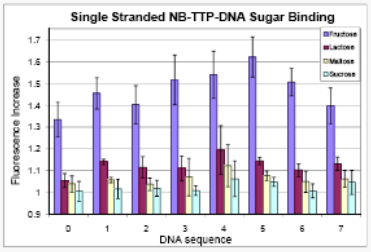

Fluorescence response of single stranded NB-TTP-DNA (Template 0~7, 0.5 μM) to 0.1 M fructose, lactose, maltose and sucrose (λ_{ex}: 490 nm)

From *in vitro* to *in vivo* ?

- NB-TTP can be recognized by DNA polymerase
- NB fluorescent properties were well retained after incorporation into DNA
- NB-TTP has suitable wavelengths (λ_{ex}: 490nm, λ_{em}: 540 nm) for FITC channel observation
- Other napthalimide-based compounds without boronic acid have been tested for anti-cancer and cell imaging studies

Preliminary HeLa Cell Imaging Studies

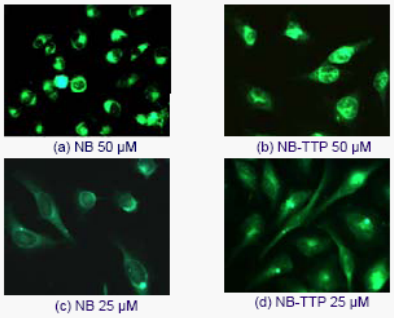

(a) NB 50 μM (b) NB-TTP 50 μM

(c) NB 25 μM (d) NB-TTP 25 μM

Note: NB was used as control compound, pictures were taken 17 h after incubation using FITC channel of fluorescent microscope (40X oil lens)

Preliminary HeLa Cell Imaging Studies

- Both NB and NB-TTP showed good membrane permeability
- Both NB and NB-TTP retained fluorescence after entering cell
- NB-TTP had more significant accumulation in nucleus area than NB
- Potential application of NB-TTP in studies of nuclear labeling, cell division tracing, ROS sensing, BNCT…

Conclusions

- NB-TTP (naphthalimide-based boronic acid modified TTP) was successfully synthesized in total 13 steps
- NB-TTP demonstrated good photostability, and well-retained fluorescent properties of NB
- NB-TTP can be recognized by DNA polymerase
- NB-TTP modified DNA showed fluorescence intensity increases upon carbohydrate addition
- NB-TTP demonstrated good cell-membrane permeability and cell nucleus accumulation in fluorescent cell imaging studies

Acknowledgement

Professors: Dr. Binghe Wang
Dr. Zhen Huang

Postdocs: Dr. Na Lin
Dr. Junfeng Wang
Dr. Shilong Zheng
Dr. Chaofeng Dai
Dr. Guojing Sun

Graduate Students:
Shan Jin, Nanting Ni, Yunfeng (Jerry) Cheng, Suazette Reid, Weixuan Chen, Hanjing Peng, Sarah Burroughs, all previous and current group members

Special thanks: Dr. Siming Wang
Dr. Sekar Chandrasekaran

Financial Support: Georgia Cancer Coalition, Georgia Research Alliance, NIH (Grants CA123329, CA113917, GM084933), GSU MBD program

APPENDIX: NMR and MS Spectra

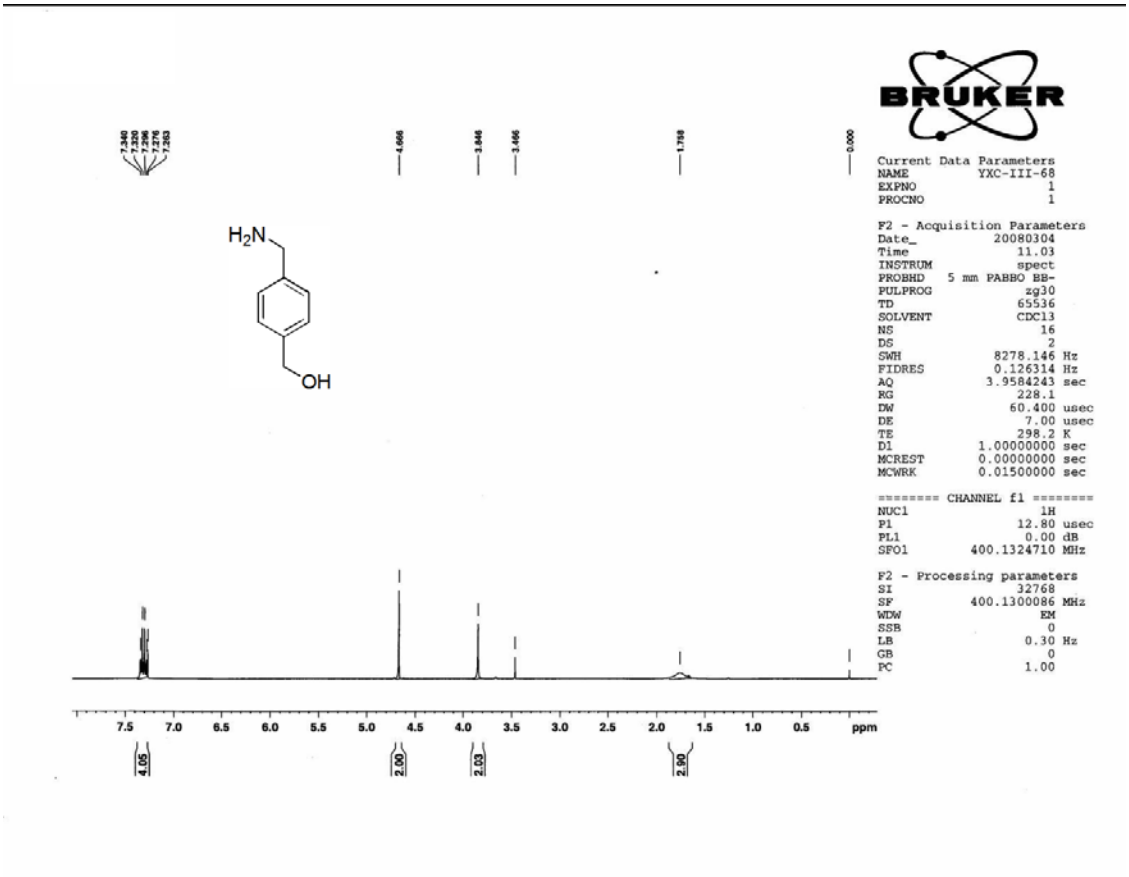

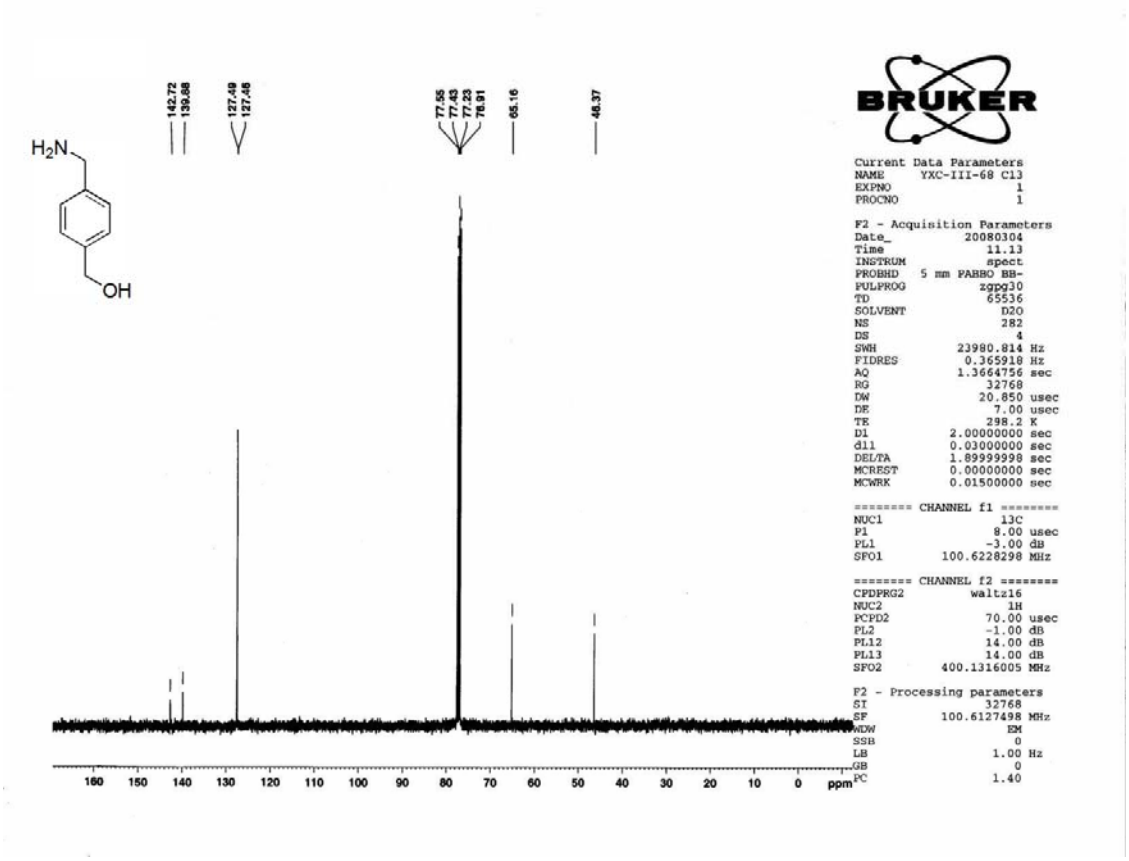
142.72
139.68
127.49
127.45
77.55
77.43
77.23
76.91
65.16
48.37
H2N
OH
160 150 140 130 120 110 100 90 80 70 60 50 40 30 20 10 0 ppm
BRUKER
Current Data Parameters
NAME YXC-III-68 C13
EXPNO 1
PROCNO 1
F2 - Acquisition Parameters
Date_ 20080304
Time 11.13
INSTRUM spect
PROBHD 5 mm PABBO BB-
PULPROG zgpg30
TD 65536
SOLVENT D2O
NS 282
DS 4
SWH 23980.814 Hz
FIDRES 0.365918 Hz
AQ 1.3664756 sec
RG 32768
DW 20.850 usec
DE 7.00 usec
TE 298.2 K
D1 2.00000000 sec
d11 0.03000000 sec
DELTA 1.89999998 sec
MCREST 0.00000000 sec
MCWRK 0.01500000 sec
======== CHANNEL f1 ========
NUC1 13C
P1 8.00 usec
PL1 -3.00 dB
SFO1 100.6228298 MHz
======== CHANNEL f2 ========
CPDPRG2 waltz16
NUC2 1H
PCPD2 70.00 usec
PL2 -1.00 dB
PL12 14.00 dB
PL13 14.00 dB
SFO2 400.1316005 MHz
F2 - Processing parameters
SI 32768
SF 100.6127498 MHz
WDW EM
SSB 0
LB 1.00 Hz
GB 0
PC 1.40

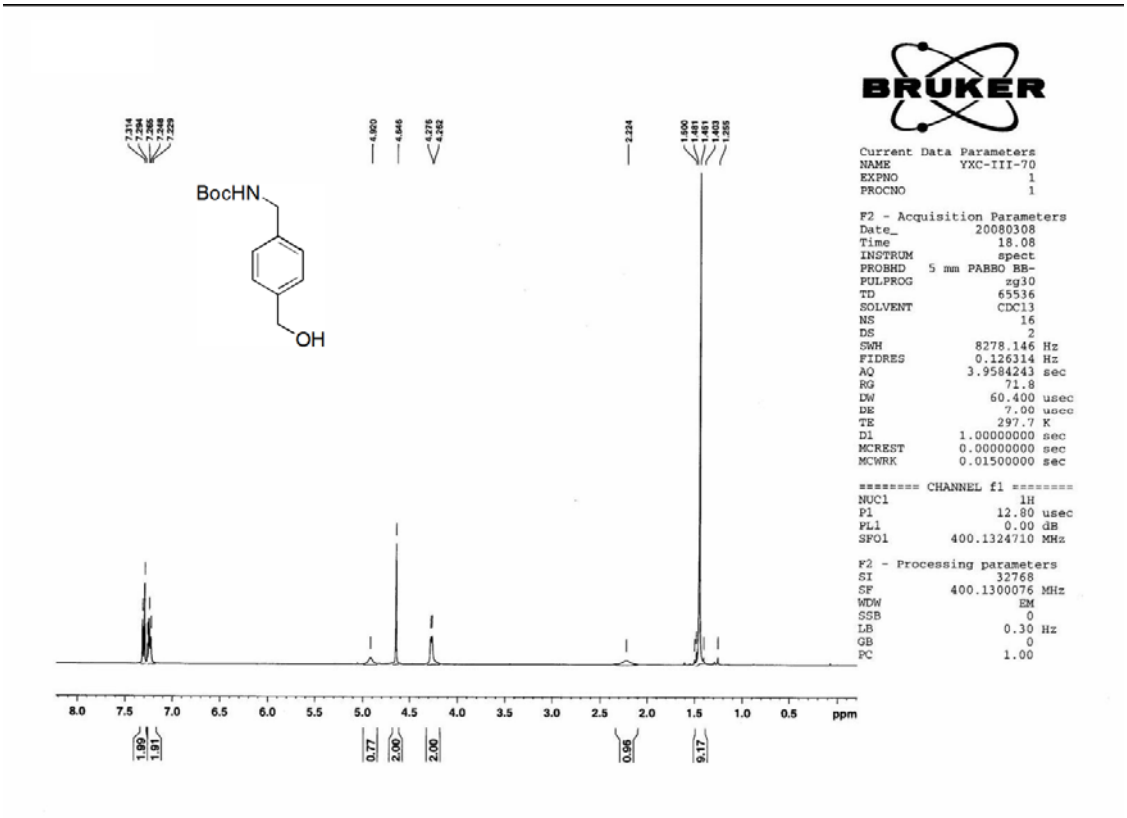
BocHN
OH
7.314
7.304
7.286
7.248
7.229
4.920
4.846
4.276
4.262
2.234
1.500
1.481
1.461
1.403
1.285
8.0
7.5
7.0
6.5
6.0
5.5
5.0
4.5
4.0
3.5
3.0
2.5
2.0
1.5
1.0
0.5
ppm
1.99
1.91
0.77
2.00
2.00
0.96
9.17
BRUKER
Current Data Parameters
NAME YXC-III-70
EXPNO 1
PROCNO 1
F2 - Acquisition Parameters
Date_ 20080308
Time 18.08
INSTRUM spect
PROBHD 5 mm PABBO BB-
PULPROG zg30
TD 65536
SOLVENT CDCl3
NS 16
DS 2
SWH 8278.146 Hz
FIDRES 0.126314 Hz
AQ 3.9584243 sec
RG 71.8
DW 60.400 usec
DE 7.00 usec
TE 297.7 K
D1 1.00000000 sec
MCREST 0.00000000 sec
MCWRK 0.01500000 sec
======== CHANNEL f1 ========
NUC1 1H
P1 12.80 usec
PL1 0.00 dB
SFO1 400.1324710 MHz
F2 - Processing parameters
SI 32768
SF 400.1300076 MHz
WDW EM
SSB 0
LB 0.30 Hz
GB 0
PC 1.00

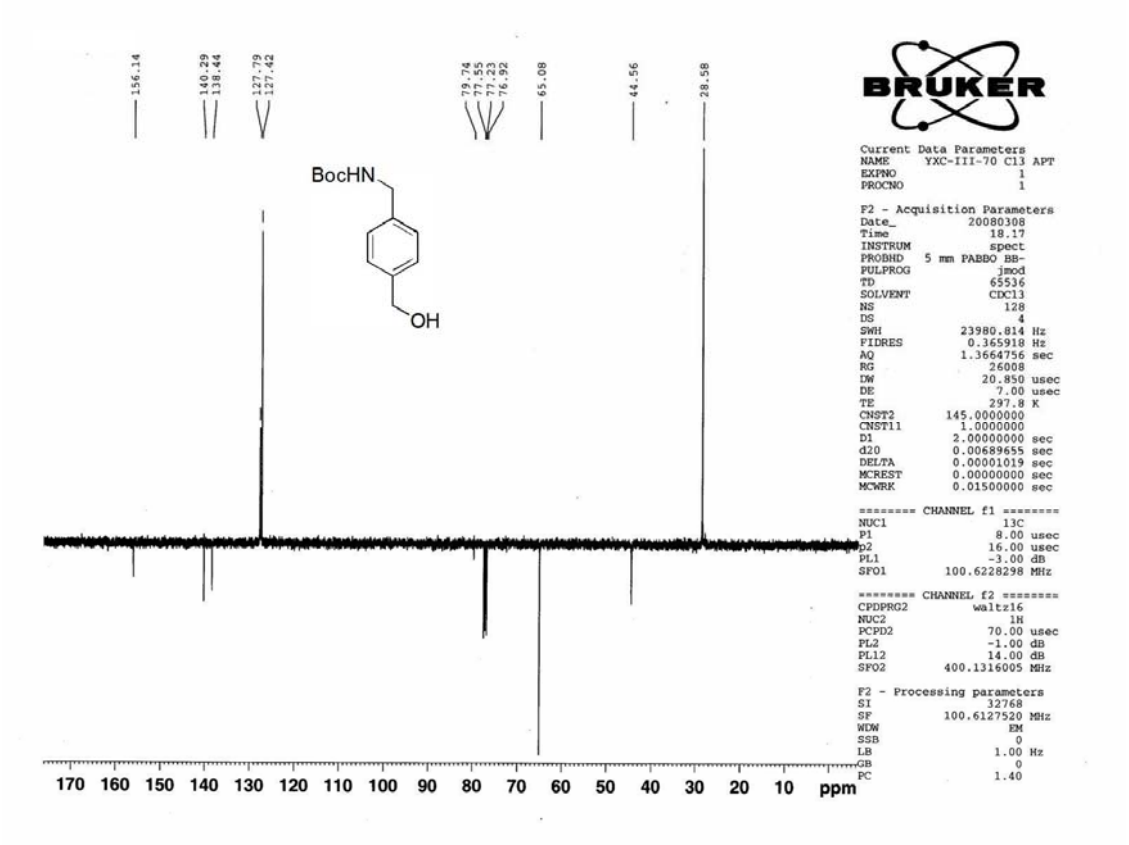
156.14
140.29
138.44
127.79
127.42
79.74
77.55
77.23
76.92
65.08
44.56
28.58
BocHN
OH
170 160 150 140 130 120 110 100 90 80 70 60 50 40 30 20 10 ppm
BRUKER
Current Data Parameters
NAME YXC-III-70 C13 APT
EXPNO 1
PROCNO 1
F2 - Acquisition Parameters
Date_ 20080308
Time 18.17
INSTRUM spect
PROBHD 5 mm PABBO BB-
PULPROG jmod
TD 65536
SOLVENT CDCl3
NS 128
DS 4
SWH 23980.814 Hz
FIDRES 0.365918 Hz
AQ 1.3664756 sec
RG 26008
DW 20.850 usec
DE 7.00 usec
TE 297.8 K
CNST2 145.0000000
CNST11 1.0000000
D1 2.00000000 sec
d20 0.00689655 sec
DELTA 0.00001019 sec
MCREST 0.00000000 sec
MCWRK 0.01500000 sec
======== CHANNEL f1 ========
NUC1 13C
P1 8.00 usec
p2 16.00 usec
PL1 -3.00 dB
SFO1 100.6228298 MHz
======== CHANNEL f2 ========
CPDPRG2 waltz16
NUC2 1H
PCPD2 70.00 usec
PL2 -1.00 dB
PL12 14.00 dB
SFO2 400.1316005 MHz
F2 - Processing parameters
SI 32768
SF 100.6127520 MHz
WDW EM
SSB 0
LB 1.00 Hz
GB 0
PC 1.40

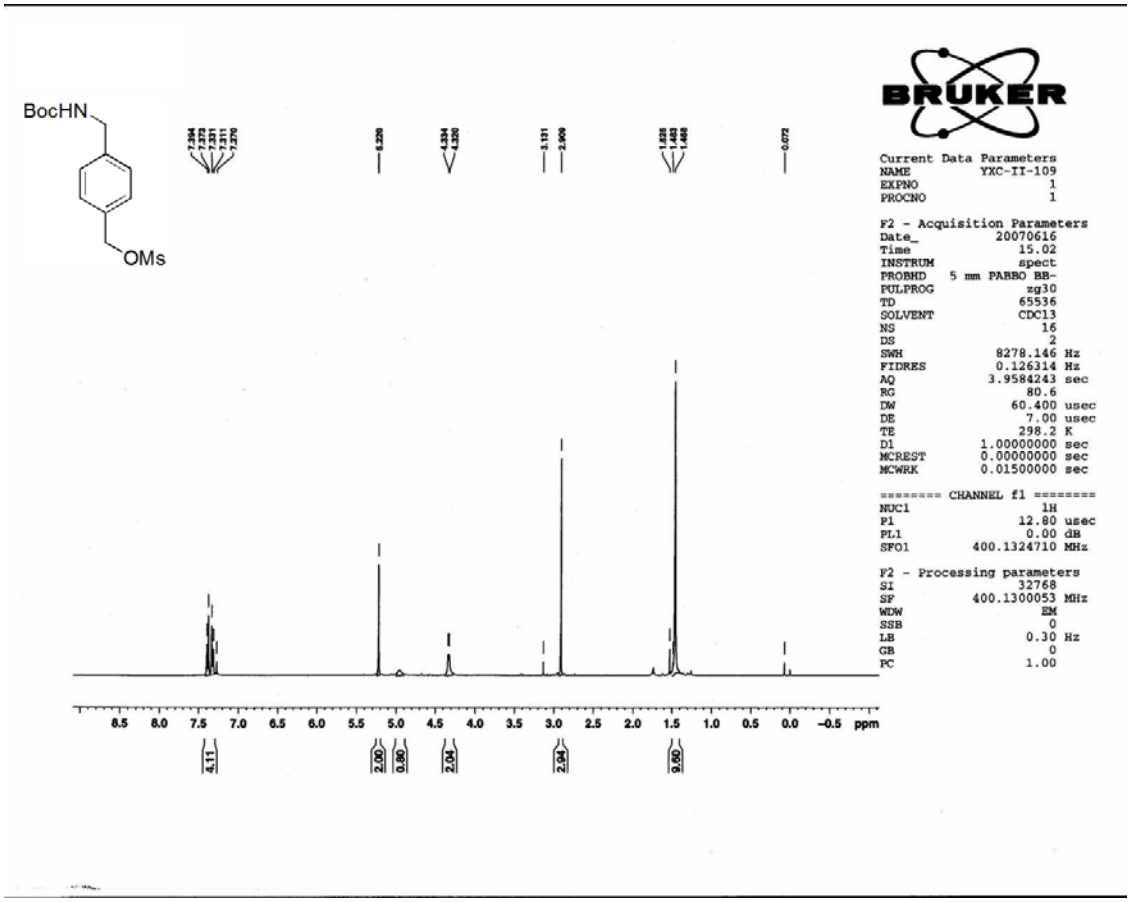

BRUKER

Current Data Parameters
NAME YXC-II-109
EXPNO 1
PROCNO 1

F2 - Acquisition Parameters
Date_ 20070616
Time 15.02
INSTRUM spect
PROBHD 5 mm PABBO BB-
PULPROG zg30
TD 65536
SOLVENT CDCl3
NS 16
DS 2
SWH 8278.146 Hz
FIDRES 0.126314 Hz
AQ 3.9584243 sec
RG 80.6
DW 60.400 usec
DE 7.00 usec
TE 298.2 K
D1 1.00000000 sec
MCREST 0.00000000 sec
MCWRK 0.01500000 sec

======== CHANNEL f1 ========
NUC1 1H
P1 12.80 usec
PL1 0.00 dB
SFO1 400.1324710 MHz

F2 - Processing parameters
SI 32768
SF 400.1300053 MHz
WDW EM
SSB 0
LB 0.30 Hz
GB 0
PC 1.00

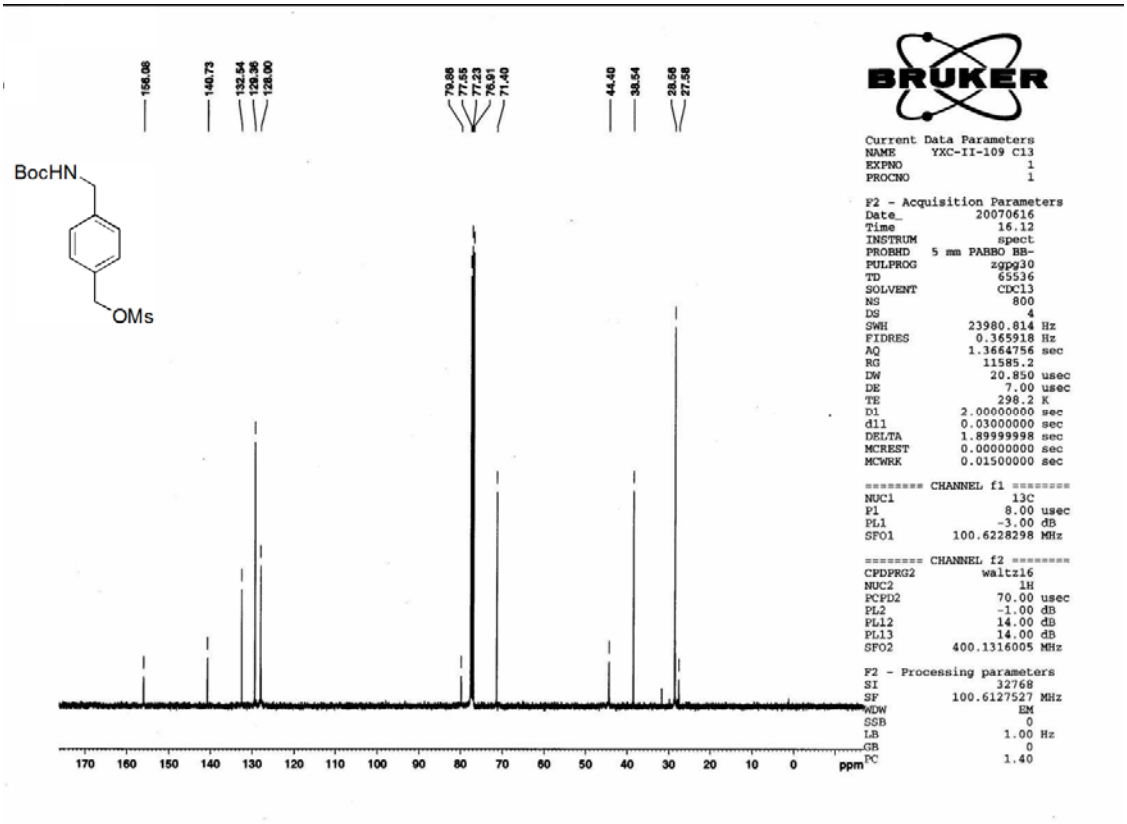
156.06
140.73
132.54
129.36
128.00
79.88
77.55
77.23
76.91
71.40
44.40
38.54
28.56
27.58
BocHN
OMs
170 160 150 140 130 120 110 100 90 80 70 60 50 40 30 20 10 0 ppm
BRUKER
Current Data Parameters
NAME YXC-II-109 C13
EXPNO 1
PROCNO 1
F2 - Acquisition Parameters
Date_ 20070616
Time 16.12
INSTRUM spect
PROBHD 5 mm PABBO BB-
PULPROG zgpg30
TD 65536
SOLVENT CDCl3
NS 800
DS 4
SWH 23980.814 Hz
FIDRES 0.365918 Hz
AQ 1.3664756 sec
RG 11585.2
DW 20.850 usec
DE 7.00 usec
TE 298.2 K
D1 2.00000000 sec
d11 0.03000000 sec
DELTA 1.89999998 sec
MCREST 0.00000000 sec
MCWRK 0.01500000 sec
======== CHANNEL f1 ========
NUC1 13C
P1 8.00 usec
PL1 -3.00 dB
SFO1 100.6228298 MHz
======== CHANNEL f2 ========
CPDPRG2 waltz16
NUC2 1H
PCPD2 70.00 usec
PL2 -1.00 dB
PL12 14.00 dB
PL13 14.00 dB
SFO2 400.1316005 MHz
F2 - Processing parameters
SI 32768
SF 100.6127527 MHz
WDW EM
SSB 0
LB 1.00 Hz
GB 0
PC 1.40

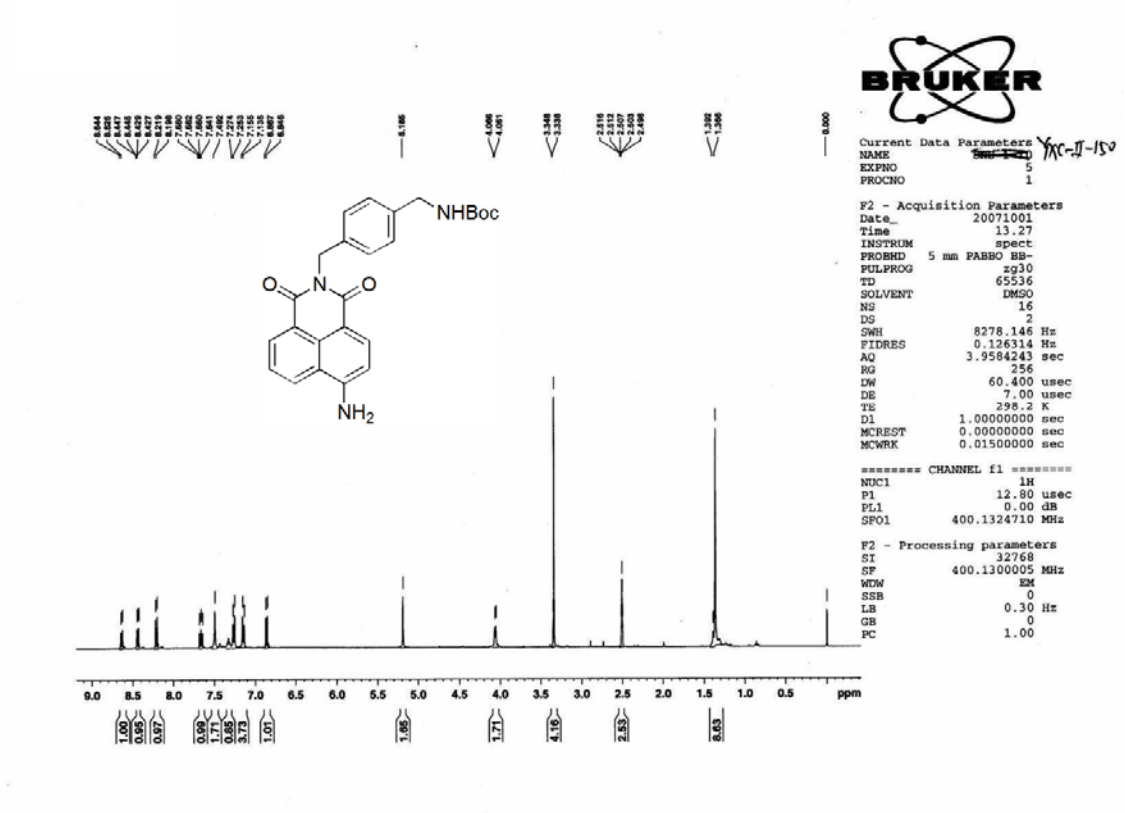

BRUKER

Current Data Parameters YXC-II-150

NAME	[redacted]
EXPNO	5
PROCNO	1

F2 - Acquisition Parameters

Date_	20071001
Time	13.27
INSTRUM	spect
PROBHD	5 mm PABBO BB-
PULPROG	zg30
TD	65536
SOLVENT	DMSO
NS	16
DS	2
SWH	8278.146 Hz
FIDRES	0.126314 Hz
AQ	3.9584243 sec
RG	256
DW	60.400 usec
DE	7.00 usec
TE	298.2 K
D1	1.00000000 sec
MCREST	0.00000000 sec
MCWRK	0.01500000 sec

======== CHANNEL f1 ========

NUC1	1H
P1	12.80 usec
PL1	0.00 dB
SFO1	400.1324710 MHz

F2 - Processing parameters

SI	32768
SF	400.1300005 MHz
WDW	EM
SSB	0
LB	0.30 Hz
GB	0
PC	1.00

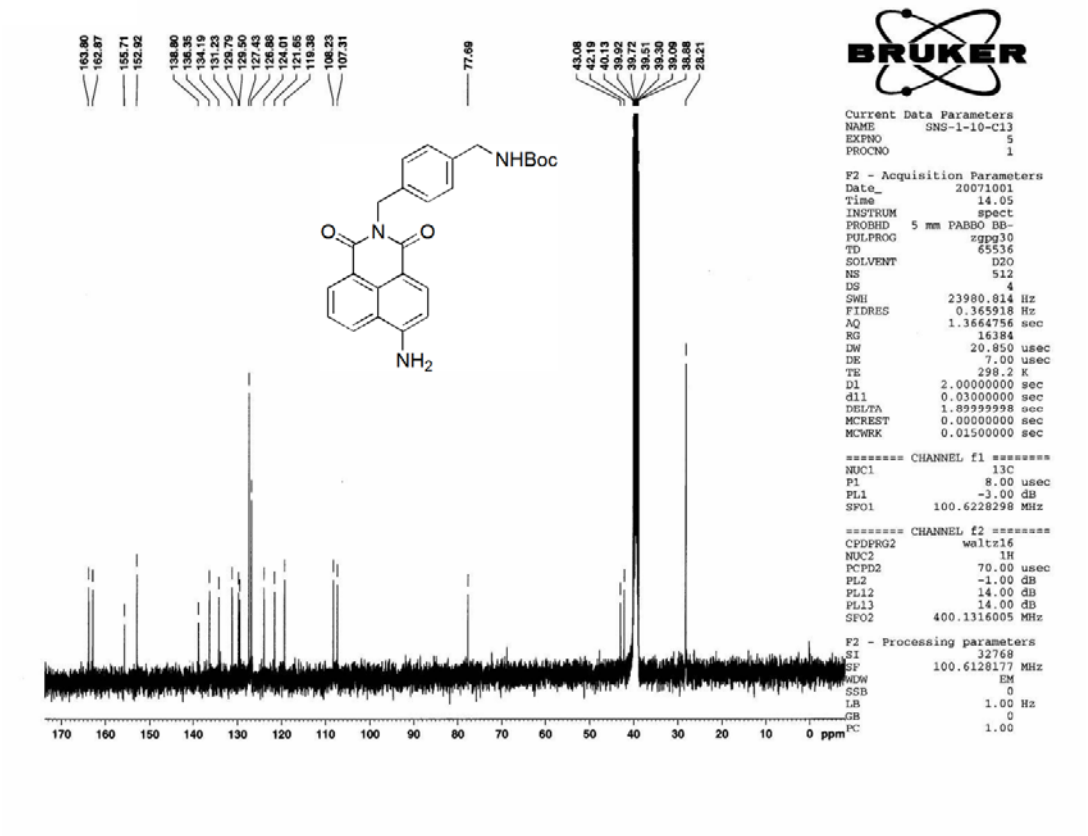
163.90
162.87
155.71
152.92
138.80
136.35
134.19
131.23
129.79
129.50
127.43
126.86
124.01
121.65
119.38
108.23
107.31
77.69
43.08
42.19
40.13
39.92
39.72
39.51
39.30
39.09
38.88
28.21
NHBoc
O
N
O
NH2
BRUKER
Current Data Parameters
NAME SNS-1-10-C13
EXPNO 5
PROCNO 1
F2 - Acquisition Parameters
Date_ 20071001
Time 14.05
INSTRUM spect
PROBHD 5 mm PABBO BB-
PULPROG zgpg30
TD 65536
SOLVENT D2O
NS 512
DS 4
SWH 23980.814 Hz
FIDRES 0.365918 Hz
AQ 1.3664756 sec
RG 16384
DW 20.850 usec
DE 7.00 usec
TE 298.2 K
D1 2.00000000 sec
d11 0.03000000 sec
DELTA 1.89999998 sec
MCREST 0.00000000 sec
MCWRK 0.01500000 sec
======== CHANNEL f1 ========
NUC1 13C
P1 8.00 usec
PL1 -3.00 dB
SFO1 100.6228298 MHz
======== CHANNEL f2 ========
CPDPRG2 waltz16
NUC2 1H
PCPD2 70.00 usec
PL2 -1.00 dB
PL12 14.00 dB
PL13 14.00 dB
SFO2 400.1316005 MHz
F2 - Processing parameters
SI 32768
SF 100.6128177 MHz
WDW EM
SSB 0
LB 1.00 Hz
GB 0
PC 1.00
170 160 150 140 130 120 110 100 90 80 70 60 50 40 30 20 10 0 ppm

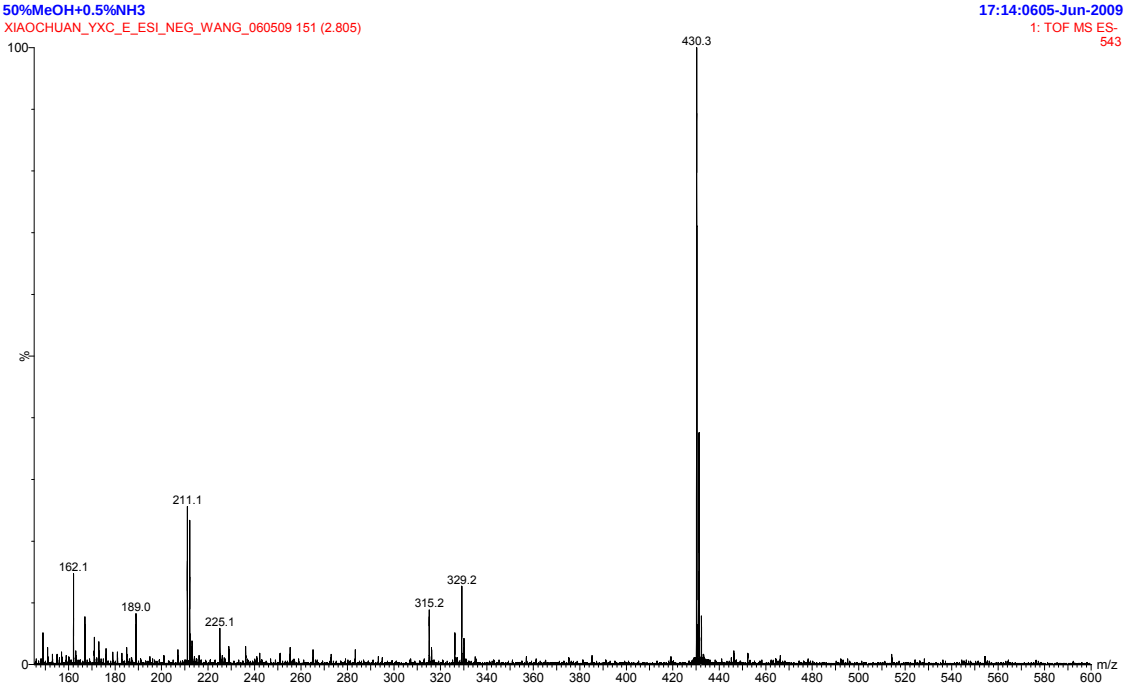
50%MeOH+0.5%NH3
XIAOCHUAN_YXC_E_ESI_NEG_WANG_060509 151 (2.805)
17:14:0605-Jun-2009
1: TOF MS ES-
543
100
%
0
430.3
211.1
162.1
189.0
225.1
315.2
329.2
160 180 200 220 240 260 280 300 320 340 360 380 400 420 440 460 480 500 520 540 560 580 600
m/z

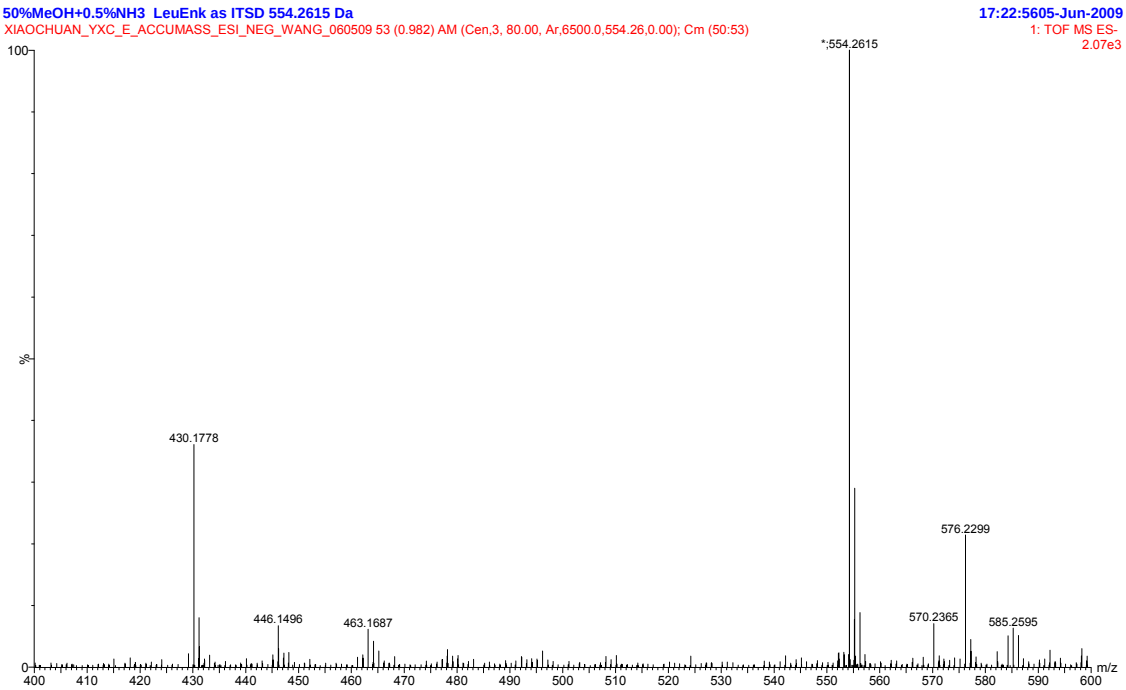
50%MeOH+0.5%NH3 LeuEnk as ITSD 554.2615 Da
17:22:5605-Jun-2009
XIAOCHUAN_YXC_E_ACCUMASS_ESI_NEG_WANG_060509 53 (0.982) AM (Cen,3, 80.00, Ar,6500.0,554.26,0.00); Cm (50:53)
1: TOF MS ES-
2.07e3
*;554.2615
430.1778
576.2299
446.1496
463.1687
570.2365
585.2595
%
m/z

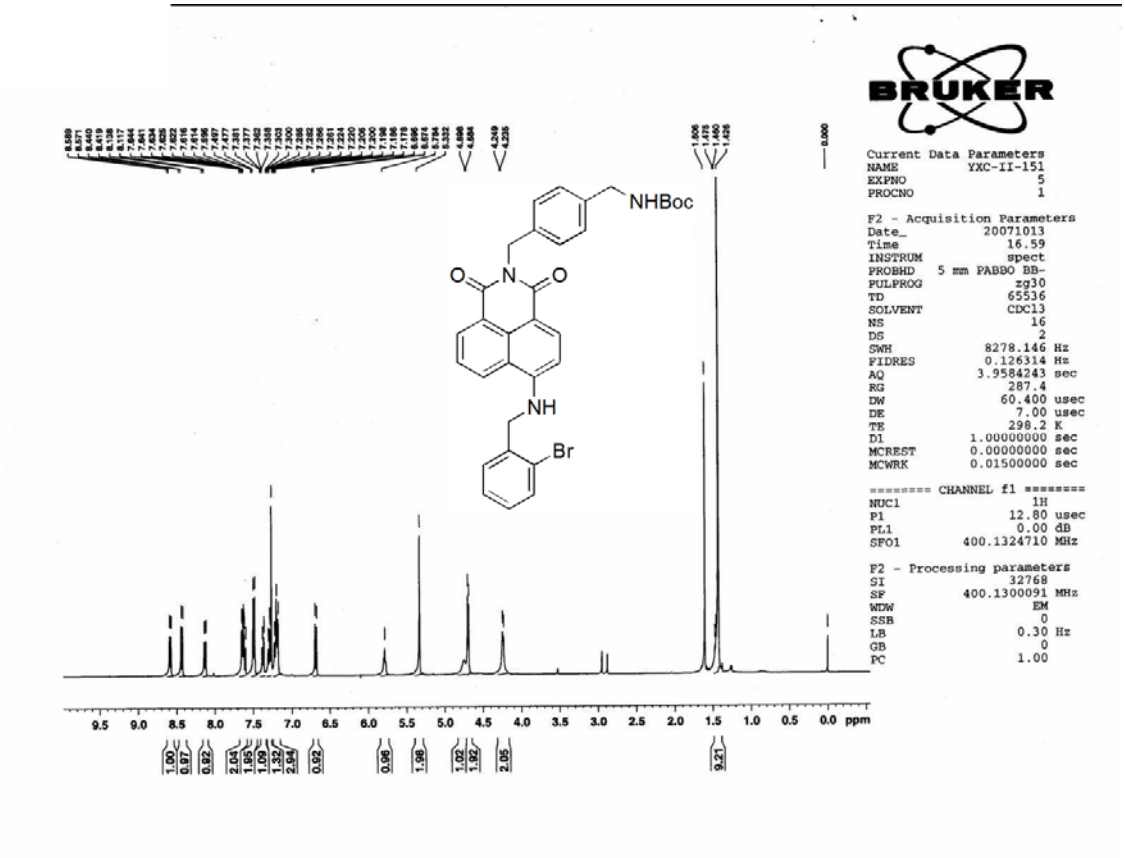
NHBoc
NH
Br
BRUKER
Current Data Parameters
NAME YXC-II-151
EXPNO 5
PROCNO 1
F2 - Acquisition Parameters
Date_ 20071013
Time 16.59
INSTRUM spect
PROBHD 5 mm PABBO BB-
PULPROG zg30
TD 65536
SOLVENT CDCl3
NS 16
DS 2
SWH 8278.146 Hz
FIDRES 0.126314 Hz
AQ 3.9584243 sec
RG 287.4
DW 60.400 usec
DE 7.00 usec
TE 298.2 K
D1 1.00000000 sec
MCREST 0.00000000 sec
MCWRK 0.01500000 sec
======== CHANNEL f1 ========
NUC1 1H
P1 12.80 usec
PL1 0.00 dB
SFO1 400.1324710 MHz
F2 - Processing parameters
SI 32768
SF 400.1300091 MHz
WDW EM
SSB 0
LB 0.30 Hz
GB 0
PC 1.00
ppm

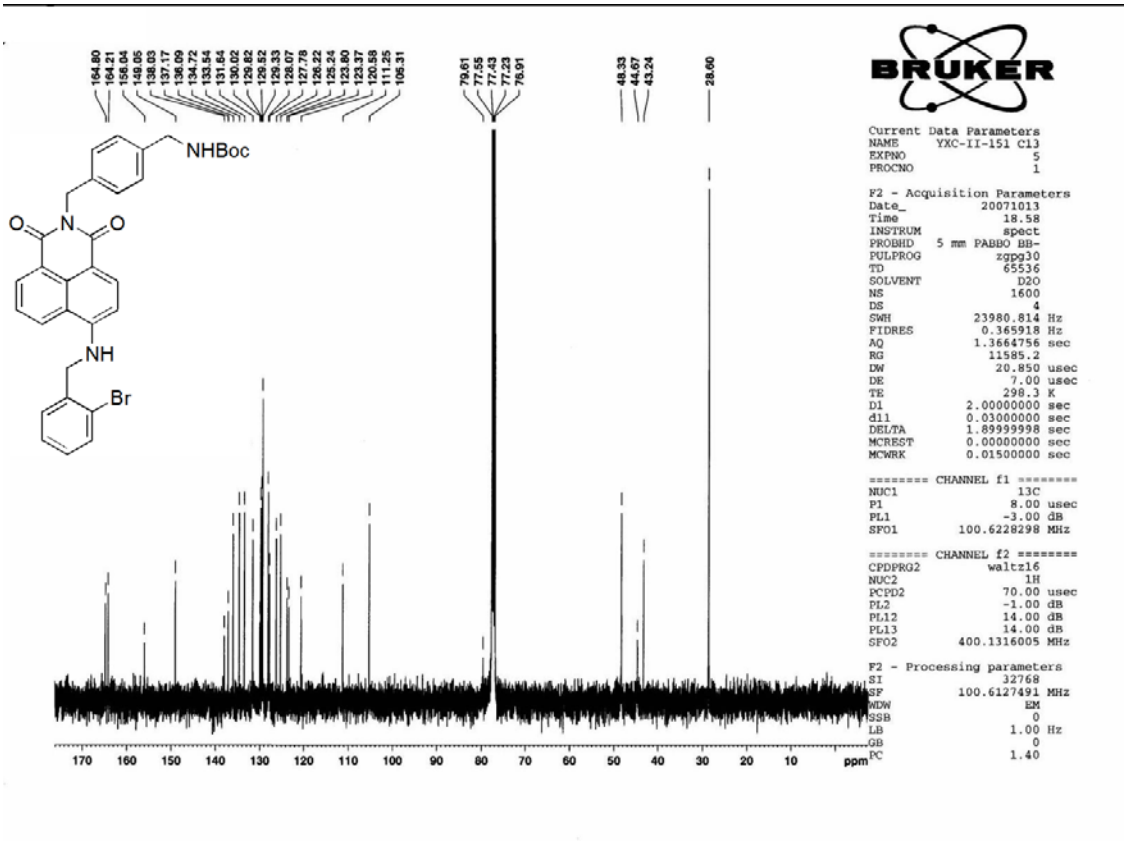
164.80
164.21
156.04
149.05
138.03
137.17
136.09
134.72
133.54
131.64
130.02
129.82
129.52
129.33
128.07
127.78
126.22
125.24
123.80
123.37
120.58
111.25
105.31
79.61
77.55
77.43
77.23
76.91
48.33
44.67
43.24
28.60
NHBoc
O
N
O
NH
Br
170 160 150 140 130 120 110 100 90 80 70 60 50 40 30 20 10 ppm
BRUKER
Current Data Parameters
NAME YXC-II-151 C13
EXPNO 5
PROCNO 1
F2 - Acquisition Parameters
Date_ 20071013
Time 18.58
INSTRUM spect
PROBHD 5 mm PABBO BB-
PULPROG zgpg30
TD 65536
SOLVENT D2O
NS 1600
DS 4
SWH 23980.814 Hz
FIDRES 0.365918 Hz
AQ 1.3664756 sec
RG 11585.2
DW 20.850 usec
DE 7.00 usec
TE 298.3 K
D1 2.00000000 sec
d11 0.03000000 sec
DELTA 1.89999998 sec
MCREST 0.00000000 sec
MCWRK 0.01500000 sec
======== CHANNEL f1 ========
NUC1 13C
P1 8.00 usec
PL1 -3.00 dB
SFO1 100.6228298 MHz
======== CHANNEL f2 ========
CPDPRG2 waltz16
NUC2 1H
PCPD2 70.00 usec
PL2 -1.00 dB
PL12 14.00 dB
PL13 14.00 dB
SFO2 400.1316005 MHz
F2 - Processing parameters
SI 32768
SF 100.6127491 MHz
WDW EM
SSB 0
LB 1.00 Hz
GB 0
PC 1.40

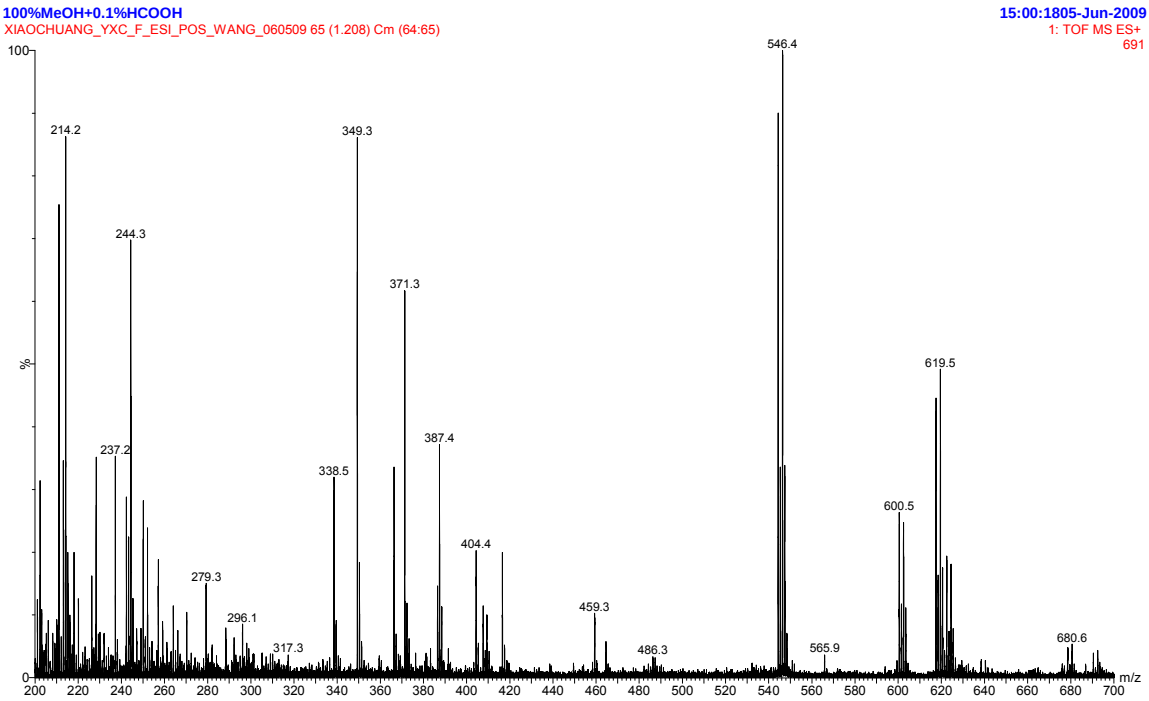
100%MeOH+0.1%HCOOH
XIAOCHUANG_YXC_F_ESI_POS_WANG_060509 65 (1.208) Cm (64:65)
15:00:1805-Jun-2009
1: TOF MS ES+
691
100
%
0
214.2
244.3
237.2
279.3
296.1
317.3
338.5
349.3
371.3
387.4
404.4
459.3
486.3
546.4
565.9
600.5
619.5
680.6
200 220 240 260 280 300 320 340 360 380 400 420 440 460 480 500 520 540 560 580 600 620 640 660 680 700 m/z

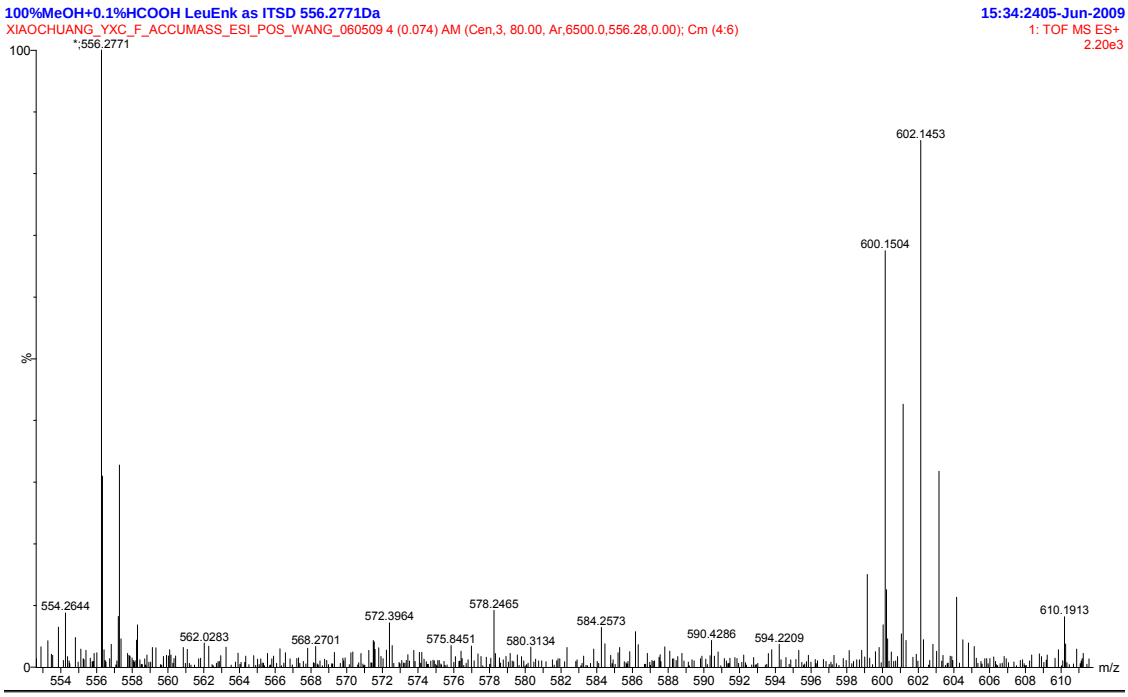

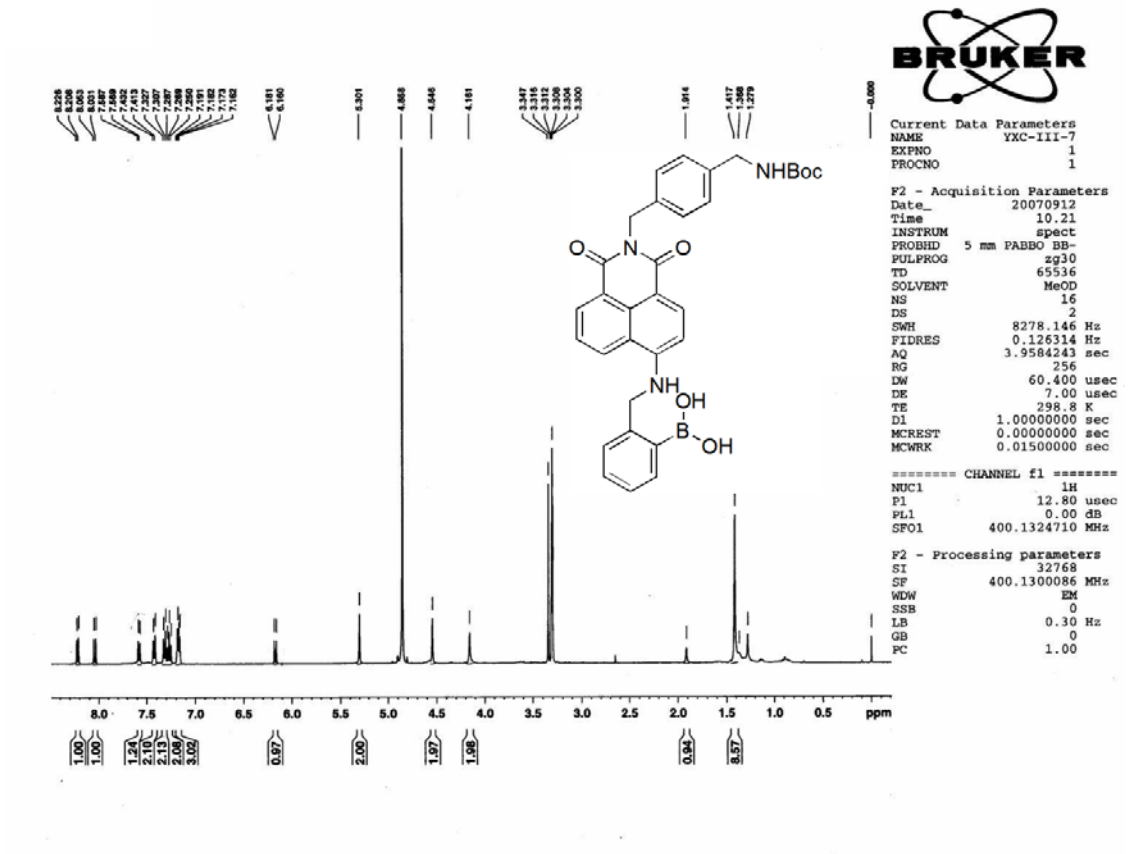

BRUKER

Current Data Parameters
NAME YXC-III-7
EXPNO 1
PROCNO 1

F2 - Acquisition Parameters
Date_ 20070912
Time 10.21
INSTRUM spect
PROBHD 5 mm PABBO BB-
PULPROG zg30
TD 65536
SOLVENT MeOD
NS 16
DS 2
SWH 8278.146 Hz
FIDRES 0.126314 Hz
AQ 3.9584243 sec
RG 256
DW 60.400 usec
DE 7.00 usec
TE 298.8 K
D1 1.00000000 sec
MCREST 0.00000000 sec
MCWRK 0.01500000 sec

======== CHANNEL f1 ========
NUC1 1H
P1 12.80 usec
PL1 0.00 dB
SFO1 400.1324710 MHz

F2 - Processing parameters
SI 32768
SF 400.1300086 MHz
WDW EM
SSB 0
LB 0.30 Hz
GB 0
PC 1.00

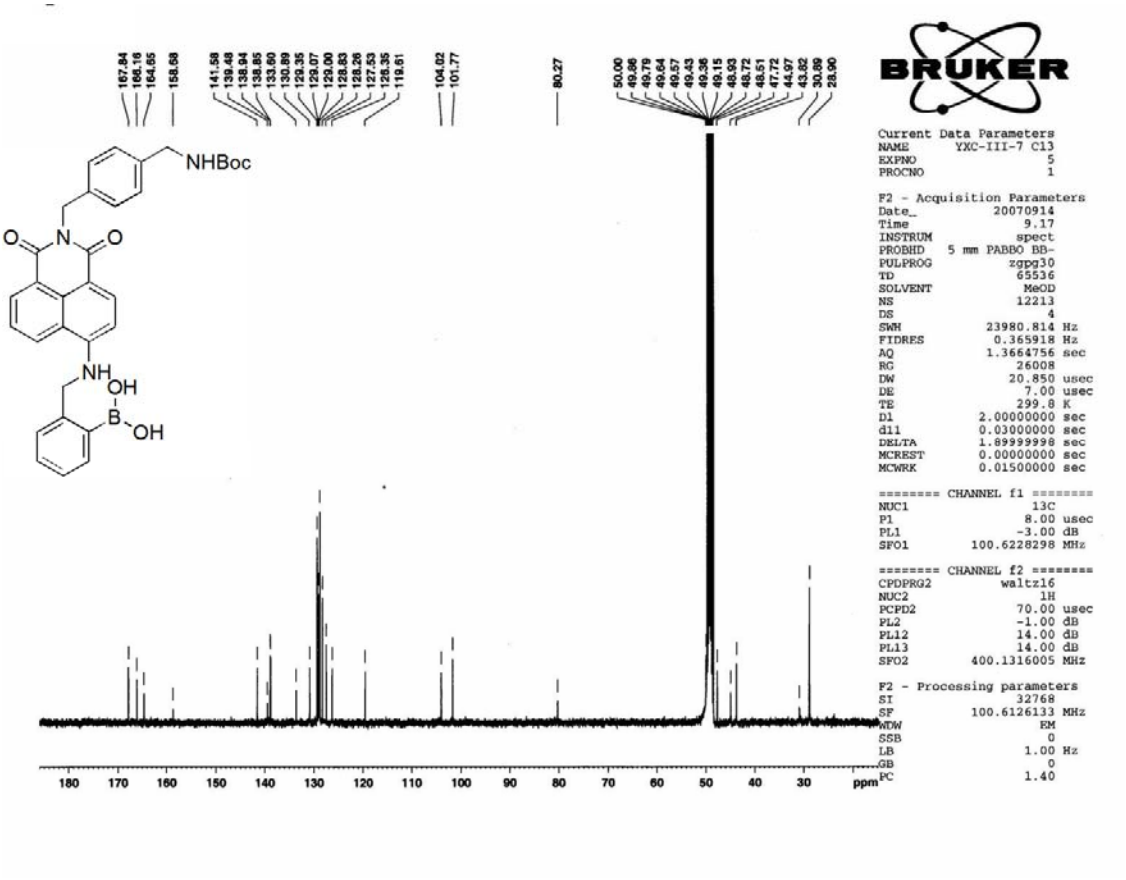
167.84
166.19
164.65
158.58
141.58
139.48
138.94
138.85
133.60
130.89
129.35
129.07
129.00
128.83
128.26
127.53
126.35
119.61
104.02
101.77
80.27
50.00
49.86
49.79
49.64
49.57
49.43
49.36
49.15
48.93
48.72
48.51
47.72
44.97
43.82
30.89
29.90
NHBoc
NH
OH
B
OH
BRUKER
Current Data Parameters
NAME YXC-III-7 C13
EXPNO 5
PROCNO 1
F2 - Acquisition Parameters
Date_ 20070914
Time 9.17
INSTRUM spect
PROBHD 5 mm PABBO BB-
PULPROG zgpg30
TD 65536
SOLVENT MeOD
NS 12213
DS 4
SWH 23980.814 Hz
FIDRES 0.365918 Hz
AQ 1.3664756 sec
RG 26008
DW 20.850 usec
DE 7.00 usec
TE 299.8 K
D1 2.00000000 sec
d11 0.03000000 sec
DELTA 1.89999998 sec
MCREST 0.00000000 sec
MCWRK 0.01500000 sec
======== CHANNEL f1 ========
NUC1 13C
P1 8.00 usec
PL1 -3.00 dB
SFO1 100.6228298 MHz
======== CHANNEL f2 ========
CPDPRG2 waltz16
NUC2 1H
PCPD2 70.00 usec
PL2 -1.00 dB
PL12 14.00 dB
PL13 14.00 dB
SFO2 400.1316005 MHz
F2 - Processing parameters
SI 32768
SF 100.6126133 MHz
WDW EM
SSB 0
LB 1.00 Hz
GB 0
PC 1.40
180 170 160 150 140 130 120 110 100 90 80 70 60 50 40 30 ppm

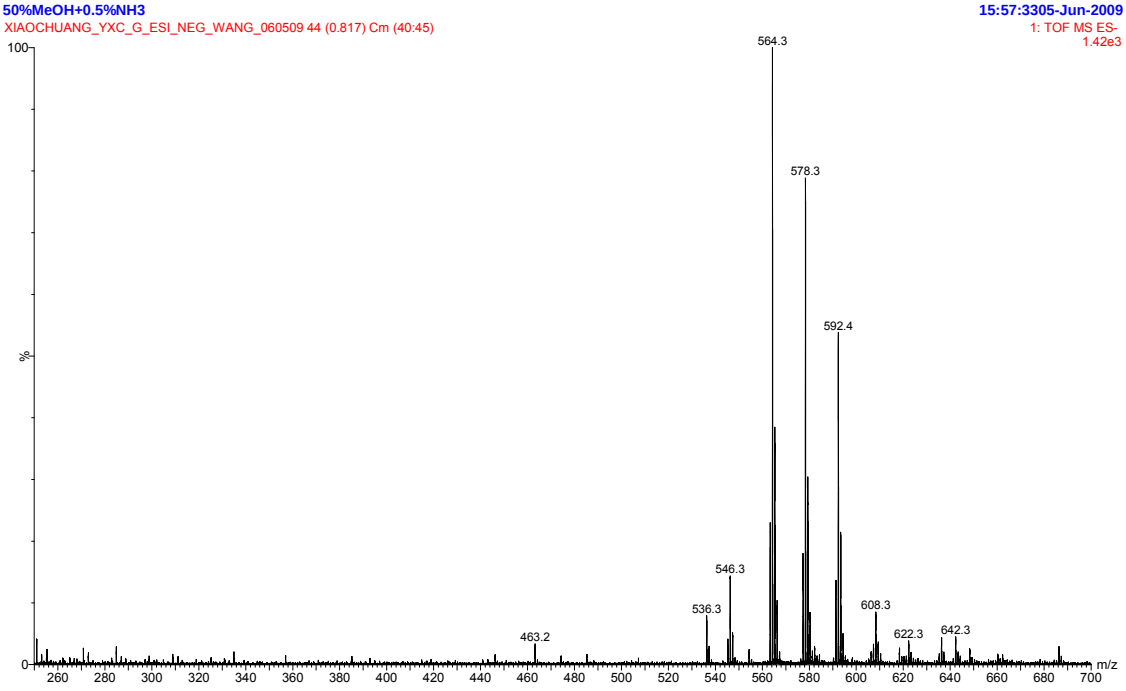
50%MeOH+0.5%NH3
XIAOCHUANG_YXC_G_ESI_NEG_WANG_060509 44 (0.817) Cm (40:45)
15:57:3305-Jun-2009
1: TOF MS ES-
1.42e3
100
%
0
564.3
578.3
592.4
546.3
536.3
608.3
622.3
642.3
463.2
260 280 300 320 340 360 380 400 420 440 460 480 500 520 540 560 580 600 620 640 660 680 700 m/z

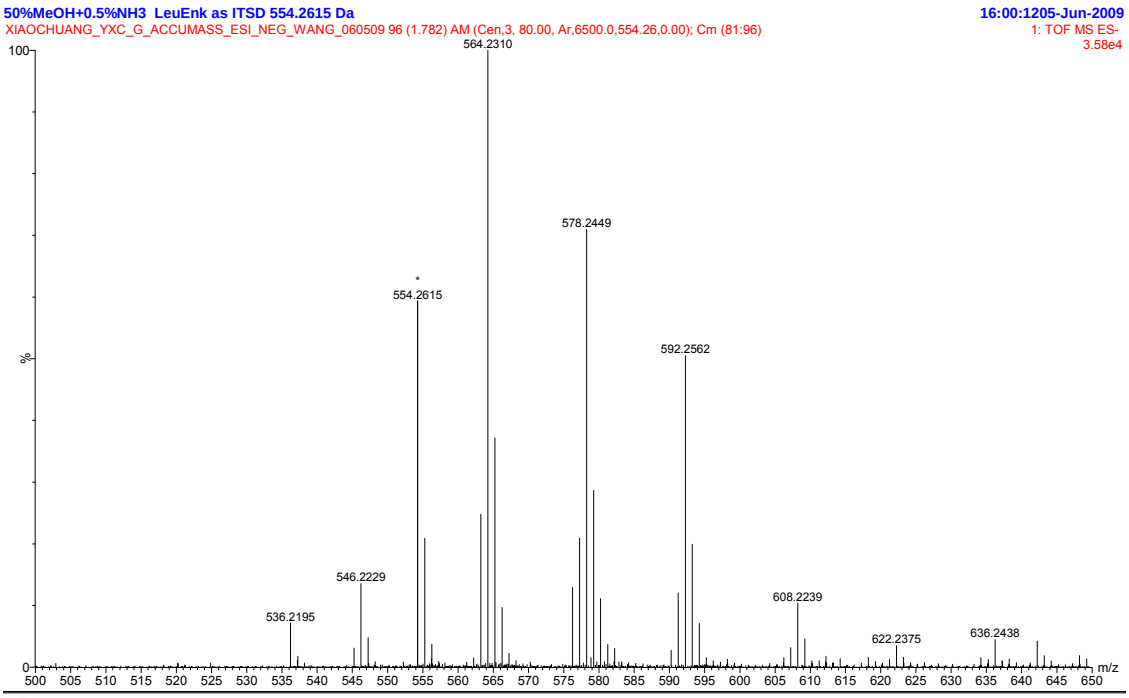
50%MeOH+0.5%NH3 LeuEnk as ITSD 554.2615 Da
16:00:1205-Jun-2009
XIAOCHUANG_YXC_G_ACCUMASS_ESI_NEG_WANG_060509 96 (1.782) AM (Cen,3, 80.00, Ar,6500.0,554.26,0.00); Cm (81:96)
1: TOF MS ES-
3.58e4
564.2310
578.2449
554.2615
592.2562
546.2229
608.2239
536.2195
622.2375
636.2438
m/z

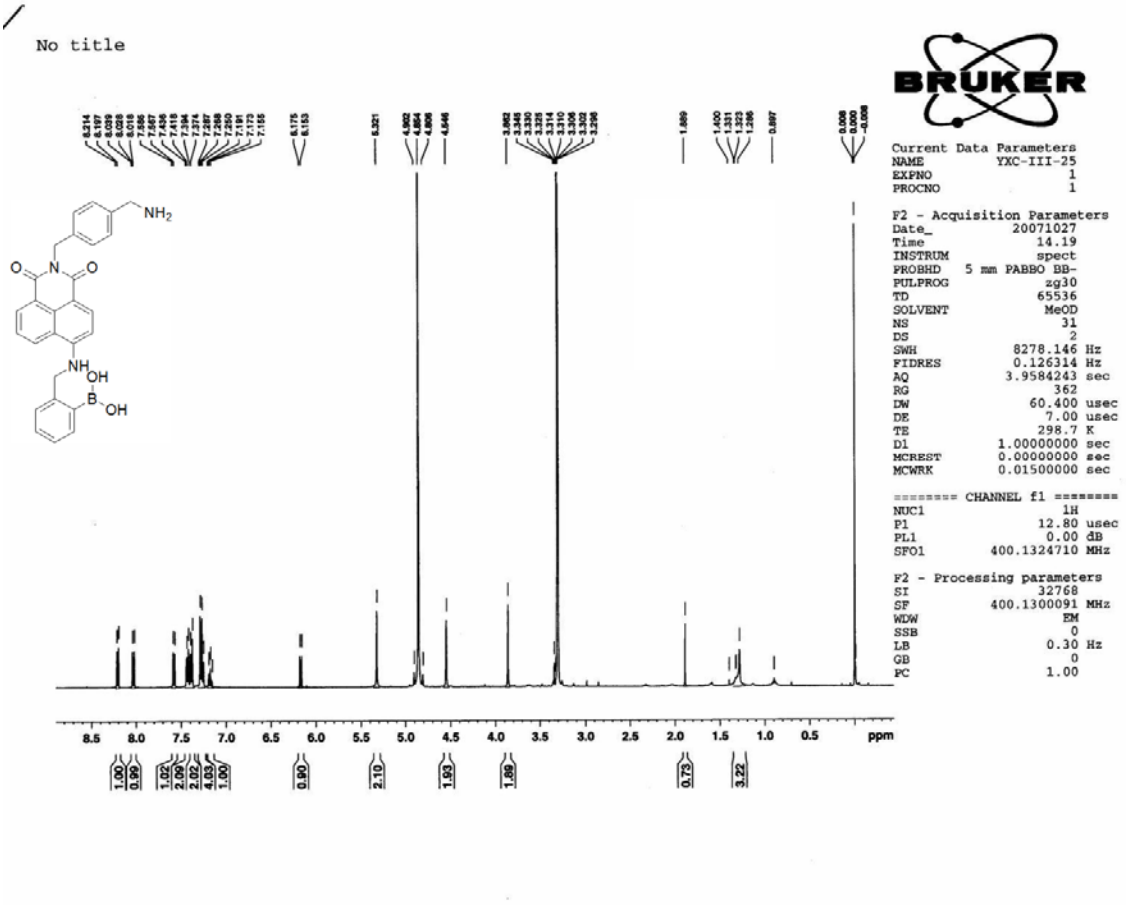
No title
BRUKER
Current Data Parameters
NAME YXC-III-25
EXPNO 1
PROCNO 1
F2 - Acquisition Parameters
Date_ 20071027
Time 14.19
INSTRUM spect
PROBHD 5 mm PABBO BB-
PULPROG zg30
TD 65536
SOLVENT MeOD
NS 31
DS 2
SWH 8278.146 Hz
FIDRES 0.126314 Hz
AQ 3.9584243 sec
RG 362
DW 60.400 usec
DE 7.00 usec
TE 298.7 K
D1 1.00000000 sec
MCREST 0.00000000 sec
MCWRK 0.01500000 sec
======== CHANNEL f1 ========
NUC1 1H
P1 12.80 usec
PL1 0.00 dB
SFO1 400.1324710 MHz
F2 - Processing parameters
SI 32768
SF 400.1300091 MHz
WDW EM
SSB 0
LB 0.30 Hz
GB 0
PC 1.00
ppm

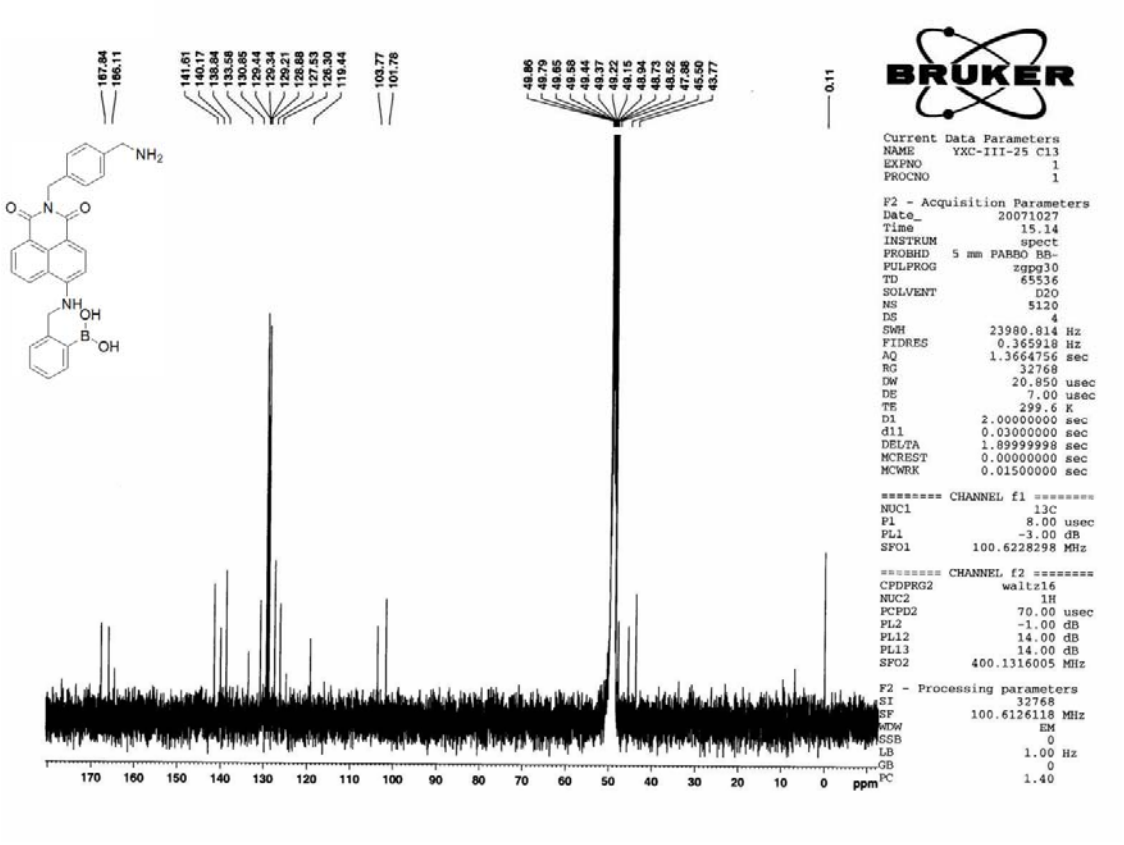
167.84
166.11
141.61
140.17
138.84
133.58
130.85
129.44
129.34
129.21
128.88
127.53
126.30
119.44
103.77
101.78
49.86
49.79
49.65
49.58
49.44
49.37
49.22
49.15
48.94
48.73
48.52
47.88
45.50
43.77
0.11
NH2
O
N
O
NH
OH
B
OH
170 160 150 140 130 120 110 100 90 80 70 60 50 40 30 20 10 0 ppm
BRUKER
Current Data Parameters
NAME YXC-III-25 C13
EXPNO 1
PROCNO 1
F2 - Acquisition Parameters
Date_ 20071027
Time 15.14
INSTRUM spect
PROBHD 5 mm PABBO BB-
PULPROG zgpg30
TD 65536
SOLVENT D2O
NS 5120
DS 4
SWH 23980.814 Hz
FIDRES 0.365918 Hz
AQ 1.3664756 sec
RG 32768
DW 20.850 usec
DE 7.00 usec
TE 299.6 K
D1 2.00000000 sec
d11 0.03000000 sec
DELTA 1.89999998 sec
MCREST 0.00000000 sec
MCWRK 0.01500000 sec
======== CHANNEL f1 ========
NUC1 13C
P1 8.00 usec
PL1 -3.00 dB
SFO1 100.6228298 MHz
======== CHANNEL f2 ========
CPDPRG2 waltz16
NUC2 1H
PCPD2 70.00 usec
PL2 -1.00 dB
PL12 14.00 dB
PL13 14.00 dB
SFO2 400.1316005 MHz
F2 - Processing parameters
SI 32768
SF 100.6126118 MHz
WDW EM
SSB 0
LB 1.00 Hz
GB 0
PC 1.40

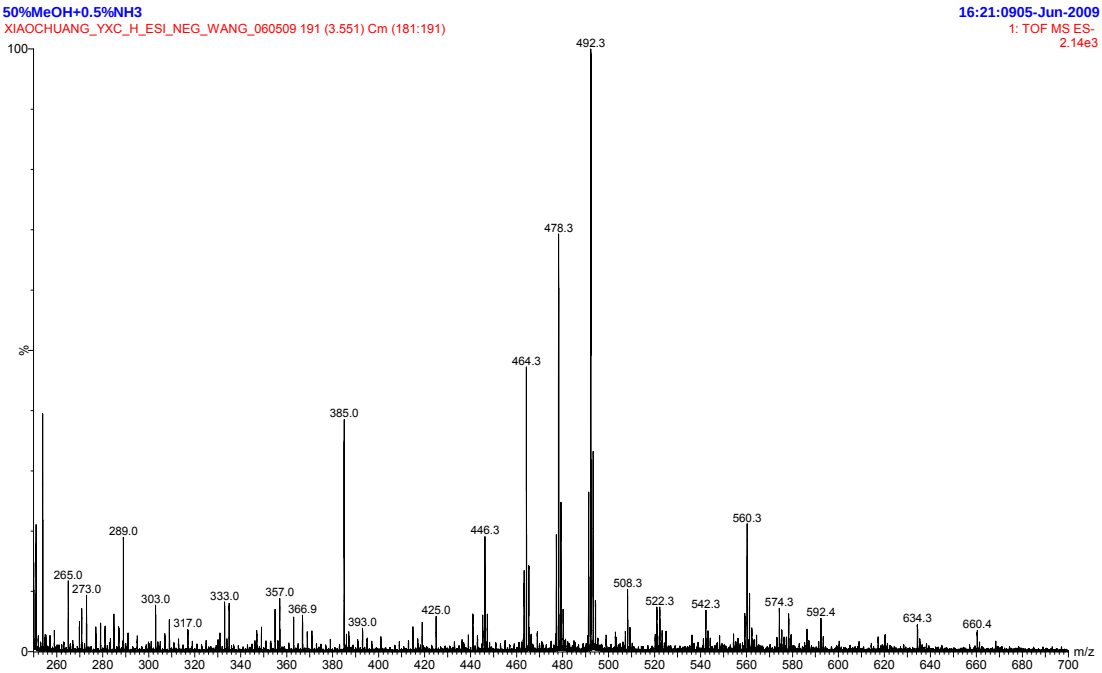
50%MeOH+0.5%NH3
XIAOCHUANG_YXC_H_ESI_NEG_WANG_060509 191 (3.551) Cm (181:191)
16:21:0905-Jun-2009
1: TOF MS ES-
2.14e3
100
%
0
492.3
478.3
464.3
385.0
446.3
560.3
289.0
265.0
273.0
303.0
317.0
333.0
357.0
366.9
393.0
425.0
508.3
522.3
542.3
574.3
592.4
634.3
660.4
260 280 300 320 340 360 380 400 420 440 460 480 500 520 540 560 580 600 620 640 660 680 700 m/z

50%MeOH+0.5%NH3 LeuEnk as ITSD 554.2615 Da **16:36:0805-Jun-2009**

XIAOCHUANG_YXC_H_ACCUMASS_ESI_NEG_WANG_060509 153 (2.840) AM (Cen,3, 80.00, Ar,6500.0,554.26,0.00); Cm (147:153) 1: TOF MS ES-

3.31e3

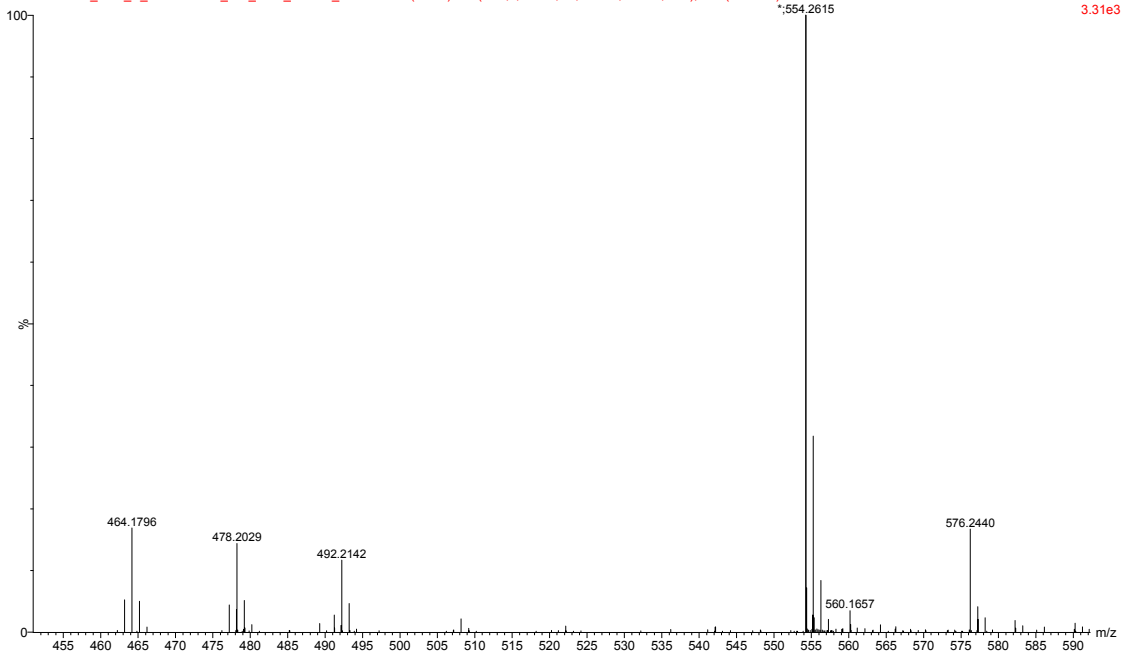

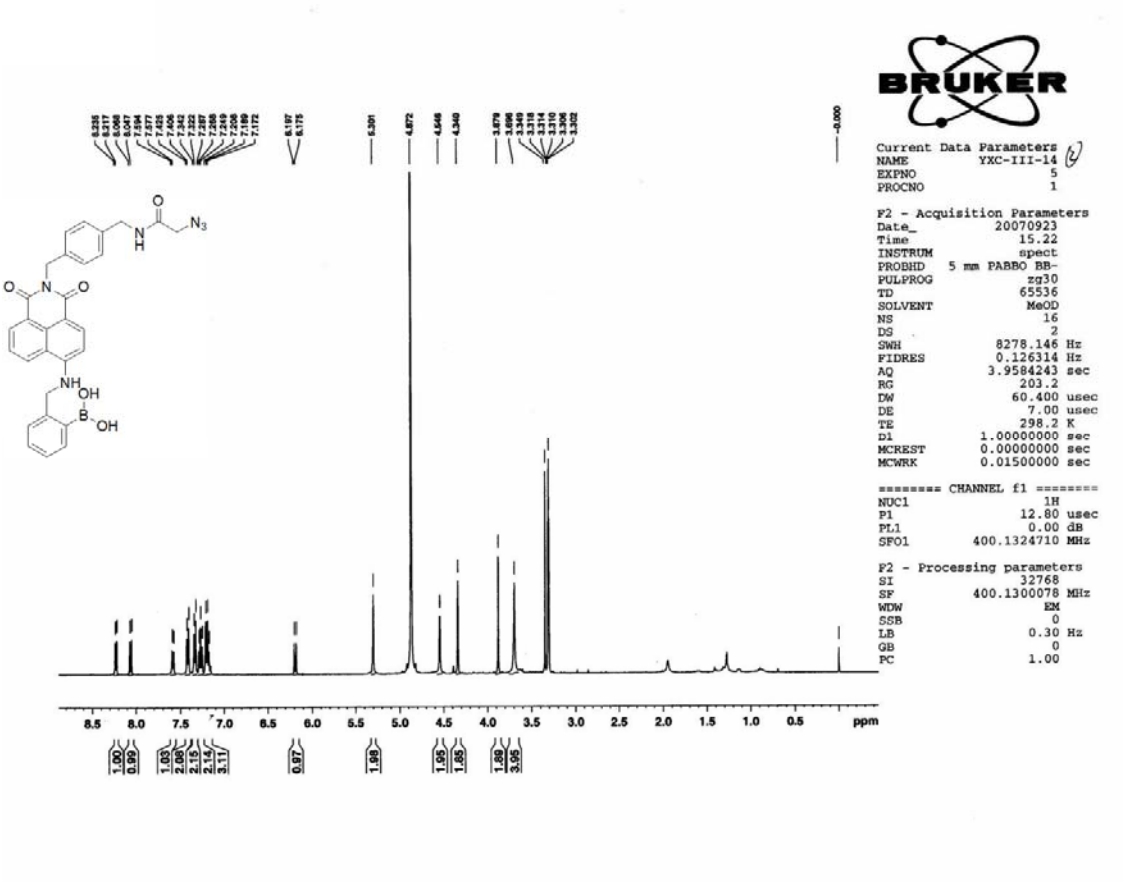

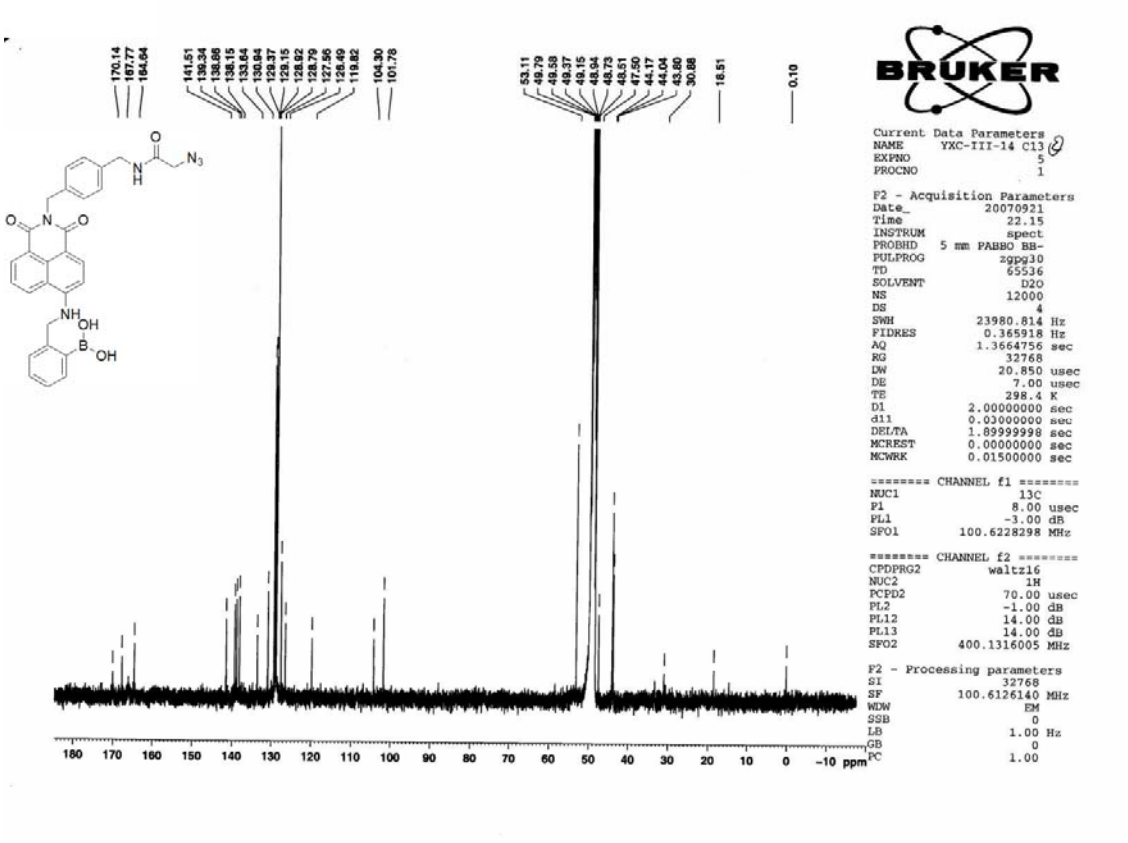

50%MeOH+0.5%NH3
XIAOCHUANG_YXC_I_ESI_NEG_WANG_060509 31 (0.574) Cm (28:32)

16:11:5005-Jun-2009
1: TOF MS ES-
381

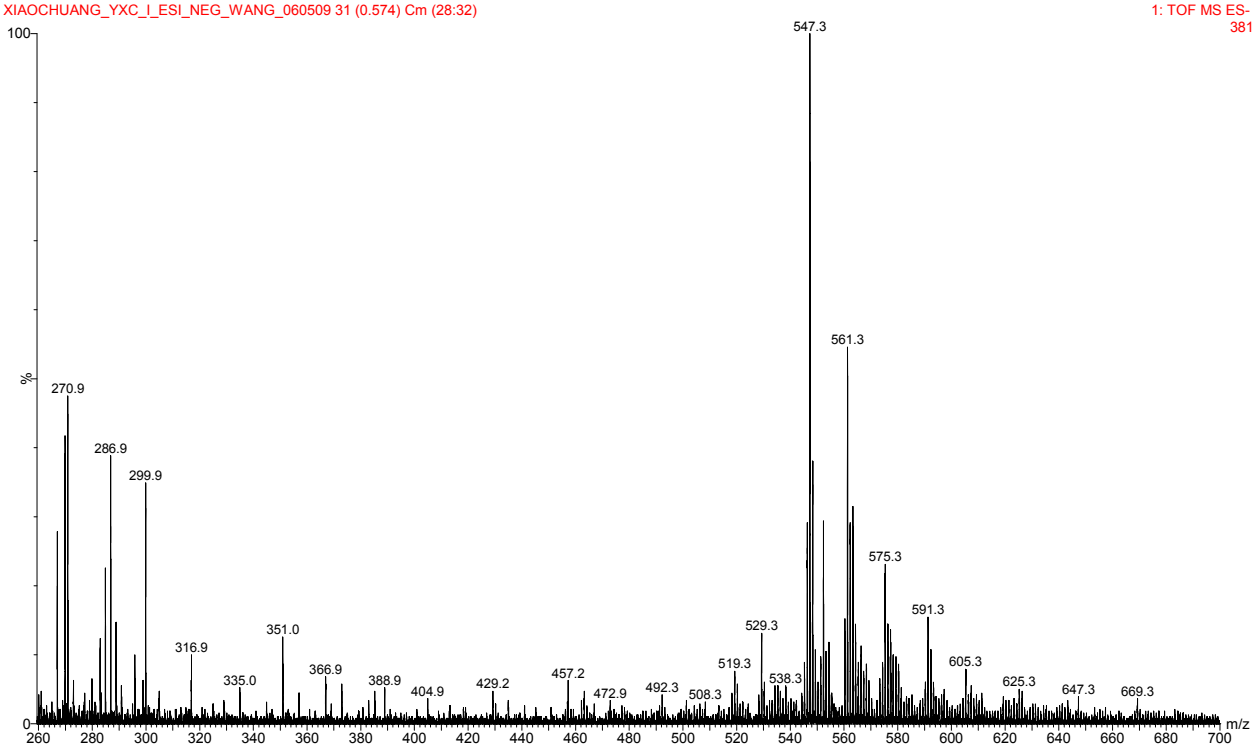

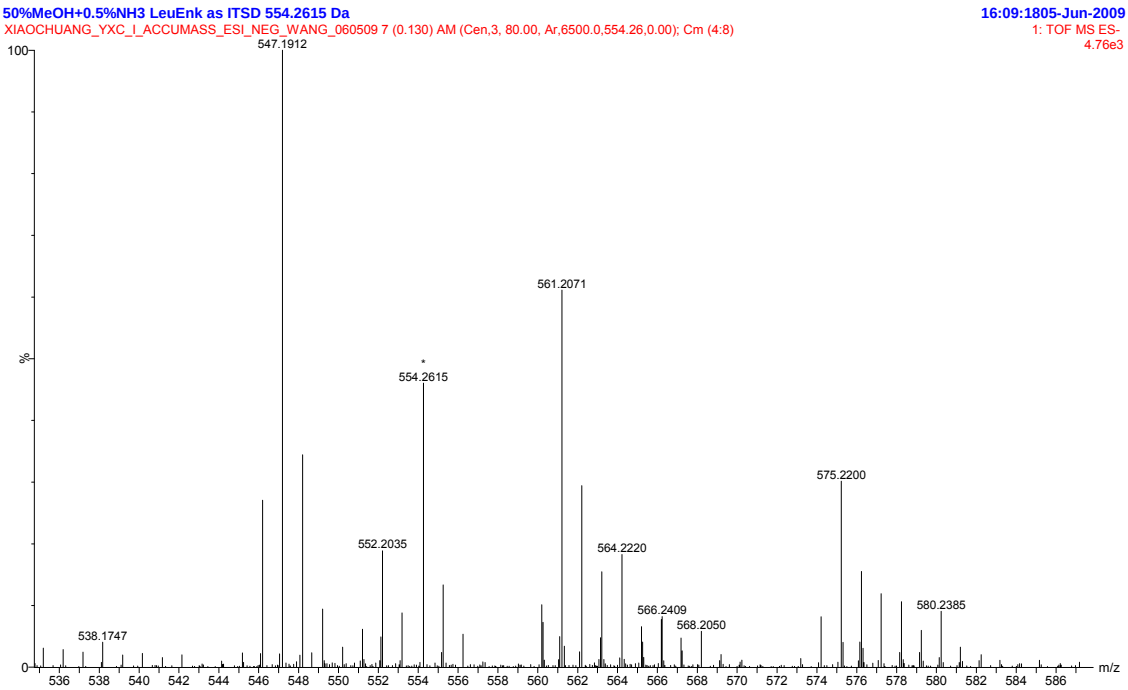
50%MeOH+0.5%NH3 LeuEnk as ITSD 554.2615 Da
XIAOCHUANG_YXC_I_ACCUMASS_ESI_NEG_WANG_060509 7 (0.130) AM (Cen,3, 80.00, Ar,6500.0,554.26,0.00); Cm (4:8)
16:09:1805-Jun-2009
1: TOF MS ES-
4.76e3
547.1912
561.2071
554.2615
575.2200
552.2035
564.2220
580.2385
566.2409
568.2050
538.1747
%
m/z

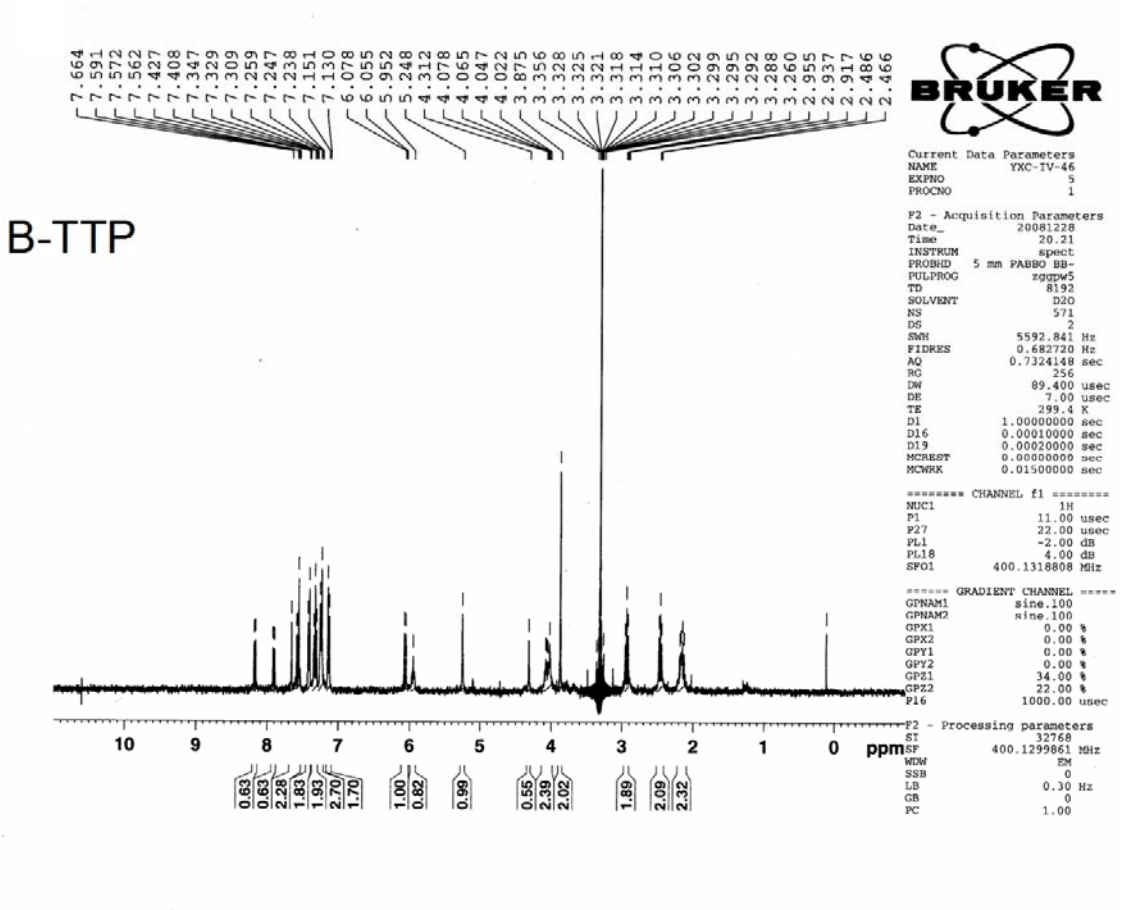
B-TTP
BRUKER
Current Data Parameters
NAME YXC-IV-46
EXPNO 5
PROCNO 1
F2 - Acquisition Parameters
Date_ 20081228
Time 20.21
INSTRUM spect
PROBHD 5 mm PABBO BB-
PULPROG zgqpw5
TD 8192
SOLVENT D2O
NS 571
DS 2
SWH 5592.841 Hz
FIDRES 0.682720 Hz
AQ 0.7324148 sec
RG 256
DW 89.400 usec
DE 7.00 usec
TE 299.4 K
D1 1.00000000 sec
D16 0.00010000 sec
D19 0.00020000 sec
MCREST 0.00000000 sec
MCWRK 0.01500000 sec
======== CHANNEL f1 ========
NUC1 1H
P1 11.00 usec
P27 22.00 usec
PL1 -2.00 dB
PL18 4.00 dB
SFO1 400.1318808 MHz
====== GRADIENT CHANNEL =====
GPNAM1 sine.100
GPNAM2 sine.100
GPX1 0.00 %
GPX2 0.00 %
GPY1 0.00 %
GPY2 0.00 %
GPZ1 34.00 %
GPZ2 22.00 %
P16 1000.00 usec
F2 - Processing parameters
SI 32768
SF 400.1299861 MHz
WDW EM
SSB 0
LB 0.30 Hz
GB 0
PC 1.00
ppm

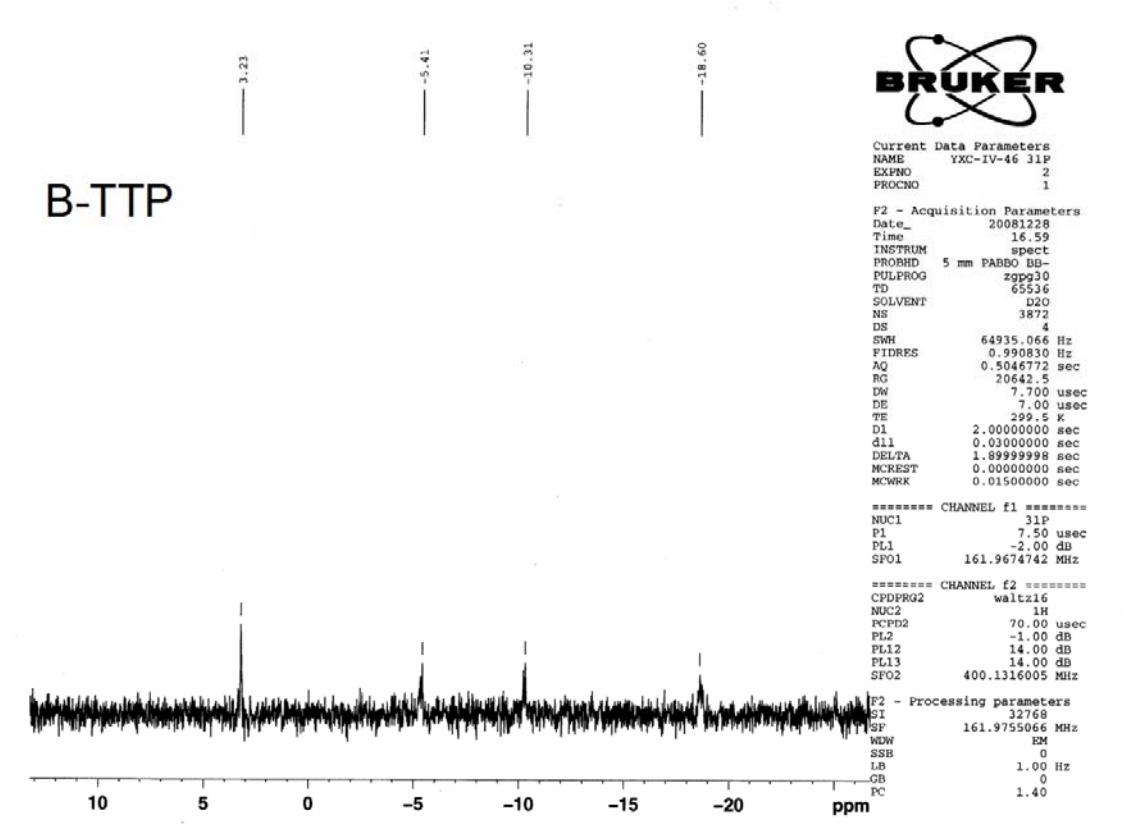
B-TTP
3.23
-5.41
-10.31
-18.60
BRUKER
Current Data Parameters
NAME YXC-IV-46 31P
EXPNO 2
PROCNO 1
F2 - Acquisition Parameters
Date_ 20081228
Time 16.59
INSTRUM spect
PROBHD 5 mm PABBO BB-
PULPROG zgpg30
TD 65536
SOLVENT D2O
NS 3872
DS 4
SWH 64935.066 Hz
FIDRES 0.990830 Hz
AQ 0.5046772 sec
RG 20642.5
DW 7.700 usec
DE 7.00 usec
TE 299.5 K
D1 2.00000000 sec
d11 0.03000000 sec
DELTA 1.89999998 sec
MCREST 0.00000000 sec
MCWRK 0.01500000 sec
======== CHANNEL f1 ========
NUC1 31P
P1 7.50 usec
PL1 -2.00 dB
SFO1 161.9674742 MHz
======== CHANNEL f2 ========
CPDPRG2 waltz16
NUC2 1H
PCPD2 70.00 usec
PL2 -1.00 dB
PL12 14.00 dB
PL13 14.00 dB
SFO2 400.1316005 MHz
F2 - Processing parameters
SI 32768
SF 161.9755066 MHz
WDW EM
SSB 0
LB 1.00 Hz
GB 0
PC 1.40
10
5
0
-5
-10
-15
-20
ppm

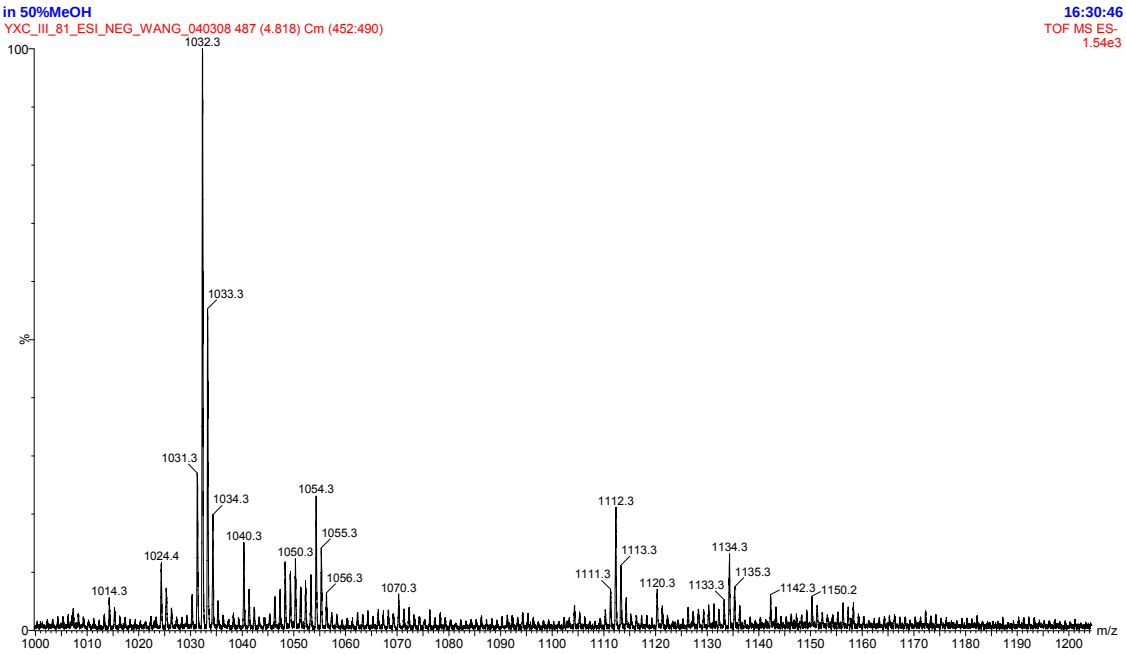
in 50%MeOH
YXC_III_81_ESI_NEG_WANG_040308 487 (4.818) Cm (452:490)
16:30:46
TOF MS ES-
1.54e3
100
%
0
1032.3
1033.3
1031.3
1034.3
1054.3
1055.3
1040.3
1050.3
1024.4
1056.3
1014.3
1070.3
1112.3
1113.3
1111.3
1134.3
1135.3
1120.3
1133.3
1142.3
1150.2
1000
1010
1020
1030
1040
1050
1060
1070
1080
1090
1100
1110
1120
1130
1140
1150
1160
1170
1180
1190
1200
m/z

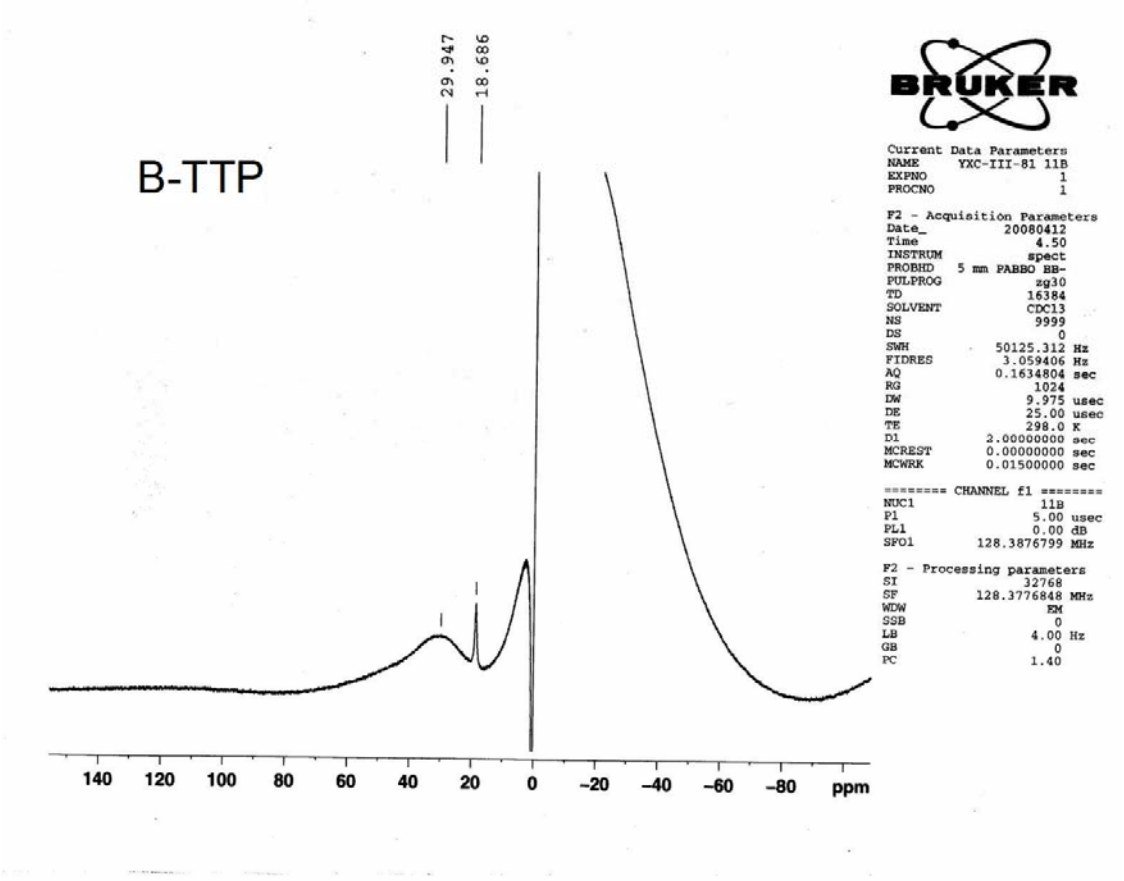
B-TTP
29.947
18.686
140 120 100 80 60 40 20 0 -20 -40 -60 -80 ppm
BRUKER
Current Data Parameters
NAME YXC-III-81 11B
EXPNO 1
PROCNO 1
F2 - Acquisition Parameters
Date_ 20080412
Time 4.50
INSTRUM spect
PROBHD 5 mm PABBO BB-
PULPROG zg30
TD 16384
SOLVENT CDCl3
NS 9999
DS 0
SWH 50125.312 Hz
FIDRES 3.059406 Hz
AQ 0.1634804 sec
RG 1024
DW 9.975 usec
DE 25.00 usec
TE 298.0 K
D1 2.00000000 sec
MCREST 0.00000000 sec
MCWRK 0.01500000 sec
======== CHANNEL f1 ========
NUC1 11B
P1 5.00 usec
PL1 0.00 dB
SFO1 128.3876799 MHz
F2 - Processing parameters
SI 32768
SF 128.3776848 MHz
WDW EM
SSB 0
LB 4.00 Hz
GB 0
PC 1.40

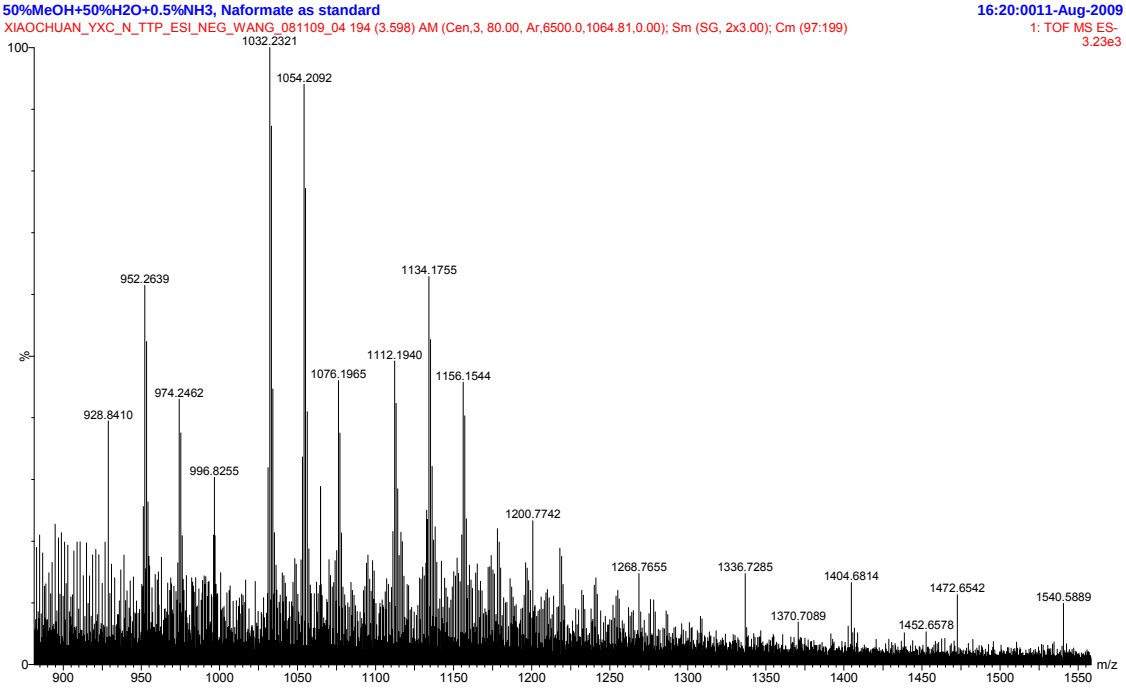
50%MeOH+50%H2O+0.5%NH3, Naformate as standard
16:20:0011-Aug-2009
XIAOCHUAN_YXC_N_TTP_ESI_NEG_WANG_081109_04 194 (3.598) AM (Cen,3, 80.00, Ar,6500.0,1064.81,0.00); Sm (SG, 2x3.00); Cm (97:199)
1: TOF MS ES-
3.23e3
100
%
0
1032.2321
1054.2092
952.2639
1134.1755
1112.1940
1076.1965
1156.1544
974.2462
928.8410
996.8255
1200.7742
1268.7655
1336.7285
1404.6814
1370.7089
1472.6542
1452.6578
1540.5889
900 950 1000 1050 1100 1150 1200 1250 1300 1350 1400 1450 1500 1550
m/z

REFERENCES

(1) Cook-Deegan, R. M. *Genomics* **1989**, *5*, 661.

(2) Lander, E. S.; Linton, L. M.; Birren, B.; Nusbaum, C.; Zody, M. C.; Baldwin, J.; Devon, K.; Dewar, K.; Doyle, M.; FitzHugh, W.; Funke, R.; Gage, D.; Harris, K.; Heaford, A.; Howland, J.; Kann, L.; Lehoczky, J.; LeVine, R.; McEwan, P.; McKernan, K.; Meldrim, J.; Mesirov, J. P.; Miranda, C.; Morris, W.; Naylor, J.; Raymond, C.; Rosetti, M.; Santos, R.; Sheridan, A.; Sougnez, C.; Stange-Thomann, N.; Stojanovic, N.; Subramanian, A.; Wyman, D.; Rogers, J.; Sulston, J.; Ainscough, R.; Beck, S.; Bentley, D.; Burton, J.; Clee, C.; Carter, N.; Coulson, A.; Deadman, R.; Deloukas, P.; Dunham, A.; Dunham, I.; Durbin, R.; French, L.; Grafham, D.; Gregory, S.; Hubbard, T.; Humphray, S.; Hunt, A.; Jones, M.; Lloyd, C.; McMurray, A.; Matthews, L.; Mercer, S.; Milne, S.; Mullikin, J. C.; Mungall, A.; Plumb, R.; Ross, M.; Shownkeen, R.; Sims, S.; Waterston, R. H.; Wilson, R. K.; Hillier, L. W.; McPherson, J. D.; Marra, M. A.; Mardis, E. R.; Fulton, L. A.; Chinwalla, A. T.; Pepin, K. H.; Gish, W. R.; Chissoe, S. L.; Wendl, M. C.; Delehaunty, K. D.; Miner, T. L.; Delehaunty, A.; Kramer, J. B.; Cook, L. L.; Fulton, R. S.; Johnson, D. L.; Minx, P. J.; Clifton, S. W.; Hawkins, T.; Branscomb, E.; Predki, P.; Richardson, P.; Wenning, S.; Slezak, T.; Doggett, N.; Cheng, J. F.; Olsen, A.; Lucas, S.; Elkin, C.; Uberbacher, E.; Frazier, M. *Nature* **2001**, *409*, 860.

(3) Venter, J. C.; Adams, M. D.; Myers, E. W.; Li, P. W.; Mural, R. J.; Sutton, G. G.; Smith, H. O.; Yandell, M.; Evans, C. A.; Holt, R. A.; Gocayne, J. D.; Amanatides, P.;

Ballew, R. M.; Huson, D. H.; Wortman, J. R.; Zhang, Q.; Kodira, C. D.; Zheng, X. Q. H.; Chen, L.; Skupski, M.; Subramanian, G.; Thomas, P. D.; Zhang, J. H.; Miklos, G. L. G.; Nelson, C.; Broder, S.; Clark, A. G.; Nadeau, C.; McKusick, V. A.; Zinder, N.; Levine, A. J.; Roberts, R. J.; Simon, M.; Slayman, C.; Hunkapiller, M.; Bolanos, R.; Delcher, A.; Dew, I.; Fasulo, D.; Flanigan, M.; Florea, L.; Halpern, A.; Hannenhalli, S.; Kravitz, S.; Levy, S.; Mobarry, C.; Reinert, K.; Remington, K.; Abu-Threideh, J.; Beasley, E.; Biddick, K.; Bonazzi, V.; Brandon, R.; Cargill, M.; Chandramouliswaran, I.; Charlab, R.; Chaturvedi, K.; Deng, Z. M.; Di Francesco, V.; Dunn, P.; Eilbeck, K.; Evangelista, C.; Gabrielian, A. E.; Gan, W.; Ge, W. M.; Gong, F. C.; Gu, Z. P.; Guan, P.; Heiman, T. J.; Higgins, M. E.; Ji, R. R.; Ke, Z. X.; Ketchum, K. A.; Lai, Z. W.; Lei, Y. D.; Li, Z. Y.; Li, J. Y.; Liang, Y.; Lin, X. Y.; Lu, F.; Merkulov, G. V.; Milshina, N.; Moore, H. M.; Naik, A. K.; Narayan, V. A.; Neelam, B.; Nusskern, D.; Rusch, D. B.; Salzberg, S.; Shao, W.; Shue, B. X.; Sun, J. T.; Wang, Z. Y.; Wang, A. H.; Wang, X.; Wang, J.; Wei, M. H.; Wides, R.; Xiao, C. L.; Yan, C. H. *Science* **2001**, *291*, 1304.

(4) Mann, M.; Jensen, O. N. *Nat. Biotechnol.* **2003**, *21*, 255.

(5) Graves, D. J.; Martin, B. L.; Wang, J. H. *Co- and Post-translational Modification of Proteins : Chemical Principles and Biological Effects*; Oxford University Press: New York 1994.

(6) *Post-translational Processing : a Practical Approach*; New York : Oxford University Press: Oxford 1999; Vol. 203.

(7) Bode, A. M.; Dong, Z. G. *Nat. Rev. Cancer* **2004**, *4*, 793.

(8) Gabius, H.-J.; Gabius, S. *Glycosciences : Status and Perspectives*; New York : Chapman & Hall: London 1997.

(9) Varki, A.; al., e. *Essentials of Glycobiology*; 2nd ed.; Cold Spring Harbor Laboratory Press: Cold Spring Harbor, N.Y. , 2009.

(10) Taylor, M. E.; Drickamer, K. *Introduction to Glycobiology*; Oxford University Press: New York, 2003.

(11)Lis, H.; Sharon, N. *Eur. J. Biochem.* **1993**, *218*, 1.

(12) Lowe, J. B.; Marth, J. D. *Annu. Rev. Biochem.* **2003**, *72*, 643.

(13) Brownlee, M. *Annu. Rev. Med.* **1995**, *46*, 223.

(14) Hakomori, S. *Proc. Natl. Acad. Sci. U. S. A.* **2002**, *99*, 10231.

(15) Rudd, P. M.; Elliott, T.; Cresswell, P.; Wilson, I. A.; Dwek, R. A. *Science* **2001**, *291*, 2370.

(16) Raman, R.; Raguram, S.; Venkataraman, G.; Paulson, J. C.; Sasisekharan, R. *Nat. Methods* **2005**, *2*, 817.

(17) Ohtsubo, K.; Marth, J. D. *Cell* **2006**, *126*, 855.

(18) Spiro, R. G. *Glycobiology* **2002**, *12*, 43R.

(19) Schachter, H. *Glycoconj. J.* **2000**, *17*, 465.

(20) Yan, A. X.; Lennarz, W. J. *J. Biol. Chem.* **2005**, *280*, 3121.

(21) Kukuruzinska, M. A.; Lennon, K. *Crit. Rev. Oral Biol. Med.* **1998**, *9*, 415.

(22) Van den Steen, P.; Rudd, P. M.; Dwek, R. A.; Opdenakker, G. *Crit. Rev. Biochem. Mol. Biol.* **1998**, *33*, 151.

(23) Iozzo, R. V. *Annu. Rev. Biochem.* **1998**, *67*, 609.

(24) Esko, J. D.; Selleck, S. B. *Annu. Rev. Biochem.* **2002**, *71*, 435.

(25) Scott, J. E. *Faseb J.* **1992**, *6*, 2639.

(26) Maccioni, H. J. F.; Giraudo, C. G.; Daniotti, J. L. *Neurochem. Res.* **2002**, *27*, 629.

(27) Hakomori, S. I.; Igarashi, Y. In *Advances in Lipid Research, Vol 25*; Academic Press Inc: San Diego, 1993; Vol. 25, p 147.

(28) Hart, G. W. *Annu. Rev. Biochem.* **1997**, *66*, 315.

(29) Zhang, F. X.; Su, K. H.; Yang, X. Y.; Bowe, D. B.; Paterson, A. J.; Kudlow, J. E. *Cell* **2003**, *115*, 715.

(30) O'Donnell, N.; Zachara, N. E.; Hart, G. W.; Marth, J. D. *Mol. Cell. Biol.* **2004**, *24*, 1680.

(31) Zachara, N. E.; Hart, G. W. *Biochim. Biophys. Acta-Gen. Subj.* **2004**, *1673*, 13.

(32) Ioffe, E.; Stanley, P. *Proc. Natl. Acad. Sci. U. S. A.* **1994**, *91*, 728.

(33) Metzler, M.; Gertz, A.; Sarkar, M.; Schachter, H.; Schrader, J. W.; Marth, J. D. *Embo J.* **1994**, *13*, 2056.

(34) Wang, L. C.; Fuster, M.; Sriramarao, P.; Esko, J. D. *Nat. Immunol.* **2005**, *6*, 902.

(35) Morris, M. A.; Ley, K. *Curr. Mol. Med.* **2004**, *4*, 431.

(36) van Gisbergen, K.; Geijtenbeek, T. B. H.; van Kooyk, Y. *Trends Immunol.*

2005, *26*, 626.

(37) Rosen, S. D. *Annu. Rev. Immunol.* **2004**, *22*, 129.

(38) Lowe, J. B. *Curr. Opin. Cell Biol.* **2003**, *15*, 531.

(39) Barton, G. M.; Medzhitov, R. *Science* **2003**, *300*, 1524.

(40) Geijtenbeek, T. B. H.; van Vliet, S. J.; Engering, A.; t Hart, B. A.; van Kooyk, Y. *Annu. Rev. Immunol.* **2004**, *22*, 33.

(41) van Die, I.; Cummings, R. D. *Chem. Immunol. Allergy* **2006**, *90*, 91.

(42) Takahashi, K.; Ezekowitz, R. A. *Clin. Infect. Dis.* **2005**, *41 Suppl 7*, S440.

(43) Kishore, U.; Greenhough, T. J.; Waters, P.; Shrive, A. K.; Ghai, R.; Kamran, M. F.; Bernal, A. L.; Reid, K. B.; Madan, T.; Chakraborty, T. *Mol. Immunol.* **2006**, *43*, 1293.

(44) Cambi, A.; Koopman, M.; Figdor, C. G. *Cell. Microbiol.* **2005**, *7*, 481.

(45) Geijtenbeek, T. B.; van Vliet, S. J.; Engering, A.; t Hart, B. A.; van Kooyk, Y. *Annu. Rev. Immunol.* **2004**, *22*, 33.

(46) Ashwell, G.; Harford, J. *Annu. Rev. Biochem.* **1982**, *51*, 531.

(47) Ellies, L. G.; Ditto, D.; Levy, G. G.; Wahrenbrock, M.; Ginsburg, D.; Varki, A.; Le, D. T.; Marth, J. D. *Proc. Natl. Acad. Sci. U. S. A.* **2002**, *99*, 10042.

(48) Ornitz, D. M.; Yayon, A.; Flanagan, J. G.; Svahn, C. M.; Levi, E.; Leder, P. *Mol. Cell. Biol.* **1992**, *12*, 240.

(49) Belenkaya, T. Y.; Han, C.; Yan, D.; Opoka, R. J.; Khodoun, M.; Liu, H. Z.; Lin, X. H. *Cell* **2004**, *119*, 231.

(50) Jaeken, J.; Carchon, H. *Curr. Opin. Pediatr.* **2004**, *16*, 434.

(51) Freeze, H. H. *Nat. Rev. Genet.* **2006**, *7*, 537.

(52) Aebi, M.; Hennet, T. *Trends Cell Biol.* **2001**, *11*, 136.

(53) Kornfeld, S.; Sly, W. S. *Hosp. Pract.* **1985**, *20*, 71.

(54) Kudo, M.; Brem, M. S.; Canfield, W. M. *Am. J. Hum. Genet.* **2006**, *78*, 451.

(55) Gong, C. X.; Liu, F.; Grundke-Iqbal, I.; Iqbal, K. *J. Neural Transm.* **2005**, *112*, 813.

(56) Block, T. M.; Comunale, M. A.; Lowman, M.; Steel, L. F.; Romano, P. R.; Fimmel, C.; Tennant, B. C.; London, W. T.; Evans, A. A.; Blumberg, B. S.; Dwek, R. A.; Mattu, T. S.; Mehta, A. S. *Proc. Natl. Acad. Sci. U. S. A.* **2005**, *102*, 779.

(57) Ueda, K.; Katagiri, T.; Shimada, T.; Irie, S.; Sato, T. A.; Nakamura, Y.; Daigo, Y. *J. Proteome Res.* **2007**, *6*, 3475.

(58) Barrabes, S.; Pages-Pons, L.; Radcliffe, C. M.; Tabares, G.; Fort, E.; Royle, L.; Harvey, D. J.; Moenner, M.; Dwek, R. A.; Rudd, P. M.; De Llorens, R.; Peracaula, R. *Glycobiology* **2007**, *17*, 388.

(59) Saldova, R.; Wormald, M. R.; Dwek, R. A.; Rudd, P. M. *Dis. Markers* **2008**, *25*, 219.

(60) Ang, I. L.; Poon, T. C. W.; Lai, P. B. S.; Chan, A. T. C.; Ngai, S. M.; Hui, A. Y.; Johnson, P. J.; Sung, J. J. Y. *J. Proteome Res.* **2006**, *5*, 2691.

(61) Kobata, A.; Amano, J. *Immunol. Cell Biol.* **2005**, *83*, 429.

(62) Peracaula, R.; Tabares, G.; Royle, L.; Harvey, D. J.; Dwek, R. A.; Rudd, P. M.;

de Llorens, R. *Glycobiology* **2003**, *13*, 457.

(63) Tabares, G.; Radcliffe, C. M.; Barrabes, S.; Ramirez, M.; Aleixandre, R. N.; Hoesel, W.; Dwek, R. A.; Rudd, P. M.; Peracaula, R.; de Llorens, R. *Glycobiology* **2006**, *16*, 132.

(64) Kyselova, Z.; Mechref, Y.; Al Bataineh, M. M.; Dobrolecki, L. E.; Hickey, R. J.; Vinson, J.; Sweeney, C. J.; Novotny, M. V. *J. Proteome Res.* **2007**, *6*, 1822.

(65) Tabares, G.; Jung, K.; Reiche, J.; Stephan, C.; Lein, M.; Peracaula, R.; de Llorens, R.; Hoesel, W. *Clin. Biochem.* **2007**, *40*, 343.

(66) Kovalevskaya, G.; Kakuma, T.; Schlatterer, J.; O'Connor, J. F. *Mol. Cell. Endocrinol.* **2007**, *260*, 237.

(67) Valmu, L.; Alfthan, H.; Hotakainen, K.; Birken, S.; Stenman, U. H. *Glycobiology* **2006**, *16*, 1207.

(68) Cole, L. A. *Placenta* **2007**, *28*, 977.

(69) Peracaula, R.; Tabares, G.; Lopez-Ferrer, A.; Brossmer, R.; de Bolos, C.; de Llorens, R. *Glycoconjugate J.* **2005**, *22*, 135.

(70) Fernandez-Salas, E.; Peracaula, R.; Frazier, M. L.; de Llorens, R. *Eur. J. Biochem.* **2000**, *267*, 1484.

(71) Jin, S.; Cheng, Y.; Reid, S.; Li, M.; Wang, B. *Med. Res. Rev.* **2009**, (DOI: 10.1002/med.20155).

(72) Frank, R.; Hargreaves, R. *Nat. Rev. Drug Discov.* **2003**, *2*, 566.

(73) Miura, Y.; Nishimura, S. I. *Trends Glycosci. Glycotechnol.* **2008**, *20*, 17.

(74) An, H. J.; Peavy, T. R.; Hedrick, J. L.; Lebrilla, C. B. *Anal. Chem.* **2003**, *75*, 5628.

(75) Cipollo, J. F.; Costello, C. E.; Hirschberg, C. B. *J. Biol. Chem.* **2002**, *277*, 49143.

(76) Goldberg, D.; Sutton-Smith, M.; Paulson, J.; Dell, A. *Proteomics* **2005**, *5*, 865.

(77) Kameyama, A.; Kaneda, Y.; Yamanaka, H.; Yoshimine, H.; Narimatsu, H.; Shinohara, Y. *Anal. Chem.* **2004**, *76*, 4537.

(78) Morelle, W.; Slomianny, M. C.; Diemer, H.; Schaeffer, C.; van Dorsselaer, A.; Michalski, J. C. *Rapid Comm. Mass Spectrom.* **2004**, *18*, 2637.

(79) Dell, A.; Morris, H. R. *Science* **2001**, *291*, 2351.

(80) Rudd, P. M.; Colominas, C.; Royle, L.; Murphy, N.; Hart, E.; Merry, A. H.; Hebestreit, H. F.; Dwek, R. A. *Proteomics* **2001**, *1*, 285.

(81) Royle, L.; Mattu, T. S.; Hart, E.; Langridge, J. I.; Merry, A. H.; Murphy, N.; Harvey, D. J.; Dwek, R. A.; Rudd, P. M. *Anal. Biochem.* **2002**, *304*, 70.

(82) Guerrini, M.; Bisio, A.; Torri, G. *Semin. Thromb. Hemost.* **2001**, *27*, 473.

(83) Manzi, A. E.; Norgard-Sumnicht, K.; Argade, S.; Marth, J. D.; van Halbeek, H.; Varki, A. *Glycobiology* **2000**, *10*, 669.

(84) Lopez, M.; Coddeville, B.; Langridge, J.; Plancke, Y.; Sautiere, P.; Chaabihi, H.; Chirat, F.; HarduinLepers, A.; Cerutti, M.; Verbert, A.; Delannoy, P. *Glycobiology* **1997**, *7*, 635.

(85) Venkataraman, G.; Shriver, Z.; Raman, R.; Sasisekharan, R. *Science* **1999**, *286*, 537.

(86) Guerrini, M.; Raman, R.; Venkataraman, G.; Torri, G.; Sasisekharan, R.; Casu, B. *Glycobiology* **2002**, *12*, 713.

(87) Drickamer, K. *J. Biol. Chem.* **1988**, *263*, 9557.

(88) Lis, H.; Sharon, N. *Chem. Rev.* **1998**, *98*, 637.

(89) Spiess, M. *Biochemistry* **1990**, *29*, 10009.

(90) Stockert, R. J. *Physiol. Rev.* **1995**, *75*, 591.

(91) Holmskov, U.; Malhotra, R.; Sim, R. B.; Jensenius, J. C. *Immunol. Today* **1994**, *15*, 67.

(92) Epstein, J.; Eichbaum, Q.; Sheriff, S.; Ezekowitz, R. A. *Curr. Opin. Immunol.* **1996**, *8*, 29.

(93) Weis, W. I.; Drickamer, K. *Structure* **1994**, *2*, 1227.

(94) Weis, W. I.; Kahn, R.; Fourme, R.; Drickamer, K.; Hendrickson, W. A. *Science* **1991**, *254*, 1608.

(95) Weis, W. I.; Drickamer, K.; Hendrickson, W. A. *Nature* **1992**, *360*, 127.

(96) Sheriff, S.; Chang, C. Y.; Ezekowitz, R. A. *Nat. Struct. Biol.* **1994**, *1*, 789.

(97) Lasky, L. A. *Annu. Rev. Biochem.* **1995**, *64*, 113.

(98) O'Connell, D.; Koenig, A.; Jennings, S.; Hicke, B.; Han, H. L.; Fitzwater, T.; Chang, Y. F.; Varki, N.; Parma, D.; Varki, A. *Proc. Natl. Acad. Sci. U. S. A.* **1996**, *93*, 5883.

(99) Rosen, S. D.; Bertozzi, C. R. *Curr. Opin. Cell Biol.* **1994**, *6*, 663.

(100) McEver, R. P.; Moore, K. L.; Cummings, R. D. *J. Biol. Chem.* **1995**, *270*, 11025.

(101) Graves, B. J.; Crowther, R. L.; Chandran, C.; Rumberger, J. M.; Li, S.; Huang, K. S.; Presky, D. H.; Familletti, P. C.; Wolitzky, B. A.; Burns, D. K. *Nature* **1994**, *367*, 532.

(102) Crocker, P. R. *Curr. Opin. Pharmacol.* **2005**, *5*, 431.

(103) Varki, A.; Angata, T. *Glycobiology* **2006**, *16*, 1R.

(104) Houzelstein, D.; Goncalves, I. R.; Fadden, A. J.; Sidhu, S. S.; Cooper, D. N. W.; Drickamer, K.; Leffler, H.; Poirier, F. *Mol. Biol. Evol.* **2004**, *21*, 1177.

(105) Liu, F. T.; Rabinovich, G. A. *Nat. Rev. Cancer* **2005**, *5*, 29.

(106) Rabinovich, G. A.; Gruppi, A. *Parasite Immunol.* **2005**, *27*, 103.

(107) Simanek, E. E.; McGarvey, G. J.; Jablonowski, J. A.; Wong, C.-H. *Chem. Rev.* **1998**, *98*, 833.

(108) Ebe, Y.; Kuno, A.; Uchiyama, N.; Koseki-Kuno, S.; Yamada, M.; Sato, T.; Narimatsu, H.; Hirabayashi, J. *J. Biochem.* **2006**, *139*, 323.

(109) Hsu, K. L.; Pilobello, K. T.; Mahal, L. K. *Nat. Chem. Biol.* **2006**, *2*, 153.

(110) Rosenfeld, R.; Bangio, H.; Gerwig, G. J.; Rosenberg, R.; Aloni, R.; Cohen, Y.; Amor, Y.; Plaschkes, I.; Kamerling, J. P.; Maya, R. B. Y. *J. Biochem. Biophys. Methods* **2007**, *70*, 415.

(111) Collins, B. E.; Paulson, J. C. *Curr. Opin. Chem. Biol.* **2004**, *8*, 617.

(112) Paulson, J. C.; Blixt, O.; Collins, B. E. *Nat. Chem. Biol.* **2006**, *2*, 238.

(113) Pilobello, K. T.; Krishnamoorthy, L.; Slawek, D.; Mahal, L. K. *Chembiochem* **2005**, *6*, 985.

(114) Yan, J.; Fang, H.; Wang, B. *Med. Res. Rev.* **2005**, *25*, 490.

(115) Mazik, M.; Cavga, H. *J. Org. Chem.* **2006**, *71*, 2957.

(116) Davis, A. P.; Wareham, R. S. *Angew. Chem. Int. Ed.* **1998**, *37*, 2270.

(117) Palanisamy, U. D.; Hussain, A.; Iqbal, S.; Sproule, K.; Lowe, C. R. *J. Mol. Recognit.* **1999**, *12*, 57.

(118) Mazik, M.; Sicking, W. *Chem. Eur. J.* **2001**, *7*, 664.

(119) Lecollinet, G.; Dominey, A. P.; Velasco, T.; Davis, A. P. *Angew. Chem. Int. Ed.* **2002**, *41*, 4093.

(120) Klein, E.; Crump, M. P.; Davis, A. P. *Angew. Chem., Int. Ed.* **2005**, *44*, 298.

(121) Ferrand, Y.; Klein, E.; Barwell, N. P.; Crump, M. P.; Jimenez-Barbero, J.; Vicent, C.; Boons, G. J.; Ingale, S.; Davis, A. P. *Angew. Chem. Int. Ed.* **2009**, *48*, 1775.

(122) Hall, D. G. *Boronic Acids: Preparation, Applications in Organic Synthesis and Medicine*; 1st ed.; Wiley-VCH: Weinheim, 2005 and references cited therein.

(123) Jin, S.; Cheng, Y.; Reid, S.; Li, M.; Wang, B. *Med. Res. Rev.* **2009**, (DOI: 10.1002/med.20155) and references cited therein.

(124) Lorand, J. P.; Edwards, J. O. *J. Org. Chem.* **1959**, *24*, 769.

(125) Springsteen, G.; Wang, B. *Tetrahedron* **2002**, *58*, 5291.

(126) Yan, J.; Springsteen, G.; Deeter, S.; Wang, B. *Tetrahedron* **2004**, *60*, 11205.

(127) Jabbour, A.; Steinberg, D.; Dembitsky, V. M.; Moussaieff, A.; Zaks, B.;

Srebnik, M. *J. Med. Chem.* **2004**, *47*, 2409.

(128) Brindley, P. B.; Gerrard, W.; Lappert, M. F. *J. Chem. Soc* **1955**, 2956.

(129) Morrison, J. D.; Letsinger, R. L. *J. Org. Chem.* **1964**, *29*, 3405.

(130) Matteson, D. S.; Schaumberg, G. D. *J. Organomet. Chem.* **1967**, *8*, 359.

(131) Sienkiewicz, P. A.; Roberts, D. C. *J. Inorg. Nucl. Chem.* **1980**, *42*, 1559.

(132) DiCesare, N.; Lakowicz, J. R. *Anal. Biochem.* **2002**, *301*, 111.

(133) Badugu, R.; Lakowicz, J. R.; Geddes, C. D. *Sensor Actuat. B-Chem.* **2005**, *104*, 103.

(134) Swamy, K. M. K.; Lee, Y. J.; Lee, H. N.; Chun, J.; Kim, Y.; Kim, S. J.; Yoon, J. *J. Org. Chem.* **2006**, *71*, 8626.

(135) Oehlke, A.; Auer, A. A.; Jahre, I.; Walfort, B.; Ruffer, T.; Zoufala, P.; Lang, H.; Spange, S. *J. Org. Chem.* **2007**, *72*, 4328.

(136) Badugu, R.; Lakowicz, J. R.; Geddes, C. D. *Anal. Chem.* **2004**, *327*, 82.

(137) Badugu, R.; Lakowicz, J. R.; Geddes, C. D. *Dyes Pigments* **2005**, *64*, 49.

(138) Yoon, J.; Czarnik, A. W. *J. Am. Chem. Soc.* **1992**, *114*, 5874.

(139) James, T. D.; Sandanayake, K. R. A. S.; Iguchi, R.; Shinkai, S. *J. Am. Chem. Soc.* **1995**, *117*, 8982.

(140) Eggert, H.; Frederiksen, J.; Morin, C.; Norrild, J. C. *J. Org. Chem.* **1999**, *64*, 3846.

(141) Bielecki, M.; Eggert, H.; Norrild, J. C. *J. Chem. Soc., Perkin Trans. 2* **1999**, 449.

(142) Yang, W.; Fan, H.; Gao, S.; Gao, X.; Ni, W.; Karnati, V.; Hooks, W. B.; Carson, J.; Weston, B.; Wang, B. *Chem. Biol.* **2004**, *11*, 439.

(143) Asher, S. A.; Alexeev, V. L.; Goponenko, A. V.; Sharma, A. C.; Lednev, I. K.; Wilcox, C. S.; Finegold, D. N. *J. Am. Chem. Soc.* **2003**, *125*, 3322

(144) Wang, Z.; Zhang, D. Q.; Zhu, D. B. *J. Org. Chem.* **2005**, *70*, 5729.

(145) Gray Jr., C. W.; Houston, T. A. *J. Org. Chem.* **2002**, *67*, 5426.

(146) Wiskur, S. L.; Lavigne, J. L.; Ait-Haddou, H.; Lynch, V.; Chiu, Y. H.; Canary, J. W.; Anslyn, E. V. *Org. Lett.* **2001**, *3*, 1311.

(147) Gamsey, S.; Miller, A.; Olmstead, M. M.; Beavers, C. M.; Hirayama, L. C.; Pradhan, S.; Wessling, R. A.; Singaram, B. *J. Am. Chem. Soc.* **2007**, *129*, 1278.

(148) Cho, B. T. In *Boronic Acids*; Hall, D. G., Ed.; Wiley-VCH: Weinheim, 2005, p 411.

(149) Aharoni, R.; Bronstheyn, M.; Jabbour, A.; Zaks, B.; Srebnik, M.; Steinberg, D. *Bioorg Med Chem* **2008**, *16*, 1596.

(150) Cooper, C. R.; Spencer, N.; James, T. D. *Chem Commun* **1998**, 1365.

(151) *Boronic Acids: Preparation and Applications in Organic Synthesis and Medicine*; Hall, D. G., Ed.; Wiley-VCH, 2005.

(152) Yang, W.; He, H.; Drueckhammer, D. G. *Angew. Chem. Int. Ed* **2001**, *40*, 1714.

(153) Gray, C. W.; Johnson, L. L.; Walker, B. T.; Sleevi, M. C.; Campbell, A. S.; Plourde, R.; Houston, T. A. *Bioorg. Med. Chem. Lett.* **2005**, *15*, 5416.

(154) Roy, C. D.; Brown, H. C. *J. Organomet. Chem.* **2007**, *692*, 784.

(155) Springsteen, G.; Wang, B. H. *Chem. Commun.* **2001**, 1608.

(156) Sugihara, J. M.; Bowman, C. M. *J. Am. Chem. Soc.* **1958**, *80*, 2443.

(157) Edwards, J. O.; Sederstrom, R. J. *J. Phys. Chem.* **1961**, *65*, 862.

(158) Böeseken, J. *Adv. Carbohydr. Chem.* **1949**, *4*, 189.

(159) Letsinger, R. L.; Dandegaonker, S. H. *J. Am. Chem. Soc.* **1959**, *81*, 498.

(160) Mohler, L. K.; Czarnik, A. W. *J. Am. Chem. Soc.* **1993**, *115*, 7037.

(161) James, T. D.; Sandanayake, K.; Shinkai, S. *J. Chem. Soc.-Chem. Commun.* **1994**, 477.

(162) Yang, W.; Gao, X.; Wang, B. *Med. Res. Rev.* **2003**, *23*, 346.

(163) Springsteen, G.; Wang, B. H. *Tetrahedron* **2002**, *58*, 5291.

(164) Sorensen, M. D.; Martins, R.; Hindsgaul, O. *Angew. Chem. Int. Ed.* **2007**, *46*, 2403.

(165) Berube, M.; Dowlut, M.; Hall, D. G. *J. Org. Chem.* **2008**, *73*, 6471.

(166) Dowlut, M.; Hall, D. G. *J. Am. Chem. Soc.* **2006**, *128*, 4226

(167) Gao, X.; Zhang, Y.; Wang, B. *Org. Lett.* **2003**, *5*, 4615.

(168) Gao, X.; Zhang, Y.; Wang, B. *Tetrahedron* **2005**, *61*, 9111.

(169) Gao, X.; Zhang, Y.; Wang, B. *New J. Chem.* **2005**, *29*, 579.

(170) Jin, S.; Wang, J. F.; Li, M. Y.; Wang, B. H. *Chem. Eur. J.* **2008**, *14*, 2795.

(171) Ni, W.; Fang, H.; Springsteen, G.; Wang, B. *J. Org. Chem.* **2004**, *69*, 1999.

(172) Ni, W.; Kaur, G.; Springsteen, G.; Wang, B.; Franzen, S. *Bioorgan. Chem.*

2004, *32*, 571.

(173) Wang, J.; Jin, S.; Wang, B. *Tetrahedron Lett.* **2005**, *46*, 7003.

(174) Wang, J.; Lin, N.; Jin, S.; Wang, B. *Chem. Biol. Drug Design* **2006**, *67*, 137.

(175) Adhikiri, D. P.; Heagy, M. D. *Tetrahedron Lett.* **1999**, *40*, 7893.

(176) Cao, H.; Diaz, D. I.; DiCesare, D.; Lakowicz, J. R.; Heagy, M. D. *Org. Lett.* **2002**, *4*, 1503

(177) Cao, H.; McGill, T.; Heagy, M. D. *J. Org. Chem.* **2004**, *69*, 2959.

(178) Hutt, K.; Hernandez, R.; Heagy, M. D. *Bioorg. Med. Chem. Lett.* **2006**, *16*, 5436.

(179) Cao, H. S.; Heagy, M. D. *J. Fluoresc.* **2004**, *14*, 569.

(180) Eggert, H.; Frederiksen, J.; Morin, C.; Norrild, J. C. *J. Org. Chem.* **1999**, *64*, 3846.

(181) James, T. D.; Sandanayake, K. R. A. S.; Shinkai, S. *Nature* **1995**, *374*, 345.

(182) Franzen, S.; Ni, W. J.; Wang, B. H. *J. Phys. Chem. B* **2003**, *107*, 12942.

(183) Zhu, L.; Shabbir, S. H.; Gray, M.; Lynch, V. M.; Sorey, S.; Anslyn, E. V. *J. Am. Chem. Soc.* **2006**, *128*, 1222.

(184) Badugu, R.; Lakowicz, J. R.; Geddes, C. D. *Talanta* **2005**, *66*, 569.

(185) Badugu, R.; Lakowicz, J. R.; Geddes, C. D. *Bioorg. Med. Chem.* **2005**, *13*, 113.

(186) Yang, W.; He, H.; Drueckhammer, D. G. *Angew. Chem. Int. Edit.* **2001**, *40*, 1714.

(187) *Glycoimmunology*; Alavi, A.; Axford, J. S., Eds.; Plenum Press: New York, 1995; Vol. 376.

(188) Alexeev, V. L.; Sharma, A. C.; Goponenko, A. V.; Das, S.; Lednev, I. K.; Wilcox, C. S.; Finegold, D. N.; Asher, S. A. *Anal. Chem.* **2004**, *75*, 2316.

(189) Cooper, C. R.; James, T. D. *Chem. Lett.* **1998**, 883.

(190) Norrild, J. C.; Eggert, H. *J. Am. Chem. Soc.* **1995**, *117*, 1479.

(191) Kaur, G.; Fang, H.; Gao, X.; Li, H.; Wang, B. *Tetrahedron* **2006**, *62*, 2583.

(192) Nicholls, M. P.; Paul, P. K. C. *Org. Biomol. Chem.* **2004**, *2*, 1434.

(193) Camara, J. N.; Suri, J. T.; Cappuccio, F. E.; Wessling, R. A.; Singaram, B. *Tetrahedron Lett.* **2002**, *43*, 1139.

(194) Cordes, D. B.; Miller, A.; Gamsey, S.; Sharrett, Z.; Thoniyot, P.; Wessling, R.; Singaram, B. *Org. Biomol. Chem.* **2005**, *3*, 1708.

(195) Benesi, H. A.; Hildebrand, J. H. *J. Am. Chem. Soc.* **1949**, *71*, 2707.

(196) Burnett, T. J.; Peebles, H. C.; Hageman, J. H. *Biochem. Biophy. Res. Comm.* **1980**, *96*, 157.

(197) Davis-Mancini, K.; Lopez, I. P.; Hageman, J. H. *J. Bacteriol.* **1978**, *136*, 625.

(198) Geele, G.; Garrett, E.; Hageman, H. J. *Am. Soc. Micro.* **1975**, 391.

(199) Yang, W.; Gao, S.; Gao, X.; Karnati, V. R.; Ni, W.; Wang, B.; Hooks, W. B.; Carson, J.; Weston, B. *Bioorg. Med. Chem. Lett* **2002**, *12*, 2175.

(200) James, T. D.; Shinkai, S. *Top. Curr. Chem.* **2002**, *218*, 159.

(201) Abad, J. M.; Velez, M.; Santamaria, C.; Guisan, J. M.; Matheus, P. R.;

Vazquez, L.; Gazaryan, I.; Gorton, L.; Gibson, T.; Fernandez, V. M. *J. Am. Chem. Soc.* **2002**, *124*, 12845.

(202) Liu, J. T.; Chen, L. Y.; Shih, M. C.; Chang, Y.; Chen, W. Y. *Anal. Biochem.* **2008**, *375*, 90.

(203) Weykamp, C. W.; Penders, T. J.; Siebelder, C. W.; Muskiet, F. A.; van der Slik, W. *Clin Chem* **1993**, *39*, 138.

(204) Little, R. R.; Vesper, H.; Rohlfing, C. L.; Ospina, M.; Safar-Pour, S.; Roberts, W. L. *Clin Chem* **2005**, *51*, 264.

(205) Dickey, F. H. *Proc. Natl. Acad. Sci.* **1949**, *35*, 227.

(206) Yan, M.; Ramstrom, O. *Molecularly Imprinted Materials: Science and Technology*; Marcel Dekker, 2005.

(207) Zhang, H. Q.; Ye, L.; Mosbach, K. *J. Mol. Recognit.* **2006**, *19*, 248.

(208) Shea, K. *Trends Polym. Sci.* **1994**, *2*, 166.

(209) Wang, W.; Gao, S.; Wang, B. In *Molecularly Imprinted Materials: Science and Technology*; Yan, M., Ramstrom, O., Eds.; Marcel Dekker: 2005, p 701.

(210) Wulff, G.; Schauhoff, S. *J. Org. Chem.* **1991**, *56*, 395.

(211) Gao, S.; Wang, W.; Wang, B. *Bioorg. Chem.* **2001**, *29*, 308.

(212) Wang, W.; Gao, S.; Wang, B. *Org. Lett.* **1999**, *1*, 1209.

(213) James, T. D.; Sandanayake, K. R. A. S.; Shinkai, S. *Chem Commun* **1994**, 477.

(214) Miyahara, T.; Kurihara, K. *Chem. Lett.* **2000**, 1356.

(215) Sallacan, N.; Zayats, M.; Bourenko, T.; Kharitonov, A. B.; Willner, I. *Anal. Chem.* **2002**, *74*, 702.

(216) Granot, E.; Tel-Vered, R.; Lioubashevski, O.; Willner, I. *Adv. Funct. Mater.* **2008**, *18*, 478.

(217) Zayats, M.; Lahav, M.; Kharitonov, A. B.; Willner, I. *Tetrahedron* **2002**, *58*, 815.

(218) Rajkumar, R.; Katterle, M.; Warsinke, A.; Moehwald, H.; Scheller, F. W. *Biosens Bioelectron* **2008**, *23*, 1195.

(219) Lehn, J.-M. *Chem. Eur. J.* **1999**, *5*, 2455.

(220) Linton, B.; Hamilton, A. D. *Curr. Opin. Chem. Biol.* **1999**, *3*, 307.

(221) Otto, S.; Furlan, R. L. E.; Sanders, J. K. M. *Drug Discov. Today* **2002**, *7*, 117.

(222) Eliseev, A. V.; Lehn, J. M. *Combinatorial Chem. Biol.* **1999**, *243*, 159.

(223) Alonso, H.; Bliznyuk, A. A.; Gready, J. E. *Med Res Rev* **2006**, *26*, 531.

(224) Palanisamy, U. D.; Lowe, C. R. *J. Chromatogr. A* **2005**, *1075*, 95.

(225) Palanisamy, U. D.; Winzor, D. J.; Lowe, C. R. *J. Chromatogr. B-Anal. Tech. in Biomed. Life Sci.* **2000**, *746*, 265.

(226) Edwards, N. Y.; Sager, T. W.; McDevitt, J. T.; Anslyn, E. V. *J. Am. Chem. Soc.* **2007**, *129*, 13575.

(227) Zou, Y.; Broughton, D. L.; Bicker, K. L.; Thompson, P. R.; Lavigne, J. J. *ChemBioChem.* **2007**, *8*, 2048.

(228) Manku, S.; Hall, D. G. *Aust. J. Chem.* **2007**, *60*, 824.

(229) Duggan, P. J.; Offermann, D. A. *Aust. J. Chem.* **2007**, *60*, 829.

(230) Duggan, P. J.; Offermann, D. A. *Tetrahedron* **2009**, *65*, 109.

(231) Lin, N.; Yan, J.; Huang, Z.; Altier, C.; Li, M.; Carrasco, N.; Suyemoto, M.; Johnston, L.; Wang, S.; Wang, Q.; Fang, H.; Caton-Williams, J.; Wang, B. *Nucleic Acids Res.* **2007**, *35*, 1222.

(232) Manimala, J. C.; Wiskur, S. L.; Ellington, A. D.; Anslyn, E. V. *J. Am. Chem. Soc.* **2004**, *126*, 16515.

(233) Brustad, E.; Bushey, M. L.; Lee, J. W.; Groff, D.; Liu, W.; Schultz, P. G. *Angew. Chem., Int. Ed.* **2008**, *47*, 8220.

(234) Liu, R. W.; Mark, J.; Lam, K. S. *J. Am. Chem. Soc.* **2002**, *124*, 7678.

(235) Geysen, H. M.; Mason, T. J. *Bioorg. Med. Chem. Lett.* **1993**, *3*, 397.

(236) Wang, J. X.; Bray, A. M.; Dipasquale, A. J.; Maeji, N. J.; Geysen, H. M. *Int. J. Pept. Protein Res.* **1993**, *42*, 384.

(237) Sears, P.; Wong, C.-H. *Angew. Chem. Int. Ed.* **1999**, *38*, 2300.

(238) Gravel, M.; Kim, A.; Mark Zak, T.; Berube, C.; Hall, D. G. *J. Org. Chem.* **2002**, *67*, 3.

(239) Springsteen, G.; Wang, B. H. *Chem. Comm.* **2001**, 1608.

(240) Lam, K. S.; Salmon, S. E.; Hersh, E. M.; Hruby, V. J.; Kazmierski, W. M.; Knapp, R. J. *Nature* **1991**, *354*, 82.

(241) Wang, X.; Peng, L.; Liu, R.; Xu, B.; Lam, K. S. *J. Pept. Res.* **2005**, *65*, 130.

(242) Jeong, S.; Eom, T.; Kim, S.; Lee, S.; Yu, J. *Biochem. Biophys. Res. Comm.*

2001, *281*, 237.

(243) Ellington, A. D.; Szostak, J. W. *Nature* **1990**, *346* 818

(244) Robertson, D. L.; Joyce, G. F. *Nature* **1990**, *344*, 467.

(245) Tuerk, C.; Gold, L. *Science* **1990**, *249*, 505.

(246) Lin, N.; Yan, J.; Huang, Z.; Altier, C.; Yan, J.; Carrasco, N.; Suyemoto, M.; Johnson, L.; Fang, H.; Wang, Q.; Wang, S.; Wang, B. *Nucl. Acid Res.* **2007**, *35*, 1222.

(247) Huisgen, R. *Angew. Chem., Int. Ed.* **1963**, *2*, 565.

(248) Kolb, H. C.; Finn, M. G.; Sharpless, K. B. *Angew. Chem. Int. Ed. Engl.* **2001**, *40*, 2004.

(249) Tornoe, C. W.; Christensen, C.; Meldal, M. *J. Org. Chem.* **2002**, *67*, 3057.

(250) Yang, W.; Gao, X.; Springsteen, G.; Wang, B. *Tetrahedron Lett.* **2002**, *43*, 6339.

(251) Jin, S.; Li, M.; Zhu, C.; Tran, V.; Wang, B. *ChemBiochem.* **2008**, *9*, 1431.

(252) Nordhoff, E.; Kirpekar, F.; Roepstorff, P. *Mass Spectrom. Rev.* **1996**, *15*, 67.

(253) *Cell Biology : a Laboratory Handbook*; 3rd ed.; Boston : Elsevier Academic Press: Amsterdam, 2006.

(254) Gonzalez-Lazaro, M.; Gonzalez-Robles, A.; Hernandez-Gutierrez, R.; Arroyo, R. *Int. J. Biochem. Cell Biol.* **2005**, *37*, 166.

(255) Gierlich, J.; Burley, G. A.; Gramlich, P. M. E.; Hammond, D. M.; Carell, T. *Org. Lett.* **2006**, *8*, 3639.

(256) Bouillon, C.; Meyer, A.; Vidal, S.; Jochum, A.; Chevolot, Y.; Cloarec, J. P.;

Praly, J. P.; Vasseur, J. J.; Morvan, F. *J. Org. Chem.* **2006**, *71*, 4700.

(257) Trupp, S.; Schweitzer, A.; Mohr, G. J. *Org Biomol Chem* **2006**, *4*, 2965.

(258) Wang, J. F.; Jin, S.; Akay, S.; Wang, B. H. *Eur. J. Org. Chem.* **2007**, 2091.

(259) Kolb, H. C.; Finn, M. G.; Sharpless, K. B. *Angew. Chem., Int. Ed.* **2001**, *40*, 2004.

(260) Ambrose, W. P.; Goodwin, P. M.; Jett, J. H.; Van Orden, A.; Werner, J. H.; Keller, R. A. *Chem. Rev.* **1999**, *99*, 2929.

(261) Soper, S. A.; Nutter, H. L.; Keller, R. A.; Davis, L. M.; Shera, E. B. *Photochem. Photobiol.* **1993**, *57*, 972.

(262) Chan, T. R.; Hilgraf, R.; Sharpless, K. B.; Fokin, V. V. *Org. Lett.* **2004**, *6*, 2853.

(263) Devaraj, N. K.; Miller, G. P.; Ebina, W.; Kakaradov, B.; Collman, J. P.; Kool, E. T.; Chidsey, C. E. D. *J. Am. Chem. Soc* **2005**, *127*, 8600.

(264) Jin, S.; Choudhary, G.; Cheng, Y. F.; Dai, C. F.; Li, M. Y.; Wang, B. H. *J. Chem. Soc.-Chem. Commun.* **2009**, 5251.

(265) Connors, K. A. *Binding Constants: The Measurement of Molecular Complex Stability*; 1st ed.; John Wiley & Sons, Inc, 1987.

(266) Klenow, H.; Henningsen, I. *Proc. Natl. Acad. Sci. U S A* **1970**, *65*, 168.

(267) Bock, L. C.; Griffin, L. C.; Latham, J. A.; Vermaas, E. H.; Toole, J. J. *Nature* **1992**, *355*, 564.

(268) Cuenoud, B.; Szostak, J. W. *Nature* **1995**, *375*, 611.

(269) Daniels, D. A.; Chen, H.; Hicke, B. J.; Swiderek, K. M.; Gold, L. *Proc. Natl. Acad. Sci. U. S. A.* **2003**, *100*, 15416.

(270) Le, J. D.; Pinto, Y.; Seeman, N. C.; Musier-Forsyth, K.; Taton, T. A.; Kiehl, R. A. *Nano Lett.* **2004**, *4*, 2343.

(271) Zhang, C. Y.; Yeh, H. C.; Kuroki, M. T.; Wang, T. H. *Nat. Mater.* **2005**, *4*, 826.

(272) Petty, J. T.; Zheng, J.; Hud, N. V.; Dickson, R. M. *J. Am. Chem. Soc* **2004**, *126*, 5207.

(273) Mirkin, C. A. *MRS Bull.* **2000**, *25*, 43.

(274) Benenson, Y.; Adar, R.; Paz-Elizur, T.; Livneh, Z.; Shapiro, E. *Proc. Natl. Acad. Sci. U. S. A.* **2003**, *100*, 2191.

(275) Zhang, Z. Z.; Fan, C. H.; He, L. *Curr. Nanosci.* **2005**, *1*, 91.

(276) Yan, H.; Zhang, X. P.; Shen, Z. Y.; Seeman, N. C. *Nature* **2002**, *415*, 62.

(277) Rosi, N. L.; Mirkin, C. A. *Chem. Rev.* **2005**, *105*, 1547.

(278) Taton, T. A.; Mirkin, C. A.; Letsinger, R. L. *Science* **2000**, *289*, 1757.

(279) Sakthivel, K.; Barbas, C. F. *Angew. Chem., Int. Ed.* **1998**, *37*, 2872.

(280) Eaton, B. E.; Gold, L.; Hicke, B. J.; Janjic, N.; Jucker, F. M.; Sebesta, D. P.; Tarasow, T. M.; Willis, M. C.; Zichi, D. A. *Bioorg. Med. Chem* **1997**, *5*, 1087.

(281) Eaton, B. E.; Pieken, W. A. *Annu. Rev. Biochem.* **1995**, *64*, 837.

(282) Jensen, K. B.; Atkinson, B. L.; Willis, M. C.; Koch, T. H.; Gold, L. *Proc. Natl. Acad. Sci. U. S. A.* **1995**, *92*, 12220.

(283) Santoro, S. W.; Joyce, G. F.; Sakthivel, K.; Gramatikova, S.; Barbas, C. F. *J.*

Am. Chem. Soc **2000**, *122*, 2433.

(284) Edwards, N. Y.; Sager, T. W.; McDevitt, J. T.; Anslyn, E. V. *J. Am. Chem. Soc* **2007**, *129*, 13575.

(285) Manimala, J. C.; Wiskur, S. L.; Ellington, A. D.; Anslyn, E. V. *J. Am. Chem. Soc* **2004**, *126*, 16515.

(286) Rambo, B. M.; Lavigne, J. J. *Chem. Mat.* **2007**, *19*, 3732.

(287) Niu, W. J.; Smith, M. D.; Lavigne, J. J. *J. Am. Chem. Soc* **2006**, *128*, 16466.

(288) Severin, K. *Dalton Trans.* **2009**, 5254.

(289) Roy, D.; Cambre, J. N.; Sumerlin, B. S. *J. Chem. Soc.-Chem. Commun.* **2009**, 2106.

(290) Hisamitsu, I.; Kataoka, K.; Okano, T.; Sakurai, Y. *Pharm. Res.* **1997**, *14*, 289.

(291) Hoare, T.; Pelton, R. *Macromolecules* **2007**, *40*, 670.

(292) Randolph, J. B.; Waggoner, A. S. *Nucleic Acids Res.* **1997**, *25*, 2923.

(293) Wallner, G.; Amann, R.; Beisker, W. *Cytometry* **1993**, *14*, 136.

(294) Levinson, G. S.; Simpson, W. T.; Curtis, W. *J. Am. Chem. Soc.* **1957**, *79*, 4314.

(295) West, W.; Pearce, S.; Grum, F. *J. Phys. Chem.* **1967**, *71*, 1316.

(296) Rachofsky, E. L.; Osman, R.; Ross, J. B. A. *Biochemistry* **2001**, *40*, 946.

(297) Arkin, M. R.; Stemp, E. D. A.; Turro, C.; Turro, N. J.; Barton, J. K. *J. Am. Chem. Soc* **1996**, *118*, 2267.

(298) Hawkins, M. E.; Pfleiderer, W.; Balis, F. M.; Porter, D.; Knutson, J. R. *Anal.*

Biochem. **1997**, *244*, 86.

(299) Alexander, P.; Moroson, H. *Nature* **1962**, *194*, 882.

(300) Pfeifer, G. P.; You, Y. H.; Besaratinia, A. *Mutat. Res.* **2005**, *571*, 19.

(301) Munoz-Gamez, J. A.; Martin-Oliva, D.; Aguilar-Quesada, R.; Canuelo, A.; Nunez, M. I.; Valenzuela, M. T.; De Almodovar, J. M. R.; De Murcia, G.; Oliver, F. J. *Biochem. J.* **2005**, *386*, 119.

(302) Banasik, M.; Komura, H.; Shimoyama, M.; Ueda, K. *J. Biol. Chem.* **1992**, *267*, 1569.

(303) Brana, M. F.; Castellano, J. M.; Moran, M.; Devega, M. J. P.; Romerdahl, C. R.; Qian, X. D.; Bousquet, P.; Emling, F.; Schlick, E.; Keilhauer, G. *Anti-Cancer Drug Des.* **1993**, *8*, 257.

(304) Ghosh, U.; Bhattacharyya, N. P. *Mol. Cell. Biochem.* **2009**, *320*, 15.

(305) Rideout, D.; Schinazi, R.; Pauza, C. D.; Lovelace, K.; Chiang, L. C.; Calogeropoulou, T.; McCarthy, M.; Elder, J. H. *J. Cell. Biochem.* **1993**, *51*, 446.

(306) Chanh, T. C.; Lewis, D. E.; Allan, J. S.; Sogandaresbernal, F.; Judy, M. M.; Utecht, R. E.; Matthews, J. L. *Aids Res. Hum. Retrovir.* **1993**, *9*, 891.

(307) Chanh, T. C.; Lewis, D. E.; Judy, M. M.; Sogandaresbernal, F.; Michalek, G. R.; Utecht, R. E.; Skiles, H.; Chang, S. C.; Matthews, J. L. *Antiviral Res.* **1994**, *25*, 133.

(308) Sawa, M.; Hsu, T. L.; Itoh, T.; Sugiyama, M.; Hanson, S. R.; Vogt, P. K.; Wong, C. H. *Proc. Natl. Acad. Sci. U. S. A.* **2006**, *103*, 12371.

(309) Zhang, Z. C.; Wu, D.; Guo, X. F.; Qian, X. H.; Lu, Z.; Xu, Q.; Yang, Y. Y.;

Duan, L. P.; He, Y.; Feng, Z. *Chem. Res. Toxicol.* **2005**, *18*, 1814.

(310) Zhou, Z. G.; Yu, M. X.; Yang, H.; Huang, K. W.; Li, F. Y.; Yi, T.; Huang, C. H. *J. Chem. Soc.-Chem. Commun.* **2008**, 3387.

(311) Srikun, D.; Miller, E. W.; Dornaille, D. W.; Chang, C. J. *J. Am. Chem. Soc.* **2008**, *130*, 4596.

(312) Berque-Bestel, I.; Soulier, J. L.; Giner, M.; Rivail, L.; Langlois, M.; Sicsic, S. *J. Med. Chem.* **2003**, *46*, 2606.

(313) Otsuka, H.; Uchimura, E.; Koshino, H.; Okano, T.; Kataoka, K. *J. Am. Chem. Soc.* **2003**, *125*, 3493.

(314) Hawthorne, M. F. *Angew. Chem., Int. Ed.* **1993**, *32*, 950.

(315) Asano, T.; Nakamura, H.; Uehara, Y.; Yamamoto, Y. *Chembiochem* **2004**, *5*, 483.